



Department of Precision and Microsystems Engineering

The Influence of Porosity on the Dynamic Characteristics of Porous Air Bearings

R.M. Burghoorn

Report no : 2023.070  
Coach : Dr. ir. J. Nijssen  
Professor : Dr. ir. R.A.J. van Ostayen  
Specialisation : Mechatronic System Design  
Type of report : MSc report  
Date : 18 August 2023



# Thesis Report

## The Influence of Porosity on the Dynamic Characteristics of Porous Air Bearings

by

R.M. Burghoorn

Student number	4362446	
Project Duration:	Februari, 2022 - August, 2023	
Thesis committee:	Dr.ir. R.A.J. van Ostayen	TU Delft, supervisor
	Dr.ir. J. Nijssen	ASML, daily supervisor
	Dr.ir. J.F.L. Goosen	Independent Member

This thesis is confidential and cannot be made public until August 31, 2025.

An electronic version of this thesis is available at <https://repository.tudelft.nl>.

Cover: Inside NXE3400 - Metrology ©ASML

# Preface

This thesis was written for the completion of the Master Mechanical Engineering at the Faculty of 3ME of the Delft University of Technology. The thesis is carried out during a graduation internship at ASML in Veldhoven.

I would like to thank my supervisors: Dr. ir. R.A.J. van Ostayen from the TU Delft and Dr. ir. J. Nijssen and J. van der Sanden from ASML for their guidance and support throughout this thesis project. Without their suggestions and motivation during our meetings this project wouldn't have been possible. Additionally, I would like to thank my girlfriend Anna for helping me in the last stages of this report.

*R.M. Burghoorn  
Delft, August 2023*



# Summary

Air bearings are a vital component to high tech machines and have been in widespread use since the 1960s. They provide near frictionless motion, have high stiffness and a near infinite lifetime. When looking at existing literature the influence of the porosity on the dynamic characteristics has not been researched in depth. Especially when looking at porous air bearings with a surface restrictive layer, a discrepancy can be defined between the ideal surface restrictive layers considered in literature and layers that can be realized in reality. This report presents a model to accurately predict the dynamic characteristics of both bearings with and without a surface restrictive layer. An alternative intuitive approach is presented to explain the dynamic behaviour at low frequencies for these types of bearing based on the amount of stored air inside and underneath the bearing. This model is then used to investigate the influence of the porosity on the dynamic characteristics of a uncoated bearing. Followed by a study on the mechanics behind the surface restrictive layers and the sensitivity of the porosity of the surface restrictive layer. An existing dataset from an experiment is used to assess the viability of the model.

# Contents

<b>Preface</b>	<b>i</b>
<b>Summary</b>	<b>ii</b>
<b>Nomenclature</b>	<b>v</b>
<b>1 Introduction</b>	<b>1</b>
1.1 Construction and Operation . . . . .	1
1.2 Applications . . . . .	3
1.3 State of the Art . . . . .	4
1.4 Problem statement . . . . .	5
1.5 Research objective . . . . .	5
1.6 Thesis Outline . . . . .	5
<b>2 Theoretical modelling</b>	<b>6</b>
2.1 Thin film flow . . . . .	6
2.1.1 Incompressible flow . . . . .	6
2.1.2 Compressible flow . . . . .	7
2.2 Porous flow . . . . .	7
2.2.1 Resistance model . . . . .	7
2.2.2 Storage model . . . . .	8
2.3 Perturbation . . . . .	8
2.3.1 Perturbation thin film flow . . . . .	9
2.3.2 Perturbation porous flow . . . . .	9
2.4 Solving . . . . .	10
2.4.1 Boundary conditions . . . . .	10
2.4.2 Porous flow boundary conditions . . . . .	11
2.4.3 Solving strategy . . . . .	12
2.4.4 Post processing of the results . . . . .	12
2.5 Stability . . . . .	13
2.5.1 System dynamics . . . . .	13
2.5.2 Nyquist criterion . . . . .	14
2.6 Determine permeability coefficients from pressure and flow data for multi-layer bearings	15
2.7 Measuring porosity . . . . .	16
<b>3 Mechanics</b>	<b>17</b>
3.1 Equivalent spring damper model . . . . .	17
3.2 Damping in porous air bearings . . . . .	17
3.2.1 Accuracy and limitations of using $dm/dh$ vs calculating the damping coefficient . . . . .	21
3.3 Sensitivity of porosity on the dynamic behaviour . . . . .	22
3.4 Improve dynamics with a surface restrictive layer . . . . .	24
3.4.1 Addition of a surface restrictive layer with a change in static performance . . . . .	27
3.4.2 Static performance with reduced normalized total permeability . . . . .	27
3.4.3 Dynamic performance with reduced total normalized permeability . . . . .	28
3.5 Addition of a surface restrictive layer without a change in static performance . . . . .	29
<b>4 Case Study</b>	<b>31</b>
4.1 Measurement set-up . . . . .	31
4.2 Lumped Dynamic model . . . . .	32
4.3 Results . . . . .	33
<b>5 Conclusion</b>	<b>37</b>

<b>6 Recommendations</b>	<b>39</b>
<b>References</b>	<b>41</b>
<b>A Baseline bearing</b>	<b>44</b>
A.1 baseline static Performance . . . . .	45
A.2 baseline dynamic performance at operating point . . . . .	46
<b>B COMSOL implementation</b>	<b>47</b>
B.1 Parameters . . . . .	47
B.2 Model setup . . . . .	48
B.3 Definitions . . . . .	49
B.3.1 Bearing variables . . . . .	49
B.3.2 Stiffness variables . . . . .	49
B.3.3 Porous material properties . . . . .	51
B.3.4 Coating material properties . . . . .	51
B.3.5 Integration over bearing surface . . . . .	52
B.4 Physics . . . . .	53
B.4.1 General form boundary PDE: Reynolds static . . . . .	53
B.4.2 General form PDE: Darcy static . . . . .	57
B.4.3 Domain ODEs and DAEs: qx static (same as qy and qz) . . . . .	61
B.4.4 General form boundary PDE: Reynolds perturbation . . . . .	63
B.4.5 General form PDE: Darcy perturbation . . . . .	68
B.4.6 Domain ODEs and DAEs: qx perturbation (same as qy and qz) . . . . .	72
B.5 Solver settings . . . . .	74
B.6 Suggestions for figures . . . . .	76
B.6.1 Dynamic stiffness . . . . .	76

# Nomenclature

## Symbols

Symbol	Definition	Unit
$D_{dyn}$	frequency dependant dynamic stiffness	[N/m]
$h$	gap/flying height	[m]
$h_0$	height at perturbation point	[Pa]
$\tilde{h}$	perturbation height	[Pa]
$H$	height of porous medium	[m]
$K_{dyn}$	frequency dependant damping coefficient	[Ns/m]
$m$	mass of air inside bearing	[kg]
$M$	mass	[kg]
$p$	pressure	[Pa]
$p_s$	supply pressure	[Pa]
$p_a$	ambient pressure	[Pa]
$p_0$	pressure at perturbation point	[Pa]
$\tilde{p}$	perturbation pressure	[Pa]
$q$	flow speed	[m/s]
$R_s$	specific gas constant	[J /(kg K)]
$T$	Temperature	[K]
$x, y, z$	spatial coordinates inside material or in air film	[m]
$\epsilon$	porosity	[ ]
$\kappa_v$	viscous permeability coefficient	[m <sup>2</sup> ]
$\kappa_i$	inertial permeability coefficient	[m]
$K_v$	normalized viscous permeability coefficient	[m]
$K_i$	normalised permeability coefficient	[ ]
$\mu$	dynamic viscosity	[Pa s]
$\rho$	density	[kg /m <sup>3</sup> ]
$\omega$	perturbation frequency	[rad/s]

# 1

## Introduction

Air bearings are a vital component to high tech machines and have been in widespread use since the 1960s. They provide near frictionless motion, have high stiffness and a near infinite lifetime. Using air as an lubricant makes them suitable for very clean environments, which explains their popularity in semiconductor applications. The subject of this thesis are porous bearings, they are easy to manufacture compared to some other types of air bearings and have a high load capacity and stiffness for their size[12]. When designing porous air bearings special attention needs to be taken when selecting a porous material. As the choice of material has a large influence on both the static and dynamic characteristics of the bearing. This report focusses on the influence of the porosity on the dynamic characteristics of the bearing.

### 1.1. Construction and Operation

Aerostatic porous thrust bearings are very simple in their construction, requiring only a few components to operate. In Figure 1.1 a schematic representation of a porous thrust bearing is given. In the figure the relevant parts needed to make an air bearing can be seen: air supply, a housing and a block of porous material. The operation of the bearing relies on the fact that the air film underneath the bearing is very small. Because of the small gap the air encounters resistance against the flow. This causes the pressure to build up underneath the bearing and causes the bearing to float on a thin film of air.

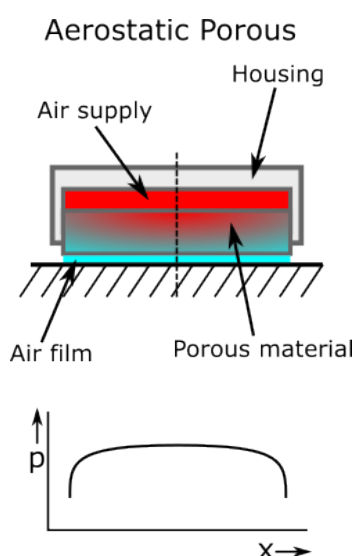


**Figure 1.1:** Schematic drawing of a circular porous bearing with the shape of the pressure profile underneath the bearing.

The resistance in the gap together with the resistance in the restrictor, can be approximated by a first order electrical analogy as can be seen in Figure 1.2. Using this analogy, the fundamental operation of the bearing can be explained. During the operation of the bearing, the air flows from the supply to the outside. Because the gap between the bearing and the counter-surface provides a resistance, the pressure underneath the bearing builds up allowing the bearing to float. As the resistance of the gap depends on the fly height, the pressure in the gap goes down as the bearing goes up. This coupling between the fly height and pressure is what gives the bearing stiffness.

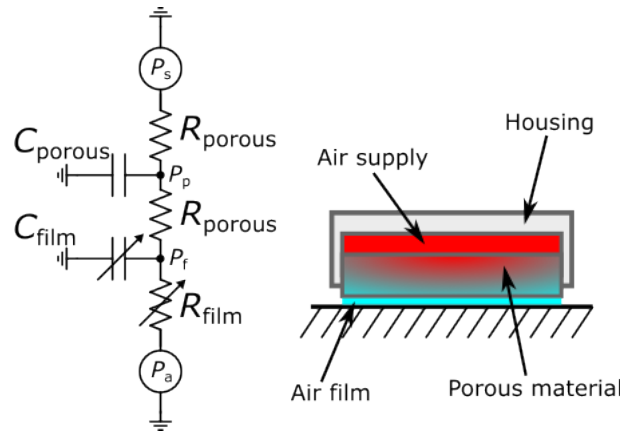


**Figure 1.2:** A first order electrical analogy of a porous air bearing.

Because the air is compressible, the pressure in the different parts of the bearing determines how much air is stored inside the bearing. In the electrical analogy this is represented by the capacitance. When the bearing changes height these capacitances in the material need to be filled or emptied, causing a delay on the system. To counter this effect a surface restrictive layer is often used. A schematic drawing of a bearing with and without a restrictive layer is shown in Figure 1.3. The idea behind this approach is to use a base material with a low resistance combined with a high resistance coating. This keeps the porous material at the supply pressure while the pressure drop occurs over the coating. This makes that the capacitance of the porous material has little to no influence on the dynamic behaviour of the bearing. Leading to a reduction in the lag compared to the uncoated bearing.

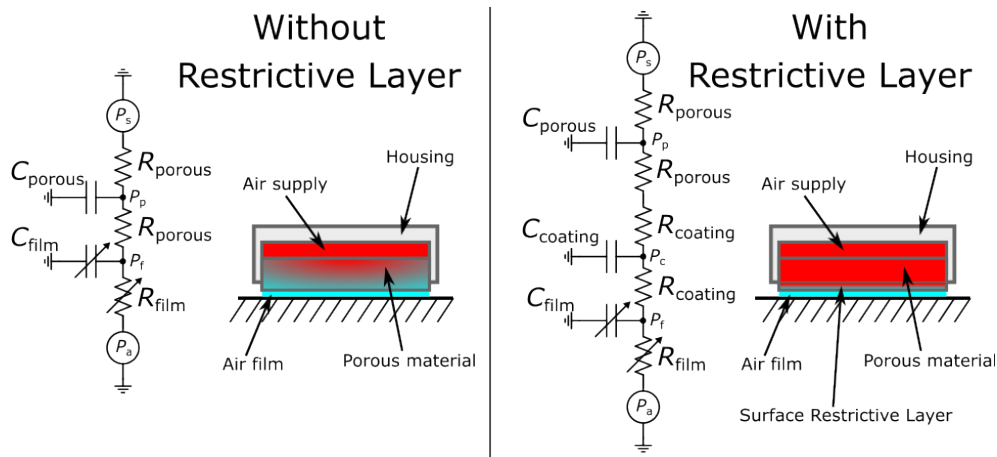


**Figure 1.3:** Schematic drawing of porous bearings with and without surface restrictive layer along with their first order electrical analogy

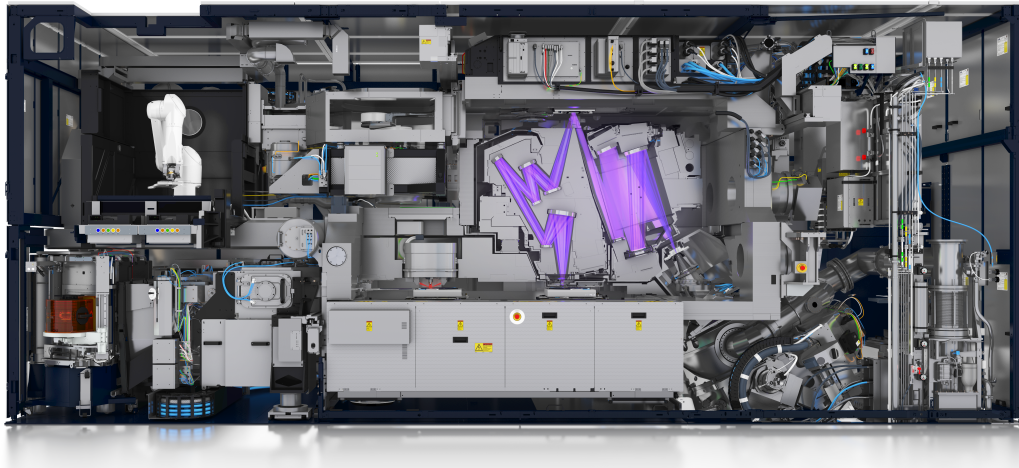


Figure 1.4: ASML NXE3400

## 1.2. Applications

Because porous air bearings need a constant supply of air they are not often found in everyday devices. However the specific combination of high stiffness, extremely low friction and a clean lubricant makes them popular in high precision, semiconductor and metrology applications such as the machines produced by ASML (Figure 1.4). High stiffness and low friction are necessary to achieve the positional accuracy needed for these machines to operate at nanometre resolution. Although the same stiffness can also be reached with hydrostatic bearings, the amount of friction is much higher. Also the use of a dirty lubricant like oil or water would increase the complexity of the machine because special care has to be taken to prevent contamination of the clean parts of the machine.

Another kind of application where air bearings are beneficial, is in high speed spindles, where the very low viscosity of gas makes very high speeds possible without high losses in friction. Because of the low friction losses these kinds of spindles can reach speeds upwards of 100.000 rpm allowing the use of very small tooling.

To give an idea of what is possible some examples of common types of porous bearings are shown below in Figures 1.5, 1.6, 1.7 and 1.8.



Figure 1.5: Example of a rectangular flat porous bearing by New Way Air Bearings [1]

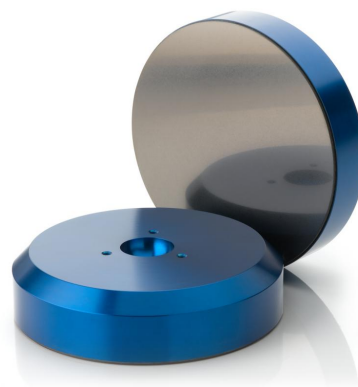


Figure 1.6: Example of a round flat porous bearing by New Way Air Bearings [1]



**Figure 1.7:** Example of a round porous bearing by Specialty Components [7]



**Figure 1.8:** Example of a spherical porous bearing by Specialty Components [6]

### 1.3. State of the Art

Development on models describing the static characteristics of porous air bearings started around the 1960s, while development of models describing dynamic characteristics started half way through the 1970s. A very good overview of the state of the art was given in 1998 by Kwan & Korbet [12].

As this thesis is not centered around the static characteristics of porous bearings, it won't be included in detail, a overview comparing different options for modelling the statics of the bearing is given by T.S. Luong et al [14]. In this paper different options are compared and validated for modelling the slip flow at the porous surface of the bearing along with different options for the flow in the porous material. Interestingly, Luong concludes that having information about the film thickness over the bearing surface is essential. Which in previous work in general is often regarded as constant. From this work and the previously mentioned state of the art we can conclude that, the static characteristics of porous air bearings are already very well documented and that differences between measurement and theory can generally be well explained. It thus makes sense to further investigate the dynamic characteristics.

Research on the dynamic characteristics of air bearings can be found as early as 1973 by Sun [29] for thrust bearings and in 1975 for journal bearings, also by Sun[30]. His work mainly focusses on obtaining a better understanding of the stability of porous bearings as they are known to have problems with instability. As noted in these papers, the instability is caused by the capacitance of the porous material cancelling out part of the squeeze film effect. Majumdar [15] follows in 1976 by using FDM to calculate the dynamic characteristics of a rectangular bearing. This is then expanded to journal bearings by Rao [25] in 1977 and is expanded [23] in 1978 to also include the tilt damping and stiffness. In 1979 Rao & Majumdar [24] published a paper on the stability of porous journal bearings. The first notion on validating the dynamic characteristics is Chang et al. [4] in 1983 investigating the stability of porous thrust bearings. In this paper the instability is compared against the theory from Sun[29]. In testing they determined that the discrepancy between theory and experiment was small at low supply pressures but high at high supply pressures. The discrepancy was determined to be due to the air in the plenum above the porous material oscillating with the pressure in the air film, in turn influencing the dynamic characteristics.

Chattopadhyay and Majumdar [5] in 1984 investigated the dynamic characteristics of journal bearings when velocity slip is taken into account. This was followed up by Majumdar and Majumdar [16][17] in 1988 investigating stability for both journal and thrust bearings considering velocity slip.



Very recent work on porous bearing dynamics focusses on modelling bearings with a surface-restricted layer. Starting with Yoshimoto and Kohn [32] looking at bearings with different shapes and sizes for the supply area. Interesting in this paper is that they do take into account the dynamic characteristics of the uncoated porous material but assume the coating to be ideal, having zero thickness and zero porosity. Miyatake et al. [18] investigated whirling instability in a coated bearing. In their paper the surface restricted layer is assumed to be very thin (10  $\mu\text{m}$ ) and the porosity to be the same as the base material. Yuta et al. [20] in 2010 investigated the dynamic characteristics of aerostatic porous journal bearings with a surface restrictive layer using the same thin coating assumption. A overview of modelling all kinds of air bearings is given by Al-Bender [3] in his book. For porous air bearings the theory is shown for a linear Darcy model including velocity slip.

## 1.4. Problem statement

From the mentioned papers above it's clear that there is already some information about porous bearing dynamic characteristics available. However, when studying them for the influence of the porosity, there is much less information available. In the paper from Majumdar [15] it is part of the normalized restrictor coefficient where only 2 values are considered. For most other papers the value is fixed. The only conclusion that can be drawn from all papers is that the porosity needs to be as low as possible. From the work of Yoshimoto it can be concluded that a surface restrictive layer provides a large improvement of the dynamic performance compared to a non coated bearing. The restrictive layer has a capacitance that is much lower than that of the uncoated bearings, decreasing the risk of instability. The choice for modelling the coating as having a very low capacitance however is not explained.

The method used to apply a surface restrictive layer is material dependent. For ductile materials it's possible to smear the pores at the surface closed, creating a high resistance layer. For brittle materials such as graphite this is not an option and a coating is utilized impregnating the top layer.

There is little information available on the performance of these coating stating the relation between penetration depth, porosity reduction and permeability reduction. A patent by Rasnick et al. [28] suggest that using an acrylic lacquer can give penetration depths between 25  $\mu\text{m}$  and 1.25 mm. A technical report by the same author [27] claims that the porosity of the coated layer is reduced by an order of magnitude. A discrepancy can thus be identified between the literature when modelling ideal coatings and coatings that can be realized in reality. As there are no papers or other literature available, there is no way to know if the porosity in the coating poses an issue or that the influence is so small that it can be neglected. There is a clear opportunity to make an improvement by looking into the topic to see what is possible and investigate in more detail the impact of material and coating on predicted dynamic performance.

## 1.5. Research objective

The following objectives are identified in this report:

- Create a COMSOL Multiphysics™ model capable of accurately predicting the dynamic characteristics of porous air bearings with and without a surface-restrictive layer.
- Determine the sensitivity of the porosity of the porous material and coating on the dynamic characteristics.
- Investigate the existence of other methods to evaluate indicators for detecting bearing designs that pose risks of inherent instability.
- Validate the model experimentally

## 1.6. Thesis Outline

This report will be structured in 3 parts. First, the theoretical models and methods used to calculate the bearing dynamic characteristics are introduced. Second, the mechanics behind the dynamic bearing characteristics are investigated. Lastly, a testcase is discussed with the goal of validating the model.

# 2

## Theoretical modelling

In this chapter all the theoretical and mathematical concepts are discussed that are required to model the dynamics of an air bearing. To start, the physical models are introduced that describe the flow within the thin film of air in the bearing gap and the flow within the porous material. Subsequently the models were perturbed to be able to determine the stiffness and damping as a function of frequency. After this, a couple of aspects are discussed that are required to use these equations. The solving strategy is discussed along with the post processing needed to extract the stiffness and damping coefficients. After this a very short introduction to stability is given. Lastly measuring the permeability and porosity is discussed which are required to model the dynamics of the air bearing.

### 2.1. Thin film flow

Thin film flow between two plates can be modelled by evaluating the full Navier-Stokes equations, but in practice this is often not necessary. For low flow speeds the flow is laminar, which allows for a simpler approach in the form of the Reynolds equation. The Reynolds equation will be introduced below and simplified by taking out all terms that are not important for low speed applications. After this, the equation will be modified using the ideal gas law to be suitable for modelling compressible gasses.

#### 2.1.1. Incompressible flow

The terms of the Reynolds equation [9] can be subdivided onto two groups describing the Poiseuille flow (pressure driven flow) and the Couette flow (flow between two moving plates). The general description of the Reynolds equation is given as follows:

$$\overbrace{\frac{\partial}{\partial x} \left( \frac{\rho h^3}{12\mu} \frac{\partial p}{\partial x} \right) + \frac{\partial}{\partial y} \left( \frac{\rho h^3}{12\mu} \frac{\partial p}{\partial y} \right)}^{\text{Poiseuille}} = \overbrace{\frac{\partial}{\partial x} \left( \frac{\rho h u}{2} \right) + \frac{\partial}{\partial y} \left( \frac{\rho h v}{2} \right)}^{\text{Couette}} + \frac{\partial}{\partial t}(\rho h) \quad (2.1)$$

Where  $h, p, \mu, \rho$  and  $t$  are height [m], pressure [Pa], viscosity [Pa s], density [kg/m<sup>3</sup>] and time [s]. Because the bearings studied in this report operate at low relative velocities between the bearing and the counter-surface, all terms regarding the Couette flow can be neglected resulting in the following simplified equation:

$$\frac{\partial}{\partial x} \left( \frac{\rho h^3}{12\mu} \frac{\partial p}{\partial x} \right) + \frac{\partial}{\partial y} \left( \frac{\rho h^3}{12\mu} \frac{\partial p}{\partial y} \right) = \frac{\partial}{\partial t}(\rho h) \quad (2.2)$$

### 2.1.2. Compressible flow

To use the Reynolds equation for compressible flow, a relation between pressure and density needs to be established. This is done by substituting the ideal gas law in to the simplified Reynolds equation. The ideal gas law is defined as follows:

$$\rho = \frac{p}{R_s T} \quad (2.3)$$

Where  $R_s$  is the specific gas constant in  $[J \text{ kg}^{-1} \text{ K}^{-1}]$  and  $T$  is the temperature in  $[K]$ . Substituting this into Equation 2.2 yields the following description for Reynolds including compressible flow:

$$\frac{\partial}{\partial x} \left( \frac{ph^3}{12\mu R_s T} \frac{\partial p}{\partial x} \right) + \frac{\partial}{\partial y} \left( \frac{ph^3}{12\mu R_s T} \frac{\partial p}{\partial y} \right) = \frac{p}{R_s T} \frac{\partial h}{\partial t} + h \frac{\partial}{\partial t} \left( \frac{p}{R_s T} \right) \quad (2.4)$$

The final simplification required is the assumption that the process is isothermal, thus treating  $T$  as a constant. This makes the model inaccurate for very high values of  $\frac{\partial h}{\partial t}$ , which is not a problem for most applications, but makes the model inaccurate for analyses with very fast changes in pressure. Optionally  $R_s T$  can be taken out completely. This results in the final general Reynolds equation used in this report:

$$\frac{\partial}{\partial x} \left( \frac{ph^3}{12\mu R_s T} \frac{\partial p}{\partial x} \right) + \frac{\partial}{\partial y} \left( \frac{ph^3}{12\mu R_s T} \frac{\partial p}{\partial y} \right) = \frac{p}{R_s T} \frac{\partial h}{\partial t} + \frac{h}{R_s T} \frac{\partial p}{\partial t} \quad (2.5)$$

This equation can be used to model the lubricating air film underneath the air bearing for both static situations (by setting the time derivatives to zero) and dynamic situations. A term that needs to be added, which is specific to modelling porous bearings, is the flow through the bearing surface. Resulting in the following description of Reynolds equation with added flow:

$$\frac{\partial}{\partial x} \left( \frac{ph^3}{12\mu R_s T} \frac{\partial p}{\partial x} \right) + \frac{\partial}{\partial y} \left( \frac{ph^3}{12\mu R_s T} \frac{\partial p}{\partial y} \right) = \frac{p}{R_s T} \frac{\partial h}{\partial t} + \frac{h}{R_s T} \frac{\partial p}{\partial t} - \frac{p}{R_s T} (q_x n_x + q_y n_y + q_z n_z) \quad (2.6)$$

In this equation  $q_x$ ,  $q_y$  and  $q_z$  are the flow velocity  $[m/s]$  inside the porous material and  $n_x$ ,  $n_y$  and  $n_z$  are the components of the normal vector to the bearing surface.

## 2.2. Porous flow

To model the flow inside the porous material two things are needed. The first is a way to model the resistance inside the material, which causes the pressure to drop over the material. The second is a model that describes storage inside the material.

### 2.2.1. Resistance model

Darcy's law is commonly used to model porous bearings. The model was originally proposed to study the flow of water through sand [8], but was later deemed to be quite suitable to model all kinds of flow through porous materials. The general Darcy flow in 1 direction is given as follows:

$$\frac{\partial p}{\partial z} = -\frac{\mu}{k} q_z \quad (2.7)$$

Where  $k$  is the permeability in  $[m^2]$  and  $q$  is the flow velocity in  $[m]$ . The permeability is a unit of how easy it is for the fluid to move through the material, a higher permeability leads to a lower drop in pressure. Because this equation assumes only laminar flow inside the material, it is only suitable for modelling very low fluid velocities. To fix this issue there are many models that add terms to the

Darcy equation to compensate for the inertial effects, adding resistance within the material. The most common model is the Darcy-Forchheimer equation:

$$\frac{dp}{dz} = -\frac{\mu}{k_v} q_z - \frac{\rho}{k_i} q_z |q_z| = -\frac{\mu}{k_v} q_z - \frac{p}{k_i R_s T} q_z |q_z| \quad (2.8)$$

This model replaces the single permeability coefficient  $q$  with two coefficients  $q_v$  and  $q_i$ , representing the viscous and inertial components.

For the implementation of the resistance model in a 3D situation, it is required to consider conservation of mass. For static situations the balance of mass flow entering and leaving any point needs to be zero, which can also be defined as divergence of the mass flow field needing to be zero.

$$\frac{\partial}{\partial x} \left( \frac{p}{R_s T} q_x \right) + \frac{\partial}{\partial y} \left( \frac{p}{R_s T} q_y \right) + \frac{\partial}{\partial z} \left( \frac{p}{R_s T} q_z \right) = 0 \quad (2.9)$$

### 2.2.2. Storage model

The equation for conservation of mass in the previous section has no dependence on time, because the storage in the porous material is neglected. This makes the model only suitable for studying the static flow through the material or when looking at non compressible fluids, and thus not sufficient for the application described in this report. The stored air inside the material per unit volume can be calculated by multiplying the density with the porosity, where the density is given by the ideal gas law (Equation 2.3).

$$\frac{m}{V} = \epsilon \rho = \epsilon \frac{p}{R_s T} \quad (2.10)$$

Where  $\epsilon$  represents the porosity and is a number between zero and one describing the void fraction. Thus a material with zero porosity is a solid block, while a material with porosity one is pure void. Adding the derivative with respect to pressure to Equation 2.9, yields the following description for the mass flow in a porous material:

$$\frac{\partial}{\partial x} \left( \frac{p}{R_s T} q_x \right) + \frac{\partial}{\partial y} \left( \frac{p}{R_s T} q_y \right) + \frac{\partial}{\partial z} \left( \frac{p}{R_s T} q_z \right) = -\frac{\epsilon}{R_s T} \frac{\partial p}{\partial t} \quad (2.11)$$

## 2.3. Perturbation

Using the above models it is possible to model the system in the time domain. To make it easier to analyse the dynamics of a system, it is desired to investigate the system in the frequency domain. Due to the non-linear behaviour of the system, it is not possible to do a fourier transformation of the system directly. The solution is to linearize the system around an operating point. This is done by introducing a small complex perturbation in the fly height and studying the perturbed pressure response. To execute the perturbation it is needed to define some equations to substitute into the dynamic equations. First the flying height and the time derivative of the flying height is defined as giving the input to the system. The linearisation point is represented by  $h_0$  and the perturbation by  $\tilde{h} = \hat{h}e^{i\omega t}$  where  $\hat{h}$  is the amplitude of the perturbation:

$$h = h_0 + \hat{h}e^{i\omega t} \quad (2.12)$$

$$\frac{\partial h}{\partial t} = \frac{\partial h_0}{\partial t} + \hat{h}i\omega e^{i\omega t} \quad (2.13)$$

The variables  $q_x$ ,  $q_y$ ,  $q_z$  and  $p$  are perturbed in a similar fashion and function as intermediary variables and output of the system.

All of these equations can be simplified further by choosing the static solution for the linearisation point, thus making the time derivative in the operating point zero. Also a substitution is made for  $\hat{h}e^{i\omega t}$  and  $\tilde{p}e^{i\omega t}$  with  $\tilde{h}$  and  $\tilde{p}$ . Resulting in the following equations for the perturbation of the height.

$$h = h_0 + \tilde{h} \quad (2.14)$$

$$\frac{\partial h}{\partial t} = \tilde{h}i\omega \quad (2.15)$$

This procedure is repeated for  $q_x$ ,  $q_y$ ,  $q_z$  and  $p$  to get all the perturbed variables.

### 2.3.1. Perturbation thin film flow

Substituting the perturbed variables in the simplified Reynolds equation (2.6) results in the following equation:

$$\begin{aligned} \frac{\partial}{\partial x} \left( \frac{(p_0 + \tilde{p})(h_0 + \tilde{h})^3}{12\mu R_s T} \left( \frac{\partial p_0}{\partial x} + \frac{\partial \tilde{p}}{\partial x} \right) \right) + \frac{\partial}{\partial y} \left( \frac{(p_0 + \tilde{p})(h_0 + \tilde{h})^3}{12\mu R_s T} \left( \frac{\partial p_0}{\partial y} + \frac{\partial \tilde{p}}{\partial y} \right) \right) = \\ \frac{p_0 + \tilde{p}}{R_s T} \tilde{h} i \omega + \frac{h_0 + \tilde{h}}{R_s T} \tilde{p} i \omega - \frac{p_0 + \tilde{p}}{R_s T} ((q_{x0} + \tilde{q}_x)n_x + (q_{y0} + \tilde{q}_y)n_y + (q_{z0} + \tilde{q}_z)n_z) \end{aligned} \quad (2.16)$$

This solution can be evaluated at this stage to find the perturbed solution, but often two more steps are performed to reduce the amount of calculation time required. First, the static solution is subtracted from the equation. It is equal to zero by its definition as it is the solution to the static Equation 2.2, since the operating point was chosen to be a solution of that equation. This results in the following adjusted description of the perturbed Reynolds equation:

$$\begin{aligned} \frac{\partial}{\partial x} \left( \frac{(p_0 + \tilde{p})(h_0 + \tilde{h})^3}{12\mu R_s T} \left( \frac{\partial p_0}{\partial x} + \frac{\partial \tilde{p}}{\partial x} \right) - \frac{p_0 h_0^3}{12\mu R_s T} \frac{\partial p_0}{\partial x} \right) + \\ \frac{\partial}{\partial y} \left( \frac{(p_0 + \tilde{p})(h_0 + \tilde{h})^3}{12\mu R_s T} \left( \frac{\partial p_0}{\partial y} + \frac{\partial \tilde{p}}{\partial y} \right) - \frac{p_0 h_0^3}{12\mu R_s T} \frac{\partial p_0}{\partial y} \right) = \\ \frac{1}{R_s T} \left( \tilde{p} h_0 i \omega + p_0 \tilde{h} + 2\tilde{p} \tilde{h} i \omega - (p_0 \tilde{q}_x + \tilde{p} q_{x0} + \tilde{p} \tilde{q}_x) n_x - (p_0 \tilde{q}_y + \tilde{p} q_{y0} + \tilde{p} \tilde{q}_y) n_y - (p_0 \tilde{q}_z + \tilde{p} q_{z0} + \tilde{p} \tilde{q}_z) n_z \right) \end{aligned} \quad (2.17)$$

Optionally this equation can be simplified by taking out all higher order terms of  $\tilde{h}$  and  $\tilde{p}$  as they are assumed to be very small and have little influence on the final result. This results in a linear system of equations which can be directly solved.

### 2.3.2. Perturbation porous flow

To get to the perturbed equations for the flow through the porous material, the perturbed variables are substituted in Equation 2.8:

$$\frac{\partial p_0}{\partial z} + \frac{\partial \tilde{p}}{\partial z} = -\frac{\mu}{k_v} (q_{z0} + \tilde{q}_z) - \frac{p_0 + \tilde{p}}{k_i R_s T} (q_{z0} + \tilde{q}_z) |q_{z0} + \tilde{q}_z| \quad (2.18)$$

To simplify this equation the static solution is subtracted from the equation. Note that there remain a lot of term of the static solution in this equation, due to the absolute signs resulting in:

$$\frac{\partial \tilde{p}}{\partial z} = -\frac{\mu}{k_v} \tilde{q}_z - \frac{p_0 + \tilde{p}}{k_i R_s T} (q_{z0} + \tilde{q}_z) |q_{z0} + \tilde{q}_z| - \frac{p_0}{k_i R_s T} q_{z0} |q_{z0}| \quad (2.19)$$

Subsequently, the conservation of mass Equation 2.9 for the porous material can also be perturbed, resulting in the following:

$$\begin{aligned} \frac{\partial}{\partial x} \left( \frac{1}{R_s T} (p_0 + \tilde{p})(q_{x0} + \tilde{q}_x) \right) + \frac{\partial}{\partial y} \left( \frac{1}{R_s T} (p_0 + \tilde{p})(q_{y0} + \tilde{q}_y) \right) + \\ \frac{\partial}{\partial z} \left( \frac{1}{R_s T} (p_0 + \tilde{p})(q_{z0} + \tilde{q}_z) \right) = -\frac{\epsilon}{R_s T} (p_0 + \tilde{p}) \end{aligned} \quad (2.20)$$

By subtracting the stationary solution, the following complete perturbed equation of the flow in the porous material including the storage term can be defined:

$$\begin{aligned} \frac{\partial}{\partial x} \left( \frac{1}{R_s T} (p_0 \tilde{q}_x + \tilde{p} q_{x0} + \tilde{p} \tilde{q}_x) \right) + \frac{\partial}{\partial y} \left( \frac{1}{R_s T} (p_0 \tilde{q}_y + \tilde{p} q_{y0} + \tilde{p} \tilde{q}_y) \right) + \\ \frac{\partial}{\partial z} \left( \frac{1}{R_s T} (p_0 \tilde{q}_z + \tilde{p} q_{z0} + \tilde{p} \tilde{q}_z) \right) = -\frac{\epsilon}{R_s T} \tilde{p} \end{aligned} \quad (2.21)$$

## 2.4. Solving

Solving the problem is a two part process. First, the static equations are evaluated along with their boundary conditions to establish the pressure distribution at the operating point. Subsequently, the perturbed equations are solved using the data from the static solution. An overview of the two problems can be seen in Figure 2.1. Next, the boundary conditions will be discussed followed by the solving strategy used to evaluate the expressions. The post processing can then be defined to extract the stiffness and damping coefficients from the perturbed pressure.

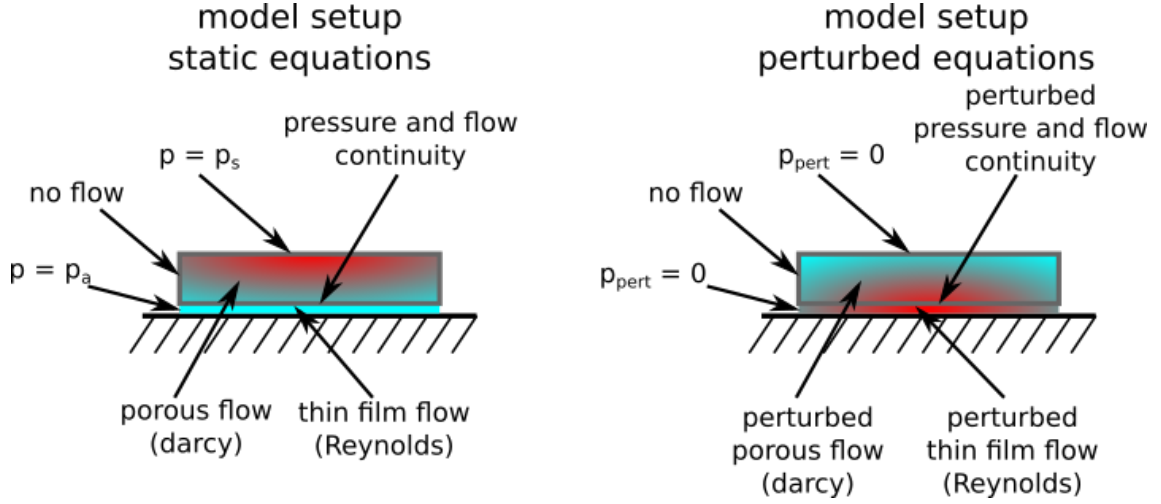


Figure 2.1: An overview of the problem setup with the boundary conditions.

### 2.4.1. Boundary conditions

#### Thin film boundary conditions

For the static solution, the Reynolds equation contains two boundary conditions. The first condition is that the pressure at the edge of the film is equal to the ambient pressure:

$$p|_{\Omega} = p_{\text{ambient}} \quad (2.22)$$

The second boundary condition is that a source term is added where the porous material and the thin film meet. This term is already introduced in Equation 2.6. It can also be implemented as a boundary condition, when a bearing with a partial porous surface is modelled. In this term the flow that is normal to the surface of the porous material is added to the flow in the thin film. At this boundary  $\vec{q}$  is the flow vector and  $\vec{n}$  is the normal vector to the surface of the porous material.

$$\text{source}|_{\Omega} = -\frac{p}{R_s T} (q_x n_x + q_y n_y + q_z n_z)|_{\Omega} \quad (2.23)$$

For the perturbed solution two more boundary conditions have to be added to make the system solvable. The first condition is set at the edges of the boundary, where we previously stated that the pressure was equal to the ambient pressure. The condition is that the perturbed pressure is equal to zero:

$$\tilde{p}|_{\Omega} = 0 \quad (2.24)$$

The second condition is to add a source term to the perturbed Reynolds equation to make sure that the perturbed flow is taken into account in the equation as well, similar to the source term added to the non perturbed equation:

$$\text{source}|_{\Omega} = \frac{1}{R_s T} (-(p_0 \tilde{q}_x + \tilde{p} q_{x0} + \tilde{p} \tilde{q}_x) n_x - (p_0 \tilde{q}_y + \tilde{p} q_{y0} + \tilde{p} \tilde{q}_y) n_y - (p_0 \tilde{q}_z + \tilde{p} q_{z0} + \tilde{p} \tilde{q}_z) n_z)|_{\Omega} \quad (2.25)$$

### 2.4.2. Porous flow boundary conditions

For the static solution of the Darcy equation it is needed to specify three boundary conditions. The first condition is that the pressure at the supply side of the bearing is equal to the supply pressure.

$$p|_{\Omega} = p_s \quad (2.26)$$

The second condition is that the pressure at the surface, where the Reynolds equation is evaluated, the pressure in the thin film and the pressure in the porous material should be equal:

$$p_{porous}|_{\Omega} = p_{film} \quad (2.27)$$

The third boundary condition is based on the fact that it is customary to seal the sides of the bearing with epoxy resin to block the airflow. A conditions is added that the flow normal to the surface has to be equal to zero:

$$-q_x n_x - q_y n_y - q_z n_z|_{\Omega} = \vec{q} \cdot \vec{n}|_{\Omega} = 0 \quad (2.28)$$

For the perturbed Darcy's equation three boundary conditions are needed as well. The first is that the perturbed pressure at the feeding surface is equal to zero:

$$\tilde{p}|_{\Omega} = 0 \quad (2.29)$$

The second boundary condition is that the perturbed pressure at the surface, where the Reynolds equations is evaluated, is equal to the perturbed pressure in the thin film:

$$p_{porous}^{\sim}|_{\Omega} = p_{film_{pert}} \quad (2.30)$$

The third boundary condition is that the perturbed flow at the sealed surfaces is equal to zero.

$$-\tilde{q}_x n_x - \tilde{q}_y n_y - \tilde{q}_z n_z|_{\Omega} = \vec{\tilde{q}} \cdot \vec{n}|_{\Omega} = 0 \quad (2.31)$$

### 2.4.3. Solving strategy

To solve the system of equations, they were implemented in COMSOL Multiphysics™ and solved in two separate steps. First, all the static equations are solved with their boundary conditions (Equations: 2.6, 2.8, 2.9, 2.22, 2.23, 2.26, 2.27, 2.28) as one fully coupled system, followed by a loop in which the perturbed equations with their boundary conditions (Equations: 2.17, 2.19, 2.21, 2.24, 2.25, 2.29, 2.30, 2.31) are solved for different values of the perturbation frequency as a fully coupled system. Solving the system as a fully coupled system forces the solver to solve all the equations at once, instead of taking steps first solving Reynolds then Darcy. The stopping criteria for both steps is that the error needs to be lower than 0.001. As this is the recommended setting, setting a smaller error has little to no effect on the results. A schematic of this procedure can be seen in Figure 2.2:

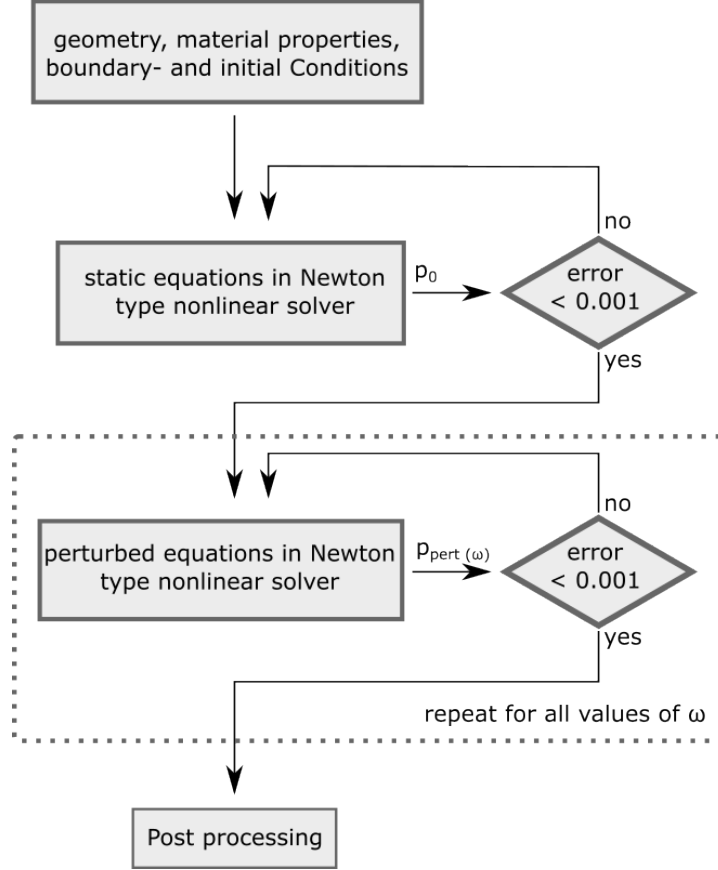


Figure 2.2: Schematic of solution procedure

### 2.4.4. Post processing of the results

The resulting output of the model is a perturbed pressure field present in the air bearing and in the porous material. These perturbed pressure profiles are very hard to interpret as is, thus the information has to be simplified to make it easier to see what the behaviour of the system is. The bearing can be simplified by introducing an equivalent frequency dependent spring and damper. This is done by integrating the perturbed pressure over the entire surface of the bearing. This result is then divided in two parts: the part of the response that is 180 degrees out of phase with the movement representing the spring and the part that is -90 degrees out of phase with the movement representing the damper. From here the stiffness and the damping coefficient can be calculated by evaluating the following equations:

$$K_{\text{dynamic}}(\omega) = \frac{-\text{Re} \left( \iint_A (\tilde{p}) dA \right)}{\tilde{h}} \quad (2.32)$$



$$D_{\text{dynamic}}(\omega) = \frac{-\text{Im} \left( \iint_A (\tilde{p}) dA \right)}{\tilde{h}i\omega} \quad (2.33)$$

## 2.5. Stability

Checking the stability of a system can be done in many ways, some methods use the time domain description others the frequency domain. In this report the Nyquist criterion is used, which is evaluated in the frequency domain. As will be demonstrated in this section, for simple systems the loop transfer functions can quite easily be derived. For more complex systems a very similar approach can be used as demonstrated by Plessers and Snoeys [22].

### 2.5.1. System dynamics

The frequency dependent stiffness and damping can be used to evaluate the stability of a system in which an air bearing is present. In this section the stability of a one degree of freedom mass spring damper system is evaluated, in which a bearing is represented by the spring and the damper. A schematic drawing of this simple system can be seen in Figure 2.3. To evaluate the stability using the Nyquist criterion the open-loop transfer function is required. This open loop transfer function can be derived from the equations of motion and using the Fourier transform or by using a block diagram like Figure 2.4. This block diagram can be used by comparing it to Figure 2.5. From the comparison Equation 2.34 is derived, which is the open loop function of this system. This function represents the coupling of the system back on itself. By using Bode or Nyquist plots this open loop can give a lot of information about the closed loop behaviour of the system.

$$L(\omega) = \frac{1}{M} \left( D(\omega) \frac{1}{i\omega} + K(\omega) \frac{1}{(i\omega)^2} \right) = \frac{1}{M} \left( -D(\omega) \frac{i}{\omega} - K(\omega) \frac{1}{\omega^2} \right) \quad (2.34)$$

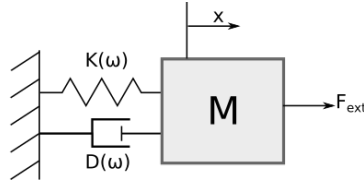


Figure 2.3: Simple 1DOF mass spring damper system

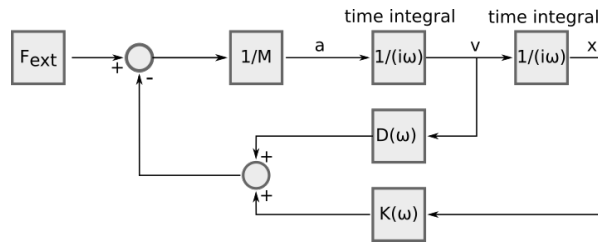


Figure 2.4: Block diagram of mass spring damper system

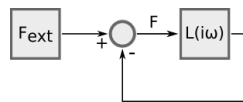


Figure 2.5: Definition of loop transfer function

### 2.5.2. Nyquist criterion

To evaluate stability the Nyquist criterion is used to see if the system is stable. The criterion states that if the open loop transfer function is plotted in the real versus imaginary plane for all frequencies starting from  $-\infty$  until  $\infty$ . The curve cannot encircle the point -1 in a clockwise motion. In practice it is not needed to look at all frequencies, only the ones that are surrounding the crossover frequency. To check for stability in these relatively simple 1D systems, it is only needed to check if the Nyquist plot passes above or below the -1 point. If the system passes below the point -1 the system is stable. If it passes above the point -1 it is unstable. Note that for more complex systems the assessment might be more complex, as systems containing more complex dynamics they can cross the circle more than once. An example of a stable and an unstable system can be seen in Figure 2.6.

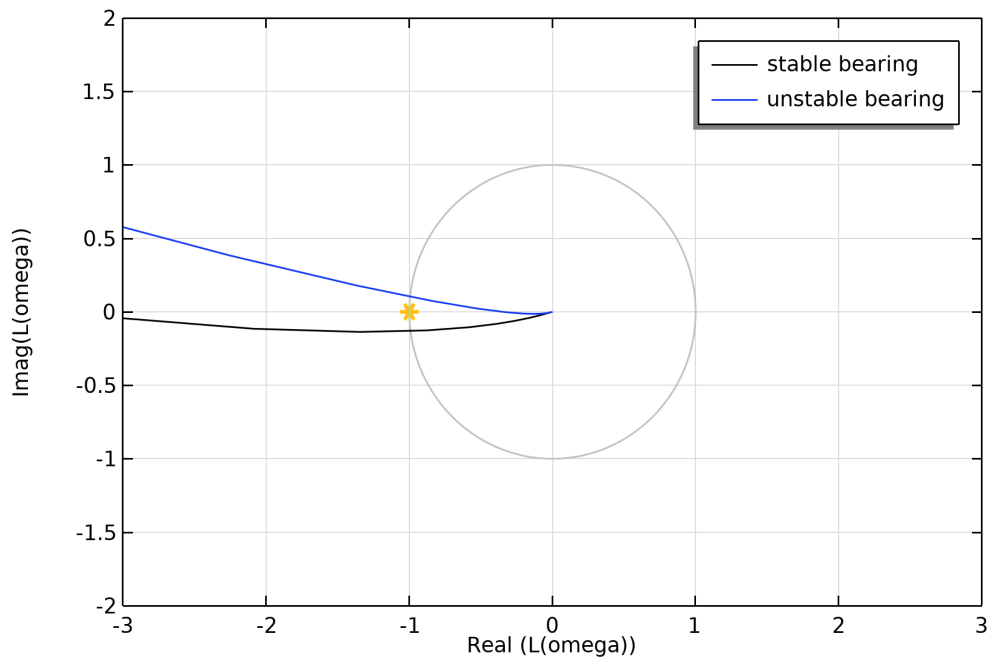
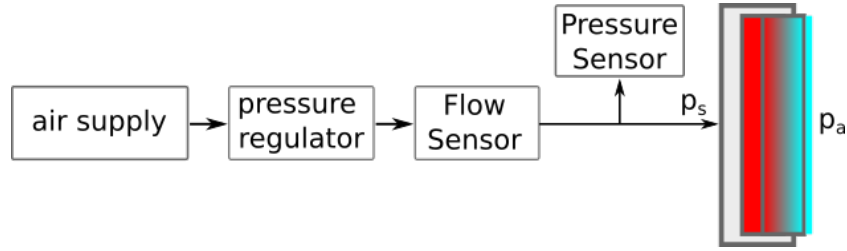


Figure 2.6: Example Nyquist Plot

## 2.6. Determine permeability coefficients from pressure and flow data for multi-layer bearings



**Figure 2.7:** Test setup for measuring permeability coefficients.

Measuring the permeability of an air bearing can be done using a relatively simple setup, using a pressure regulator and a flow sensor. The flow without a counter-surface is used to estimate the viscous and inertial permeability coefficients:  $\kappa_v$  and  $\kappa_i$ . A schematic of the measurement setup can be seen in Figure 2.7. Using this setup a sweep is made of the supply pressure and the resulting flow through the bearing is recorded. This data is then processed using the Darcy-Forchheimer equations for compressible flow as described by Kwan [11]:

$$\frac{p_s^2 - p_a^2}{2p_{ref}} = \frac{H\mu(Q/A)}{\kappa_v} + \frac{H\rho(Q/A)^2}{\kappa_i} \quad (2.35)$$

Where  $H$  is the height of the porous material in [m],  $A$  is the surface area of the bearing in [m<sup>2</sup>],  $Q$  the volumetric flow in [m<sup>3</sup>],  $\mu$  the dynamic viscosity in [Pa s] and  $\rho$  the density of the gas [kg/m<sup>3</sup>] at the reference pressure  $p_{ref}$ .

In these formula's it's possible to substitute normalized permeability defined as:

$$K_v = \kappa_v / H \quad (2.36)$$

$$K_i = \kappa_i / H \quad (2.37)$$

Substituting these into Equation 2.35 and rearranging terms yields the following general description:

$$\frac{p_s^2 - p_a^2}{2p_{ref}} = \frac{1}{K_v} \mu(Q/A) + \frac{1}{K_i} \rho(Q/A)^2 \quad (2.38)$$

As this equation is now in the form  $y = \beta_1 a + \beta_2 b$  the problem can be easily solved, as it is a linear equation with two unknowns. To average out any errors it's recommended to use a least squares estimator to determine the two permeability coefficients.

For multiple layers, which occurs when bearings are coated with the goal of improving stability [20] [18], a method is needed to determine the normalized permeability of the individual layers. To determine the normalized permeabilities of multiple layers it's necessary to do more measurements on the same bearing before and after the addition of a new layer. For this example it is assumed there are two layers. The pressure drop over the total bearing is the sum of the individual pressure drops. Evaluating Equation 2.35 for each layer and adding them together results in the following equation:

$$\frac{p_s^2 - p_a^2}{2p_{ref}} = \left( \frac{1}{K_{v1}} + \frac{1}{K_{v2}} \right) \mu(Q/A) + \left( \frac{1}{K_{i1}} + \frac{1}{K_{i2}} \right) \rho(Q/A)^2 \quad (2.39)$$

Where  $K_{v1}$  and  $K_{i1}$  are the normalized permeability coefficients of layer one and  $K_{v2}$  and  $K_{i2}$  are the coefficients of layer two. From this it can be seen that for a multilayer bearing the  $1/K_v$  and  $1/K_i$  of each layer can be added up to give the total normalized permeability. This means that it is possible to determine the normalized permeabilities for any number of layers, as long as they are added one by one, by measuring after each layer is added.

$$\frac{1}{K_{v_{total}}} = \frac{1}{K_{v_1}} + \frac{1}{K_{v_2}} + \dots + \frac{1}{K_{v_n}} \quad (2.40)$$

$$\frac{1}{K_{i_{total}}} = \frac{1}{K_{i_1}} + \frac{1}{K_{i_2}} + \dots + \frac{1}{K_{i_n}} \quad (2.41)$$

This works well if a layer is added to the material leaving the previous layer as is. But when coating a graphite bearing the coating gets drawn into the material thus replacing part of the porous material with a more dense layer. As long as the coating is relatively thin compared to the base material this is no problem, but as soon as the layer is no longer a small fraction of the base material a correction has to be made. This correction can be defined as follows:

$$K_{v_{(base \text{ after coating})}} = K_{v_{(total \text{ before coating})}} \frac{H_{base}}{H_{base} - H_{coating}} \quad (2.42)$$

$$K_{i_{(base \text{ after coating})}} = K_{i_{(total \text{ before coating})}} \frac{H_{base}}{H_{base} - H_{coating}} \quad (2.43)$$

Using the now corrected normalized permeability of the base material, it's possible to calculate the normalized permeability of the coating using Equation 2.40 and 2.41.

$$\frac{1}{K_{v_{(coating)}}} = \frac{1}{K_{v_{(total \text{ after coating})}}} - \frac{1}{K_{v_{(base \text{ after coating})}}} \quad (2.44)$$

$$\frac{1}{K_{i_{(coating)}}} = \frac{1}{K_{i_{(total \text{ after coating})}}} - \frac{1}{K_{i_{(base \text{ after coating})}}} \quad (2.45)$$

To conclude, the total workflow from start to finish is as follows. First, use the measurement set-up presented in Figure 2.7 to collect flow and pressure data before and after coating the bearing. Use the pressure and flow data from the experiment to evaluate Equation 2.39, preferably using a least squares estimate, to determine the total normalized permeability coefficients. After this the total normalized permeabilities before and after coating can be used to calculate the permeabilities of the individual layers using Equations 2.42, 2.43, 2.44 and 2.45.

## 2.7. Measuring porosity

Having an exact measurement of the open porosity is essential to determine the dynamic properties of an air bearing. There are many ways of determining the porosity, if only an average measurement is required [31]. Examples of methods that can measure the average open porosity are imbibition methods and the gas expansion method. The first is using a liquid to fill the pores of the sample. By comparing the weight before and after filling, the porosity can be calculated. The second uses a sealed container in which the sample is placed. The volume of the container can be changed and by looking at the increase and decrease in pressure, the volume of the air in the container can be calculated. The porosity can be derived from the volume of air inside the container compared to the volume of the empty container.

For measuring the local porosity in the sample the options are more involved. Optical measurements require the sample to be taken apart in small layers to take a look at the porosity [33]. This is not practical for measuring bearings as they are destroyed during the process, but can be used for model verification. Computer tomography (CT) scanning [2] is possible for porous graphite and is non-destructive, but is a rather expensive measurement at the resolutions required to map all pores in the material.

# 3

## Mechanics

In this chapter a explanation will be given on the mechanics behind porous bearings and how the porosity of the bearing influences the dynamic behaviour. The chapter is structured as follows: first, a short introduction is given to the equivalent spring damper model that is used to represent the dynamic behaviour of the bearing. Second the role of different parts of the bearing is discussed on the dynamic performance of the bearing. Third the mechanics and benefits of applying a surface restrictive layer are discussed. All examples given in this chapter use a fictional thrust bearing which can be found in appendix A.

### 3.1. Equivalent spring damper model

To improve the ease of interpretation of the dynamic behaviour the bearing dynamics are often expressed as a spring damper system. With stiffness  $K_{dyn}$  and damping coefficient  $D_{dyn}$ . These coefficients can be calculated from the perturbed pressure field, by using Equations 3.1 and 3.2.

$$K_{dyn}(\omega) = \frac{-Re \left( \iint_S (\tilde{p}) dS \right)}{\tilde{h}} \quad (3.1)$$

$$D_{dyn}(\omega) = \frac{-Im \left( \iint_S (\tilde{p}) dS \right)}{\tilde{h}i\omega} \quad (3.2)$$

In these equations the perturbed pressure is integrated over the surface of the bearing to get the force and then divided by the amplitude of the perturbation. When done for the real part of the perturbed pressure field this gives the stiffness of the bearing. When done for the out of phase (imaginary) part this give the damping coefficient.

It is possible for air bearings to have a negative damping coefficient [3]. This means that the pressure response is lagging behind the displacement of the bearing. This is problematic because this means that unlike a system with a positive damping coefficient, where the damping takes energy out of the system, the air bearing is adding energy. This unstable behaviour is known as pneumatic hammer.

### 3.2. Damping in porous air bearings

To answer how damping is created in a porous air bearing, it is needed to understand that the amount of air in the bearing changes as a function of the pressure. Which in turn relies on the resistances imposed by the porous material and the film underneath the bearing. While when a incompressible fluid is used as a lubricant the mass in the system is a simple function of the fly height:

$$m = \rho A(\epsilon H + h) \quad (3.3)$$

Where  $\rho$  is the density of the fluid [ $\text{kg/m}^3$ ],  $\epsilon$  is the porosity[],  $H$  is the height of the porous material[m],  $h$  is the flying height[m]. When looking at the derivative of the mass with respect to the flying height it is constant and always positive. Meaning that as the bearing goes down mass is squeezed out of the system and when the bearing goes up mass needs to be added to the system. As this mass cannot be squeezed out instantaneously and encounters resistance on the way out of the bearing it requires extra force. This effect is known as the squeeze-film effect [21] and adds a lead to the pressure response, which is seen in the system as damping.

When using gas as a lubricant the total amount of mass in the bearing is no longer a simple function of the flying height:

$$m = \iiint_V (\epsilon \rho) dV + \iint_A (\rho h) dA \quad (3.4)$$

Substituting the ideal gas law as described in Equation 2.3 gives us:

$$m = \iiint_V \left( \epsilon \frac{p}{R_s T} \right) dV + \iint_A \left( h \frac{p}{R_s T} \right) dA \quad (3.5)$$

As the pressure distribution influences the density there is no easy solution for these integrals, as can be seen in Figure 3.1. Going down in the flying height now has multiple contributions to the amount of air in the system. The first contribution is due to the porous material going up in pressure, which means that extra air needs to be added to this part of the bearing. The second contribution is to the film which goes up in pressure, which means that there will be more air stored per unit volume. Last the volume of the air gap is reduced, which means that less air is needed to reach the desired pressure. These three contributions are displayed in Figure 3.2 and depending on the relationship between them the pressure has either a lead or a lag on the displacement.

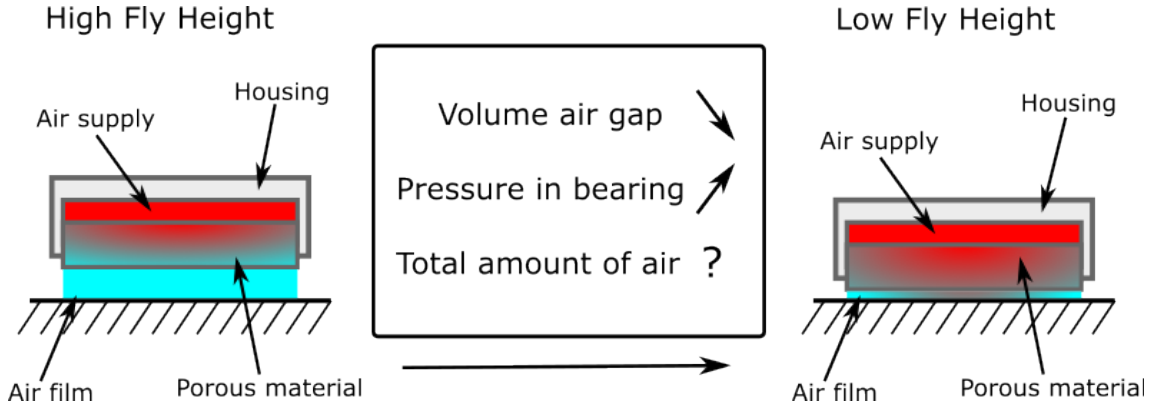


Figure 3.1: Impact of a change in height on the pressure and mass in the system

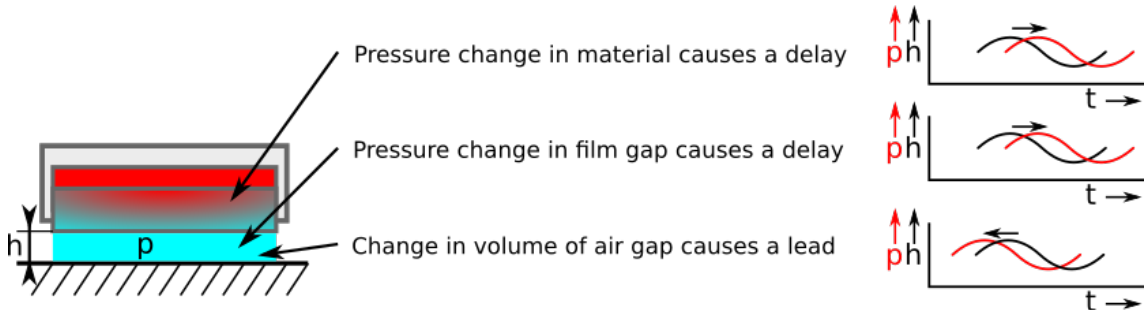
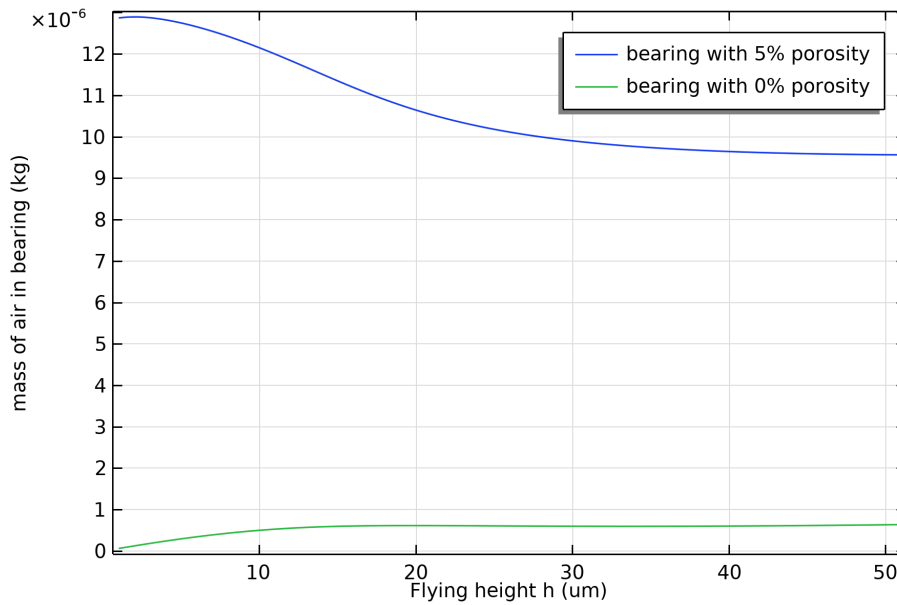


Figure 3.2: Impact of the different parts of the bearing on the pressure response of the bearing.

To show how this works in practice the amount of mass inside a bearings is shown in Figure 3.3 for 0% and 5% porosity for different flying heights, using the baseline bearing described in appendix A. For a stable bearing it's important that as the flying height goes up, so does the mass. From the figure it's clear that for a bearing with porosity this is not the case, indicating negative damping at low frequencies. It also becomes clear that this is not the ideal way to look at this data, as the slope is only of interest. The analysis is much clearer to understand looking at the derivative of the mass with respect to the flying height as shown in Figure 3.4.



**Figure 3.3:** mass of air in the bearing as a function of the flying height with and without porosity

In figure 3.4 the data is more clear and it also shows nicely that having zero porosity is no guarantee for positive damping. The air-film on it's own can cause negative damping at low frequencies.

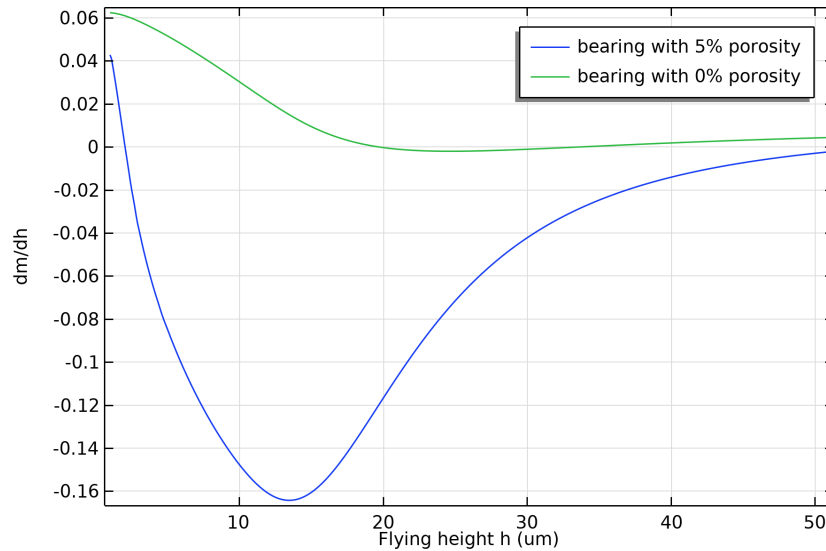


**Figure 3.4:** derivative of air in the system as a function of the flying height with and without porosity

When mapping the derivative of the mass with respect to the fly height for different fly heights and porosities, it becomes clear that there is very little room for the bearing to operate without low frequency negative damping. Only for very low fly heights and porosity there is positive damping. From Figure 3.5 it can be seen that for very high fly heights there is also a stable region but in these regions there is hardly any load capacity, thus it is unpractical to design a bearing that operates under these conditions.

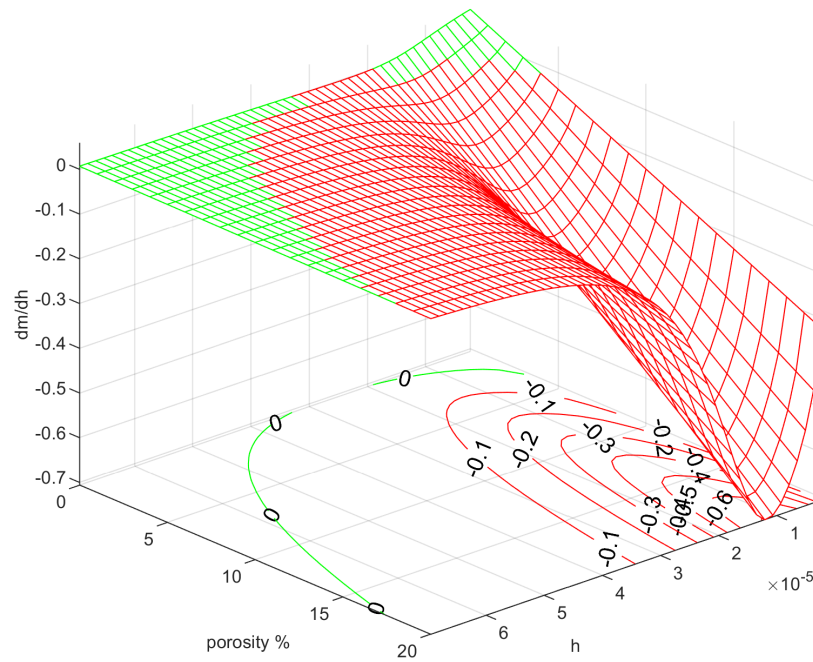


**Figure 3.5:**  $dm/dh$  mapped as a function of fly height (m) and porosity



### 3.2.1. Accuracy and limitations of using $dm/dh$ vs calculating the damping coefficient

As the relationship between  $dm/dh$  and the damping coefficient is quite complex, it can be expected that there is a error between the two. This discrepancy can be seen in Figure 3.6. From this plot it can be seen that while the lines are close, there are some small differences. In practice this means that having a positive  $dm/dh$  is not a guarantee that the bearing will have positive damping but it's a good indicator. This also means that there is no substitution for evaluating the perturbed equations for critical applications. This discrepancy is caused by the inability of using the mass as an indicator to take into account air that is redistributed within the bearing. Having the total mass in the system staying the same as a function of the fly height doesn't mean that the pressure distribution stays the same.

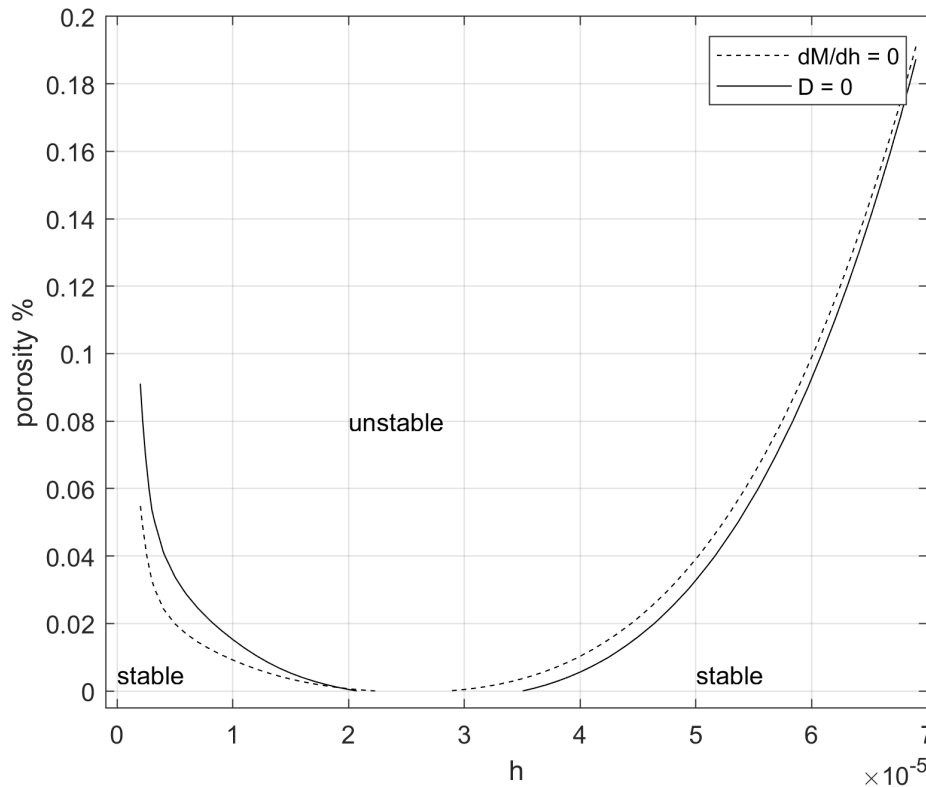


**Figure 3.6:** Comparing  $dm/dh = 0$  and calculating the  $D=0$  line using the perturbed equations

Another limitation is that using the mass only works for to relatively simple flat bearings where the description of the bearing height as a function of a coordinate  $\beta$  can be described as  $h(x, y, \beta) = C(x, y) + \beta$ . In other words, the change in gap height has to be constant over the entire surface of the bearing. This makes this method unsuitable for analysing radial or any other kind of bearing where gap height is a more complex function. When analysing systems containing more than one bearing. The analysis has to be done for each bearing individually. Only if all bearings have positive damping for all frequencies the system is certainly stable. In case one or multiple bearings showing signs of negative damping the full system dynamics has to be evaluated to ensure stability.

### 3.3. Sensitivity of porosity on the dynamic behaviour

To investigate the influence of the porosity on the dynamics, the baseline bearing which can be found in appendix A is used. In Figures 3.7 and 3.8 the dynamic performance is plotted for different porosities ranging from 0 to 20%. From these figures we can see that decreasing the porosity has a large effect on the dynamics of the bearing. For low frequencies decreasing the porosity improves damping and for high frequencies the stiffness is increased.

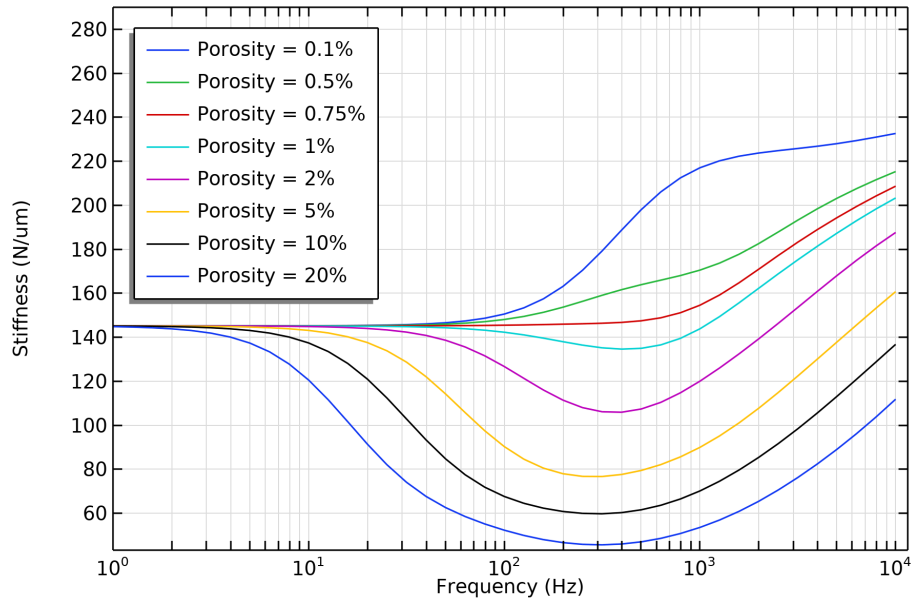


**Figure 3.7:** dynamic stiffness of baseline bearing around fly height of 13  $\mu\text{m}$  for different porosities.

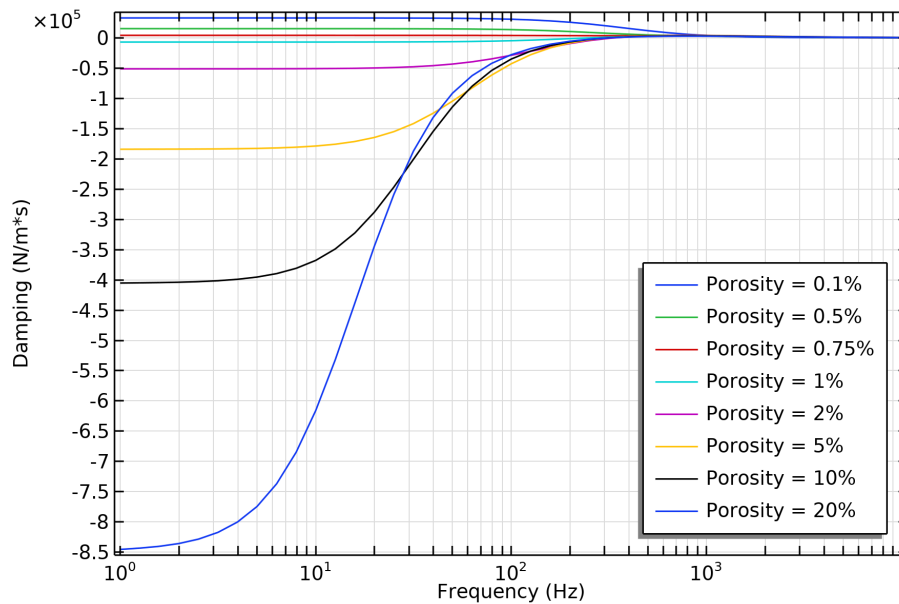


**Figure 3.8:** dynamic damping of baseline bearing around fly height of 13  $\mu\text{m}$  for different porosities.

In Figure 3.9 the zero or low frequency damping is plotted as a function of the porosity. From this figure it becomes clear that there is a linear dependency of the porosity on the low frequency damping of the bearing. From this plot it also becomes clear that the design proposed in appendix A is not very good from a dynamics point of view. As it will be difficult to find a material in practice with the presented specifications for the permeability while also having less than one percent porosity.

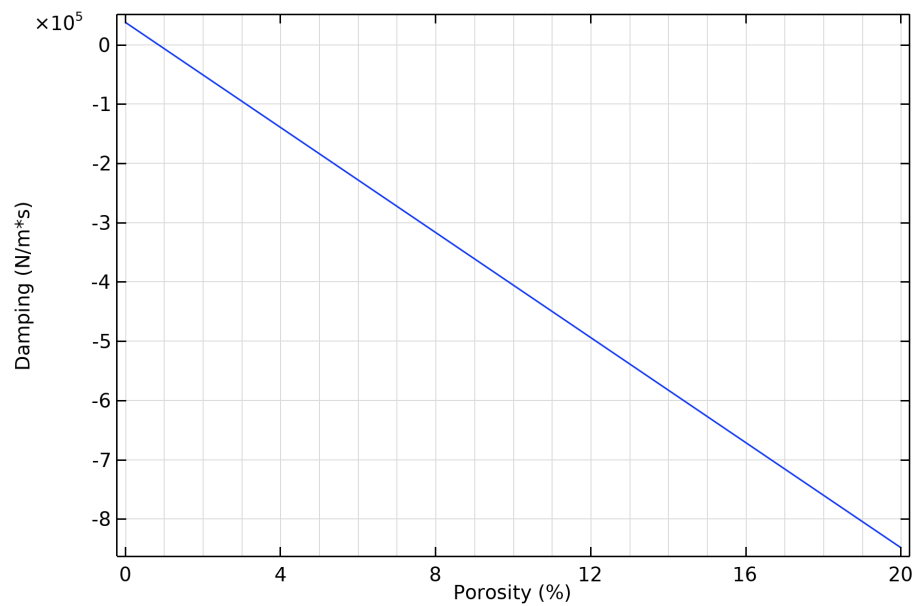


**Figure 3.9:** dynamic damping of baseline bearing around flying height of 13  $\mu\text{m}$  for different porosities at low frequency.

### 3.4. Improve dynamics with a surface restrictive layer

To improve the dynamics of the bearing a surface restrictive layer is often used. To understand why this works it is important to first look if there are other ways of improving the bearing without a coating than by reducing the porosity. In the work of Majumdar [15] only one nondimensionalized parameter contains the porosity of the bearing, this parameter is called the restrictor coefficient and it describes the dynamic behaviour of the material:

$$\gamma = \frac{\epsilon H^2}{12k} = \underbrace{(\epsilon H)}_1 \underbrace{(H/k)}_2 \frac{1}{12} \quad (3.6)$$

Where  $\epsilon$  is the porosity[],  $H$  is the height of the porous material [m] and  $k$  is the permeability of the material[m<sup>2</sup>]. It is possible to split the equation in two parts having a physical meaning. Part one is the amount of volume the bearing contains per unit area of the bearing surface and part two is the total resistance of the bearing per unit area. The first part plays no role in the static characteristics of the bearing while the second term does influence the static characteristics. Majumdar states that a lower value for the restrictor coefficient yields better dynamic performance. Assuming that the static behaviour of the bearing needs to remain the same, meaning  $H/k$  cannot change. It is possible to reduce  $\gamma$  by reducing the height of the porous material  $H$ , as long as  $k$  is also decreased in order to compensate. A reduction in height and porosity of 50% can be seen in Figures 3.10 and 3.11.

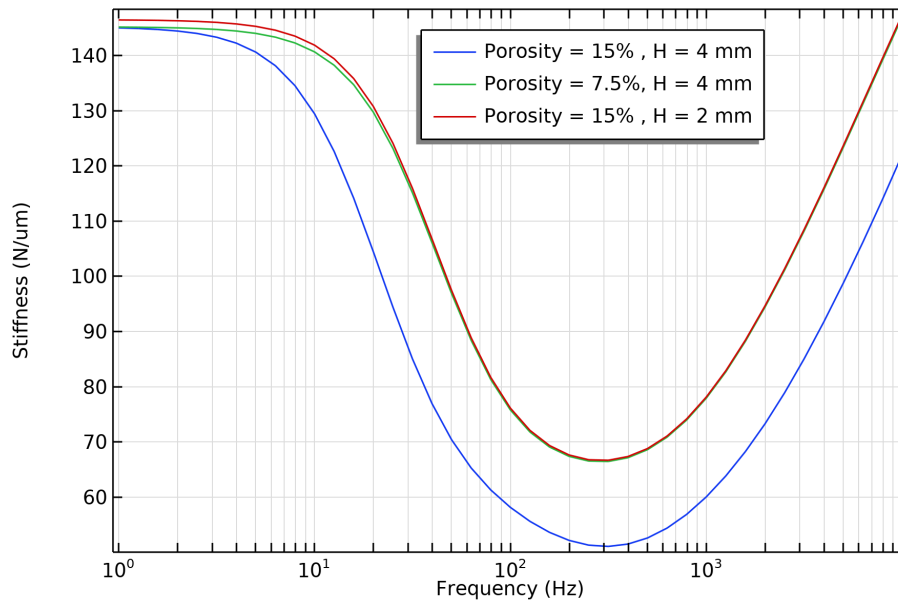


**Figure 3.10:** dynamic stiffness of baseline bearing around fly height of 13  $\mu\text{m}$ , comparing a 50% reduction in height and porosity while keeping the normalized permeability the same.

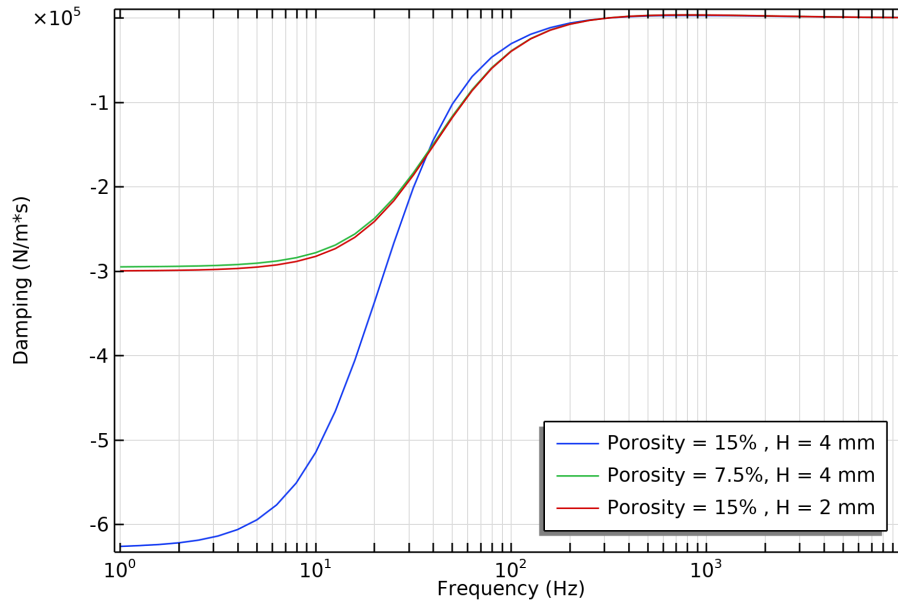


**Figure 3.11:** dynamic damping of baseline bearing around fly height of 13  $\mu\text{m}$ , comparing a 50% reduction in height and porosity while keeping the normalized permeability the same.

From these figures it can be observed that there are more options than just reducing the porosity to increase the dynamic performance. If a material is used with a lower permeability combined with a lower height of the porous material the same effect can be achieved. In practice this approach also has its limitations as a very thin layer or membrane has little mechanical stiffness and thus keeping the bearing surface flat may become an issue. The solution is to combine a base material with a high permeability, which acts as an air distribution layer and provides mechanical support, with a surface restrictive layer. The surface restrictive layer provides the resistance necessary for the operation of the bearing and ideally has a very low internal volume. In Figure 3.12 a electrical analogy is given for a uncoated and a coated bearing. If the difference in resistances is sufficiently high between the porous material and the coating, the pressure inside the base material should remain close to the supply pressure while the pressure drop occurs inside the coating. This also results in the perturbed pressure having much less influence on the pressure inside the base material. Which results in the capacitance of the base material having much less influence on the dynamics of the bearing.

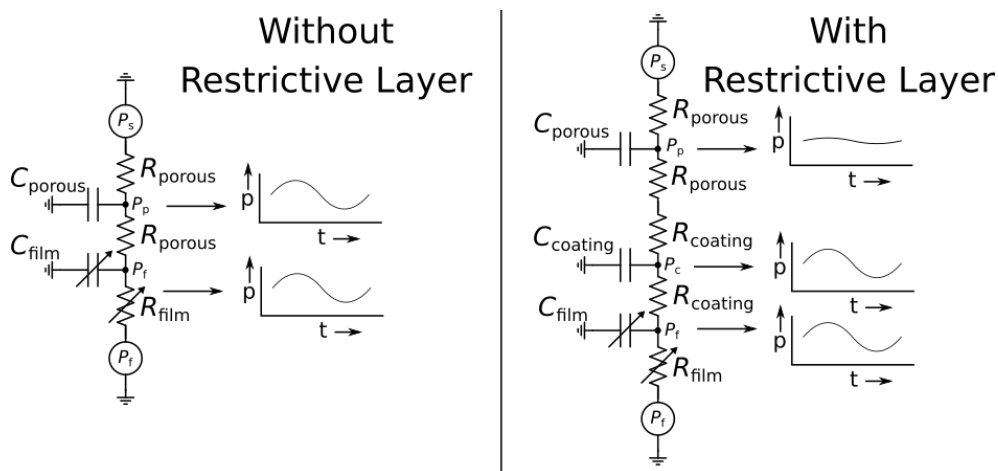


**Figure 3.12:** Schematic drawing of difference in perturbation pressure for uncoated and coated bearings

In Figures 3.13 and 3.14 the difference in the perturbed pressure response can be seen for a uncoated bearing and a coated bearing. In the uncoated bearing the perturbed pressure influences the pressure in the entire bearing, leading to a large amount of volume that needs to respond to a change in the film height. In the coated bearing the perturbed pressure influences the coating to the same extent that it does in the uncoated bearing, but the base material sees a greatly reduced change in pressure leading to less lag.

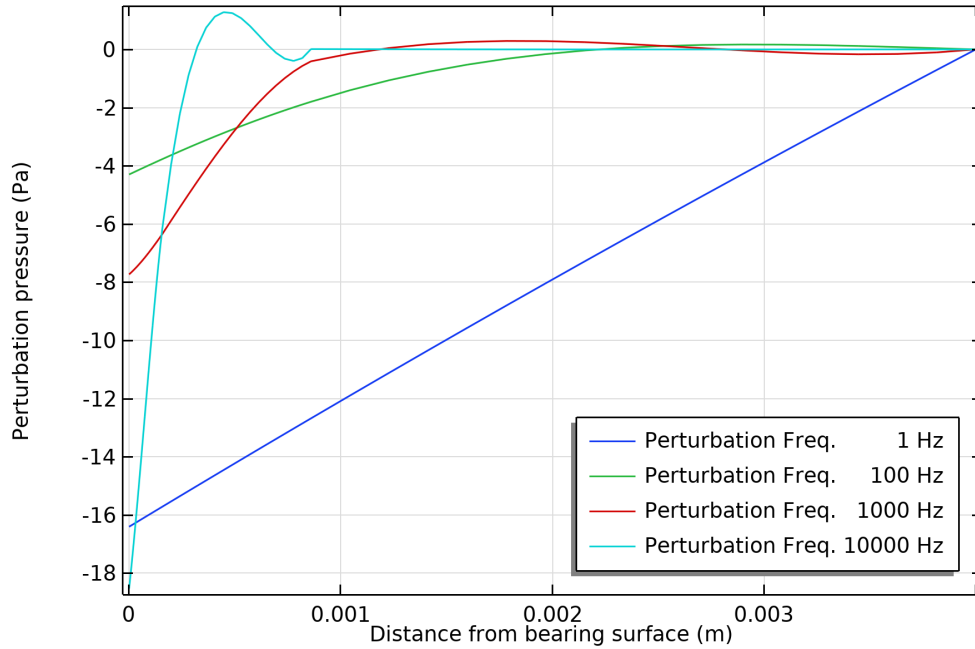


**Figure 3.13:** The perturbed pressure inside the material for a uncoated bearing in the middle of the bearing.

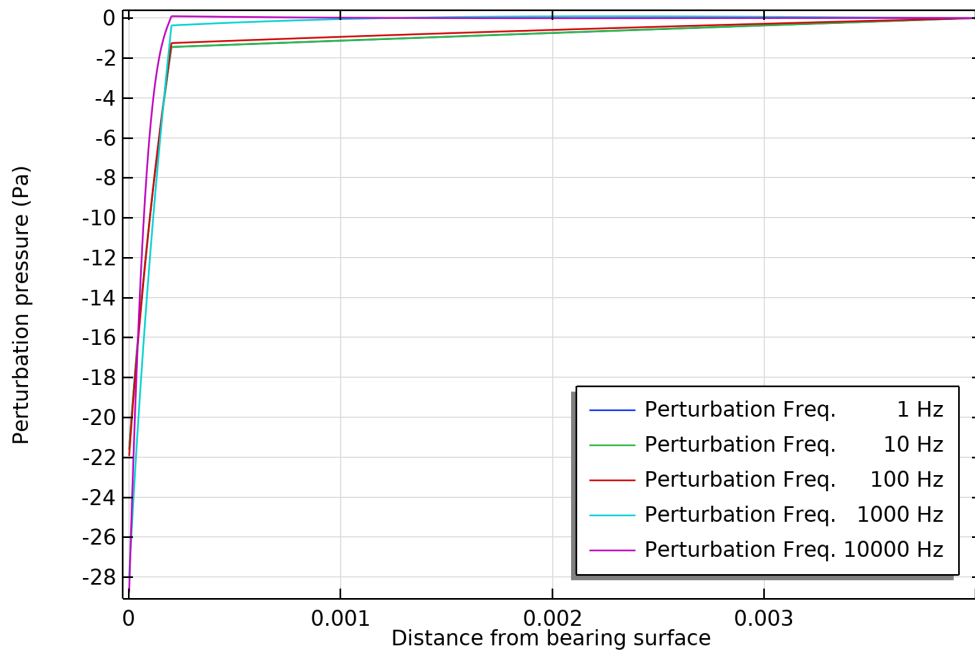


**Figure 3.14:** The perturbed pressure inside the material for a uncoated bearing in the middle of the bearing with a 0.2 mm surface restrictive layer which reduces the normalized permeability to 25% compared to the uncoated base material.

### 3.4.1. Addition of a surface restrictive layer with a change in static performance

A solution to fix unstable bearings is to add a coating to the existing bearing to improve the dynamic response of the bearing. This coating reduces the total normalized permeability and thus will influence the static performance of the bearing. By applying a coating the permeability and porosity at the surface of the bearing is reduced, creating a situation that is close to the optimal solutions found in the previous section. Because the porous material now supplies a lower contribution to the total resistance, it also contributes less to the dynamics of the bearing. Based on the literature surrounding the application of coatings [28][26][27] some assumptions were made: the coating is assumed to be around 100  $\mu\text{m}$  thick and the porosity is reduced by 10 times to 1.3% compared to the base material.

### 3.4.2. Static performance with reduced normalized total permeability

First we have to address that the static characteristics of the bearings is going to change with the addition of a coating if the base material remains unchanged. The altered bearing performance has been plotted in Figure 3.15. From the uncoated performance the operating point was chosen at 13  $\mu\text{m}$  because this is the optimal point in terms of the static stiffness being the highest. At this point the load capacity is around 2.5 kN. The assumption is made that the load needs to remain the same thus the operating point is adjusted for the different reductions in normalized permeability in order to have the same load capacity.

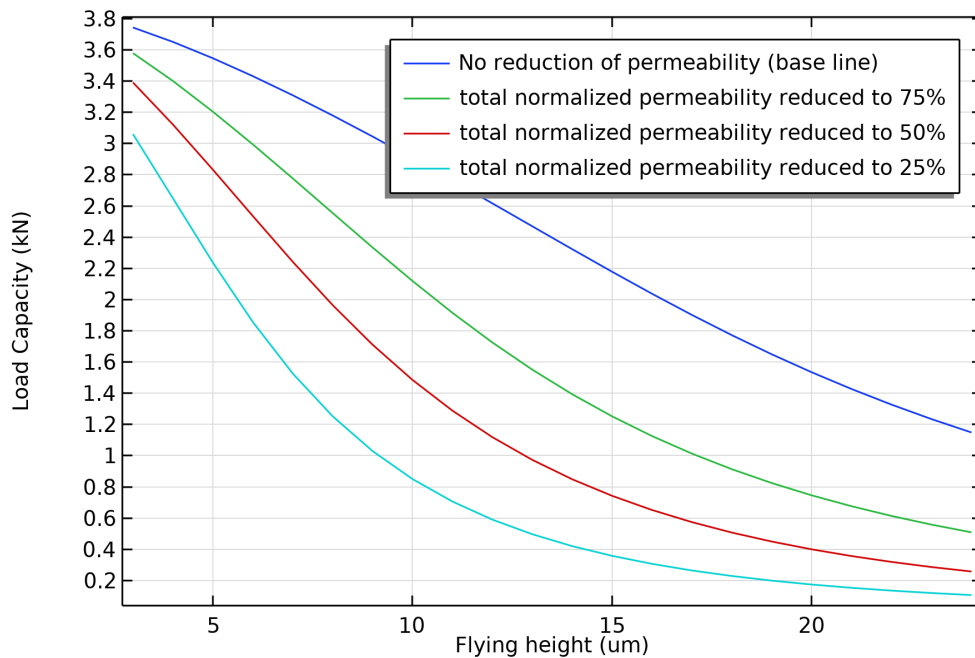


**Figure 3.15:** Load capacity of bearing for different reductions of the total permeability by applying a coating.

### 3.4.3. Dynamic performance with reduced total normalized permeability

The dynamic performance of the bearings at their new operating points is plotted in Figures 3.16 and 3.17. As we can see from the figures applying a coating to the surface of a unstable bearing to make it stable is an effective technique. It decreases the amount of volume that has to be filled within the porous material to react to a change in pressure, it also decreases the flying height of the bearing which increases the amount of squeeze film damping. It is clear that this method can be successful, it depends on the application if it's possible to use this kind of a approach because of change in static performance. In practice this might not be a ideal solution, as very low flying heights requires higher tolerances in manufacturing.

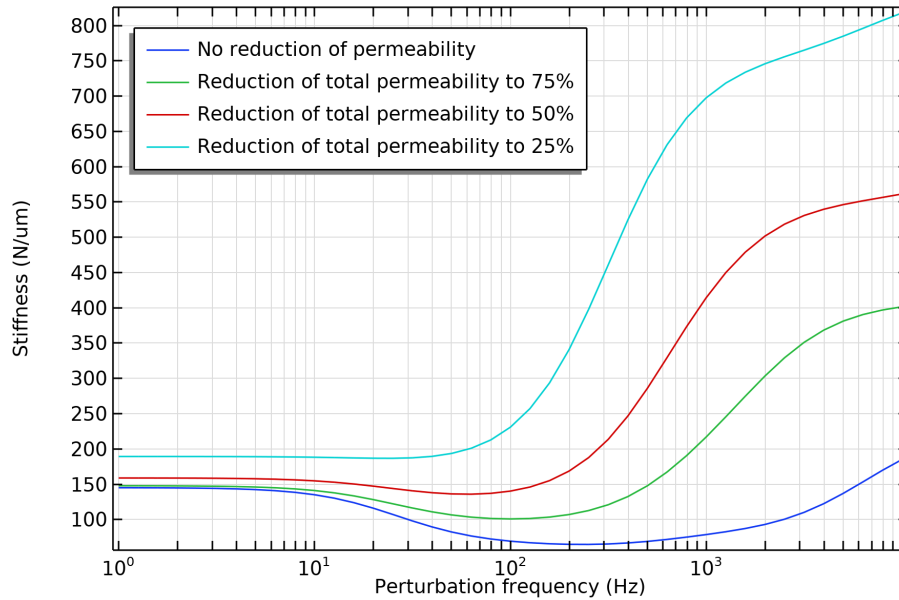


**Figure 3.16:** dynamic stiffness of coated bearing around the new operating point for different amounts of reduction of the permeability.

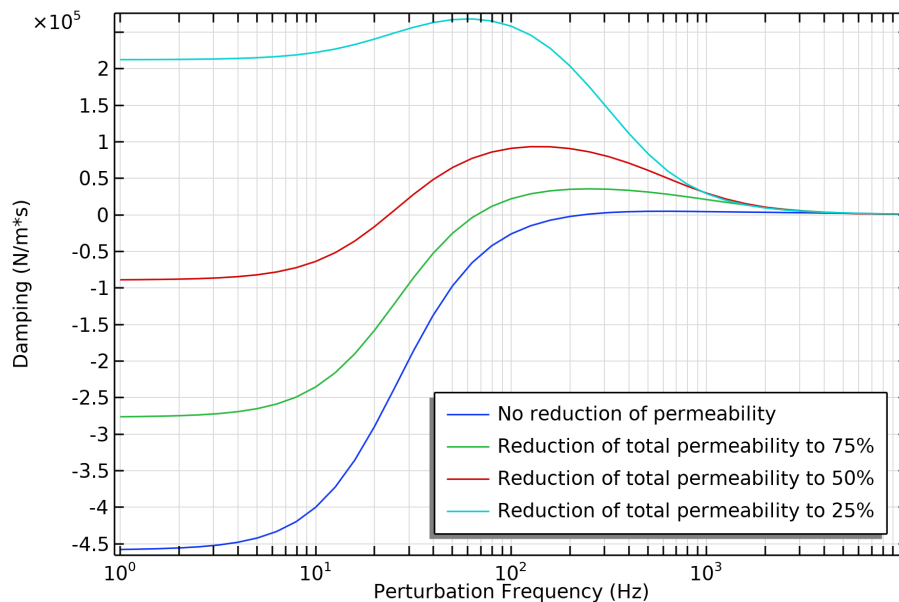


**Figure 3.17:** dynamic damping of coated bearing around the new operating point for different amounts of reduction of the permeability.



### 3.5. Addition of a surface restrictive layer without a change in static performance

From the previous example it can be seen that it is possible to improve the dynamic performance of the bearing by applying a coating to the surface of the bearing. The downside of the previous method, applying the coating as an afterthought, is that it changes the total normalized permeability and thus the static characteristics of the bearing as well. To change the dynamic performance without impacting the static performance it's necessary to keep the total normalized permeability constant when varying the amount of reduction of the coating. This requires the permeability of the base material to increase to compensate for the low permeability of the coating. The coating is assumed to be 100  $\mu\text{m}$  thick and the porosity in the coating is reduced by a factor of 10 to 1.3% compared to the base material. The limitation of this approach is that it has to be taken into account during the design of the bearing. The results of this approach applied to the test bearing found in appendix A can be seen in Figures 3.18 and 3.19.

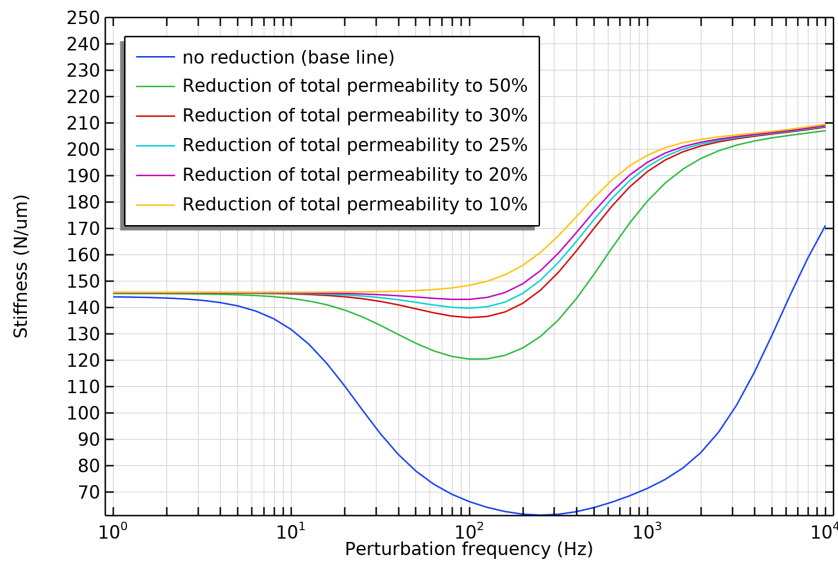


**Figure 3.18:** dynamic stiffness of coated bearing with different amounts of reduction but the same total permeability.

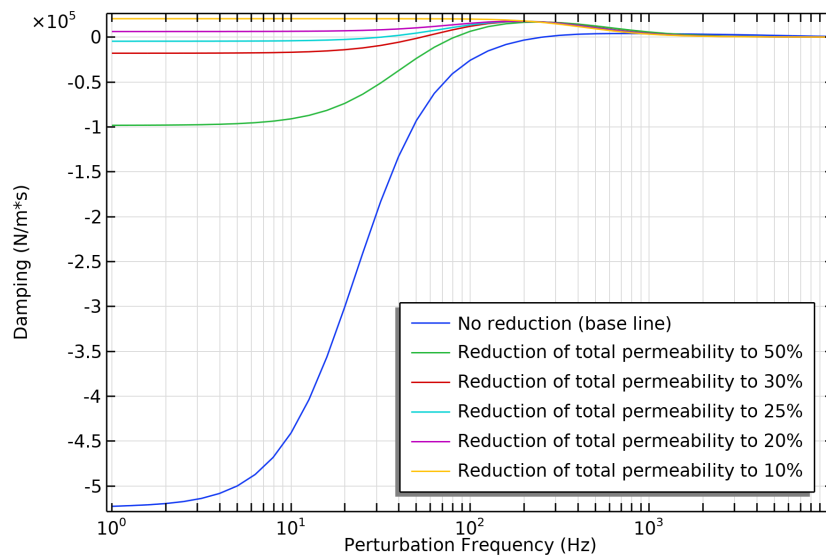


**Figure 3.19:** dynamic damping of coated bearing with different amounts of reduction but the same total permeability.

In Figure 3.20 a range of values is plotted for the permeability reduction of the coating and the amount of volume inside the bearing. It can be seen that for the baseline bearing a base material with at least five to ten times the normalized permeability is required compared to the normalized permeability of the coating. If for example it is possible to create a coating with a thickness of around 100  $\mu\text{m}$  and 10% porosity with a reduction of around 10 times, this would yield a bearing with positive damping for all frequencies.

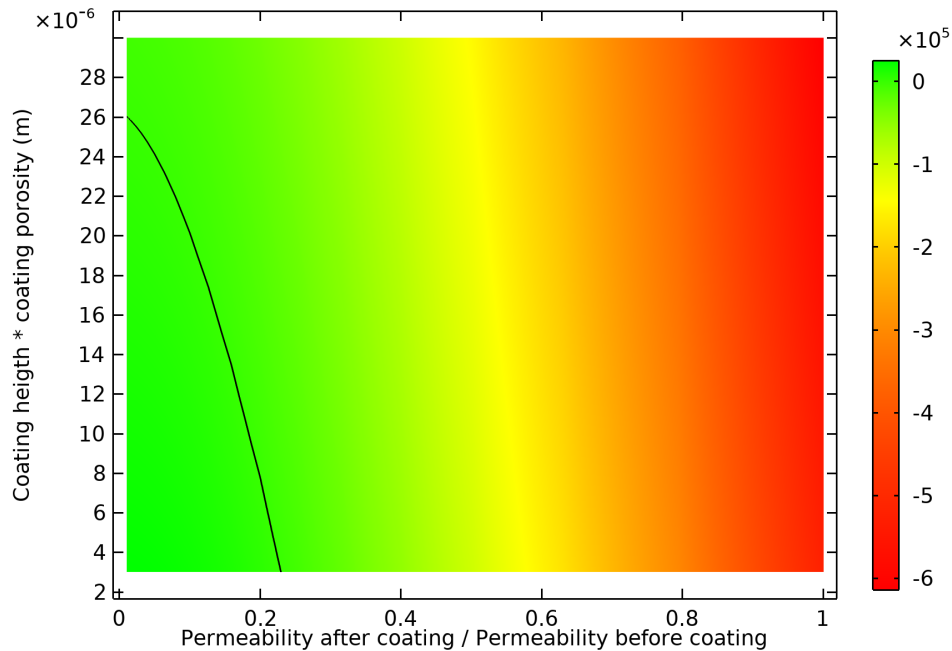


**Figure 3.20:** low frequency damping  $[\text{N}/(\text{m s})]$  of a coated bearing with the same total normalized permeability but a different ratio between the normalized permeability before and after coating and different amounts of volume per unit area inside the coating. (the black line is the edge between negative and positive damping)

# 4

## Case Study

To verify the accuracy of the model a existing dataset of 5 bearings was used. The bearing operating conditions were changed until instability was observed. Using the model of the bearing a comparison between predicted and observed instability was made.

### 4.1. Measurement set-up

A schematic drawing of the test setup used in this experiment can be seen in Figure 4.1. It consists of a load-cell with the bearing mounted upside down on top of it and a pneumatic cylinder supplying the load. The pneumatic cylinder has linear guides based on air bearings to keep the friction to a minimum. To measure the gap underneath the bearing two Tesa probes are used to measure the displacement of the bearing housing and two capacitance sensors are used to measure the displacement of the counter-surface. By calculating the difference between these two sensors the gap height can be calculated. Accelerometers were added to the set-up to better measure the moment where instability occurs.

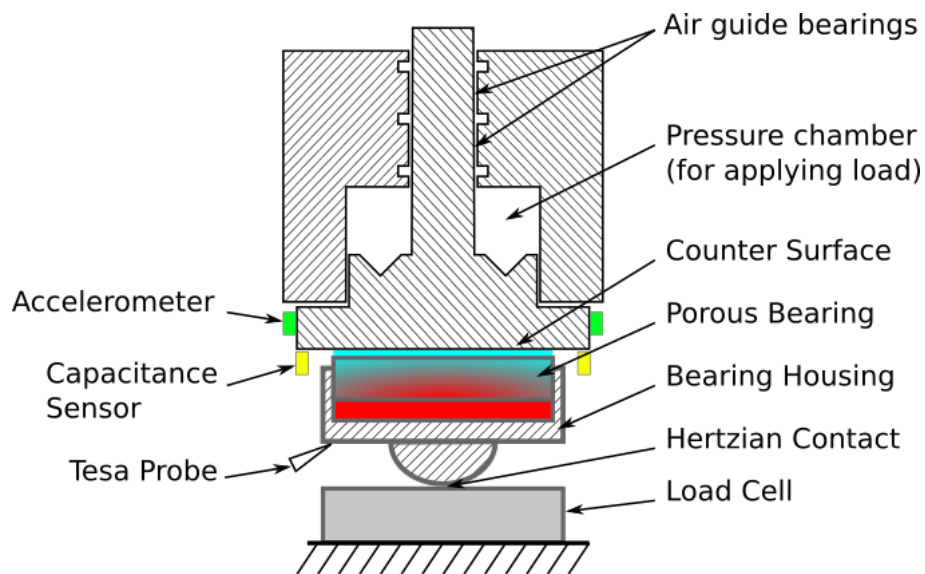


**Figure 4.1:** Schematic drawing of the testing set-up used to measure the circumstances under which the bearing shows unstable behaviour.

During the measurement the supply pressure of the bearing was set to a fixed value, while the pressure in the pressure chamber was swept up and down three times before going to the next supply pressure. After the experiment the data was examined and all the points were noted where the bearing transitioned from stable to unstable while going from low to high flying heights.

## 4.2. Lumped Dynamic model

To represent the test setup a lumped dynamics model was created simplifying the system to a 1D dynamic model. The system can be seen in Figure 4.2. It consist of a single mass representing the air cylinder and a series of springs and dampers. These represent the Hertzian contact of the bearing housing touching the load cell, the stiffness of the housing and the stiffness and damping from the bearing.

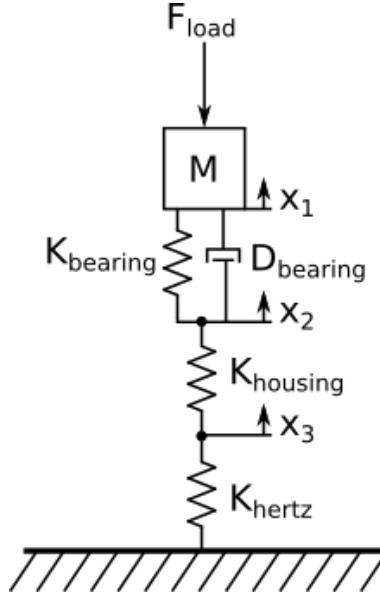


**Figure 4.2:** The lumped dynamics model used for the stability analysis

The lumped parameter model was used to calculate the open loop function of the system:

$$L(s) = \frac{1}{Ms^2} \left( -\frac{(K_{\text{bearing}} + D_{\text{bearing}}s)^2}{(K_{\text{housing}}^{-1} + K_{\text{Hertz}}^{-1})^{-1} + K_{\text{bearing}} + D_{\text{bearing}}s} + K_{\text{bearing}} + D_{\text{bearing}}s \right) \quad (4.1)$$

4.3. Results

The measurement data was compared with the model by evaluating the stability of the lumped dynamic model. The transition between stable and unstable behaviour was mapped for different supply pressures by sweeping the load on the bearing, thus sweeping the gap height. For every supply pressure the critical gap height was determined where the bearing transitioned from stable to unstable behaviour. As the porosity of the coating was unknown a range of values were plotted. The results of this procedure can be seen Figures 4.3 - 4.7. The expected behaviour is that the measured points coincide with one of the lines calculated by the model.

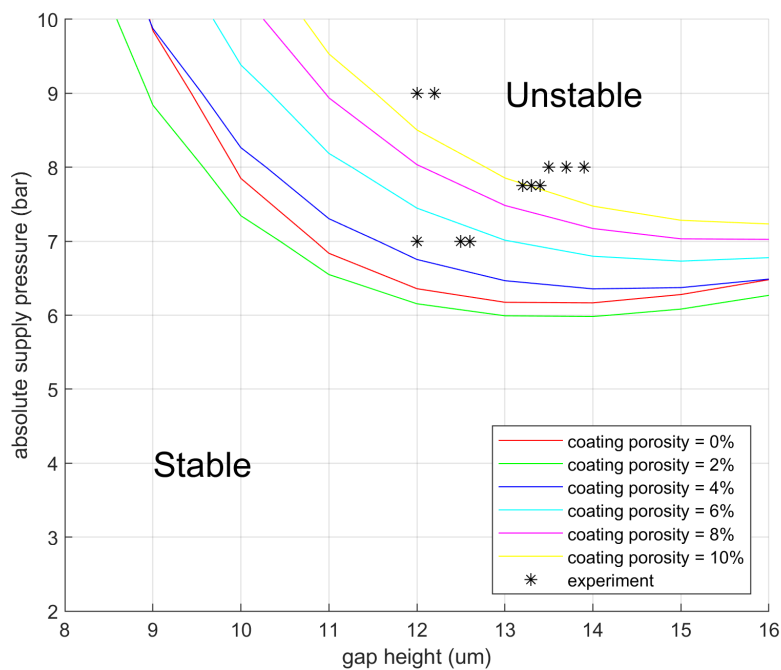


Figure 4.3: Experimental Results Bearing 1

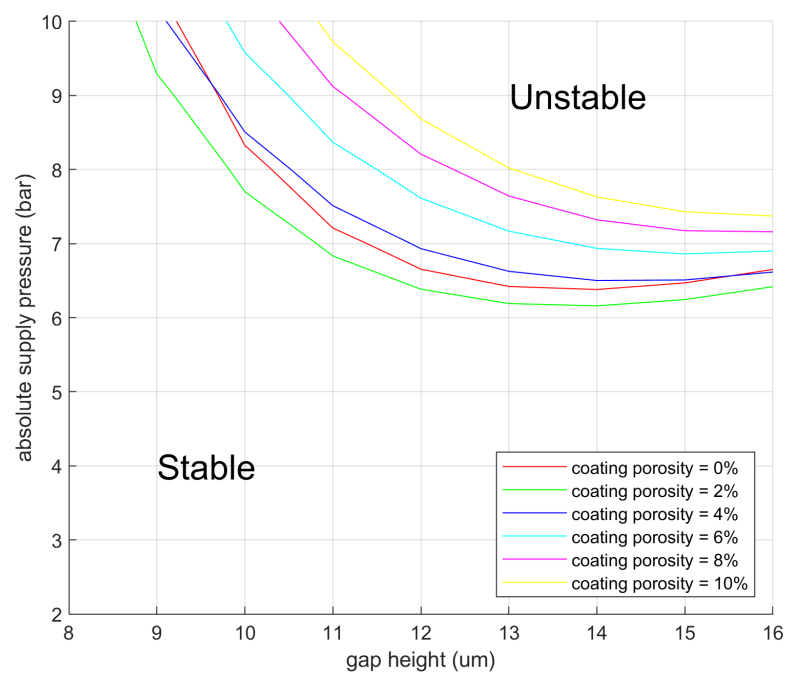


Figure 4.4: Experimental Results Bearing 2 (no instability observed)

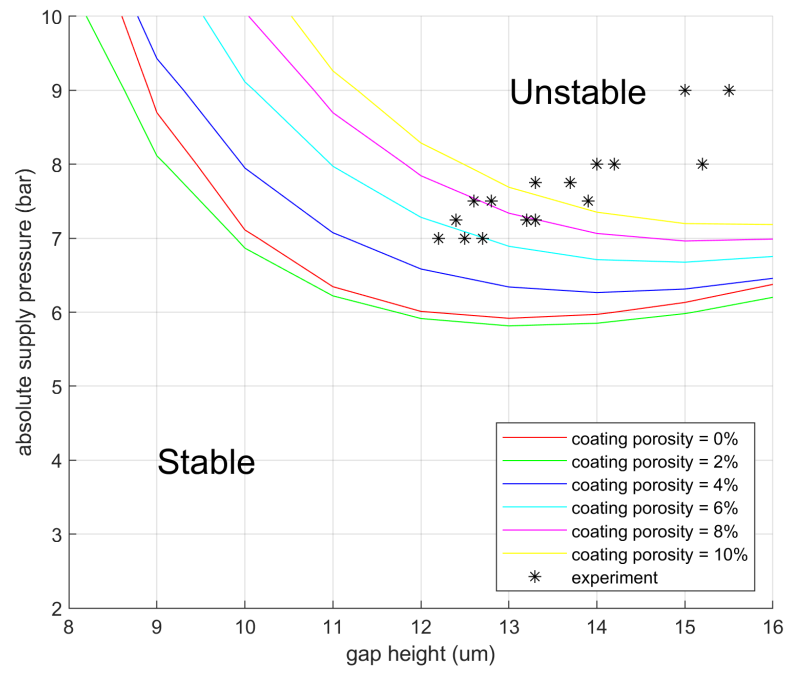


Figure 4.5: Experimental Results Bearing 3

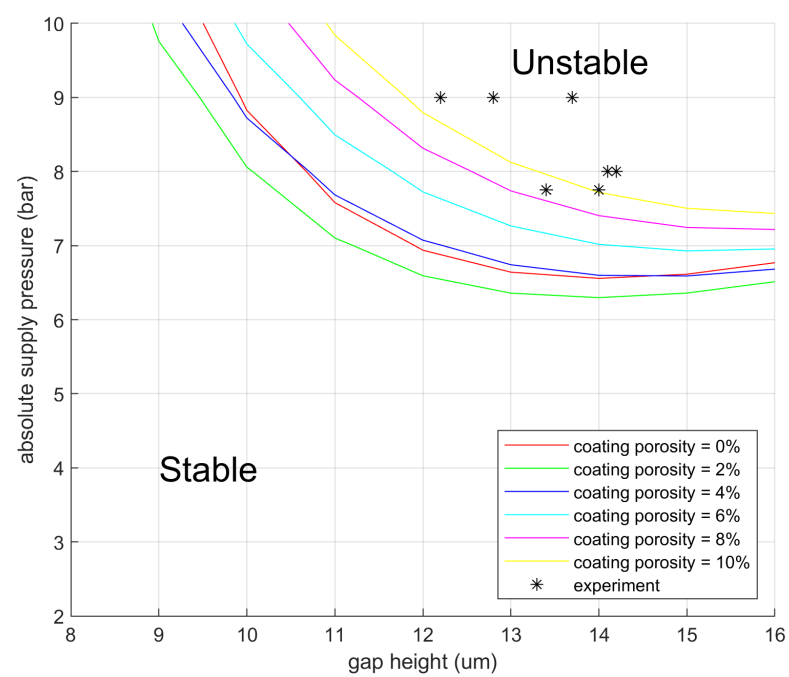


Figure 4.6: Experimental Results Bearing 4

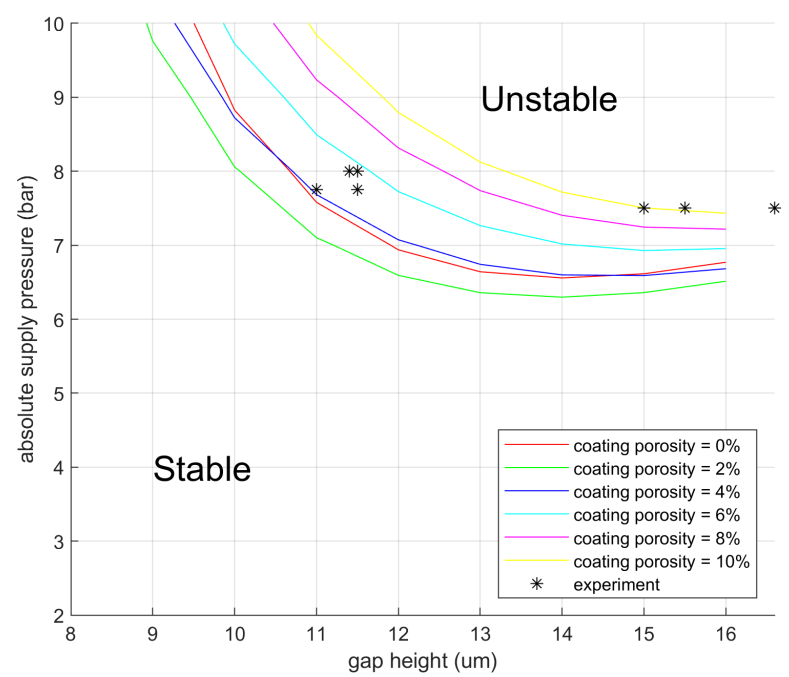


Figure 4.7: Experimental Results Bearing 5

From the results it can be concluded that only a very limited match between model and experiment can be identified. Looking at bearings 4 and 5 some resemblance can be seen with the expected model predictions. The difference between the model and the experiment could be bridged by adjusting some of the parameters in the model, such as the stiffnesses and the porosity of the bearing. For bearings 1 and 3 the trend in the measurements is very different from the expected behaviour and there is no way of adjusting the models that can explain this behaviour. This is also the case for bearing 2 where there was no instability observed.

Looking at all the results together, it is not possible to draw any conclusions from this experiment in with regards to the validity of the model. This is also due to the way in which the experiment is set up. The measurement setup is only able to identify one key point in the frequency response of the bearing, which is the point where the damping characteristic transitions from positive to negative damping. During the sweep of the fly height, the stiffness of the bearing changes, which in turn influences the eigenfrequency of the system. When the eigenfrequency falls in the range where the bearing has negative damping, this will lead to unstable behaviour. Because the exact stiffness characteristics of the housing and Hertzian contact weren't measured separately, there is no way of telling if the stiffness of the bearing or the crossover from negative to positive damping is different from the modelled values.

The measurement could be improved by first measuring the stiffness of the housing together with the Hertzian contact by loading up the bearing with no supply pressure and measure the compression of the whole stack. By evaluating the frequency at which the bearing oscillates when it becomes unstable both the stiffness of the bearing and the crossover frequency can be determined.



# 5

## Conclusion

The objectives of this report were to:

- Create a COMSOL Multiphysics™ model capable of accurately predicting the dynamic characteristics of porous air bearings with and without a surface-restrictive layer.
- Determine the sensitivity of the porosity of the porous material and coating on the dynamic characteristics.
- Investigate the existence of other methods to evaluate indicators for detecting bearing designs that pose risks of inherent instability.
- Validate the model experimentally

In order to reach these goals the following steps have been taken:

In Chapter 2 a COMSOL Multiphysics™ model was developed, using a perturbation of the Reynolds and Darcy-Forchheimer equations to predict the dynamic characteristics of a porous thrust bearing with and without a coating. A quick introduction is given to the Nyquist criterion to be able to predict instability (pneumatic hammer) in systems, using porous bearings that have negative low frequency damping. To use the model for existing air bearings, a measurement method is discussed to measure the permeability of multi layered air bearings.

In Chapter 3 the mechanics influencing dynamic behaviour are discussed and an explanation is given for the low frequency negative damping that can be present in porous bearings. This method, using the amount of mass stored in the bearing as function of the flying height, gives a more intuitive approach to understanding negative damping. The method is compared with the model discussed in chapter 2 and a small error was found along with some problems limiting the application to only simple situations, thus evaluating the perturbed equations is preferred for critical applications.

A sensitivity study on the porosity in an uncoated bearing shows a linear dependency between the low frequency damping and the porosity. This study also showed that in order to get positive low frequency damping for the studied bearing, the porosity had to be less than one percent. Revealing that the proposed bearing design can only be improved by using a coating. The addition of a surface restrictive coating is discussed and from this it is concluded that there are two conditions that have to be met for the surface restrictive layer to guarantee positive damping at low frequencies. The first condition is that the total normalized permeability has to be reduced by a large amount to decouple the capacitance of the base material from the dynamic characteristics of the bearing. The other requirement is that the porosity and height of the coating have to be small enough.

In Chapter 4 an existing dataset is used to see if the model accurately predicts instability. To predict instability using the modelled dynamic bearing characteristics a Lumped Dynamic model was created of the test setup. This model was used to evaluate the stability at different operating conditions which were then compared to the experimental results. From the comparison it was concluded that there is a very limited match between the experiment and the model.

Concluding the report three of the four objectives have been reached. A model was created capable of predicting the dynamic characteristics of porous air bearings. The sensitivity of the porosity in both

the bearing and the surface restrictive layer was investigated. An alternative method was found to predict part of the dynamic behaviour of the bearing. Unfortunately the experiment did not satisfy the goal of verifying the models.

# 6

## Recommendations

**Investigate if coating is below the surface** A method [28][26][27] that is used to make sure that bearings all have the same total permeability when doing large series is to apply a large amount of lacquer or epoxy to the bearing. The resulting layer is almost completely sealed. After this the bearing is "tuned", dissolving part of the coating to allowing air to pass through. Since this method dissolves the coating from the side of the bearing surface there is a large chance that the coating forms a restrictive layer deeper in the material. This was not considered during this report but will likely have a large influence on the dynamics. This can easily be implemented in the model by changing the locating of the restrictive layer to be deeper into the material. The challenge is not in the modelling of this layer but in determining how deep the layer sits and making it repeatable.

**A non-destructive way to measure penetration depth and porosity of coating** Knowing the capacitance of the coating is necessary to predict the dynamics of the bearing. Being able to measure these variables for research or during production would be very helpful. As CT [13] scanning every bearing is probably too expensive for most applications a more cost effective method is required.

**Alternative ways of applying a surface restrictive layer to graphite** The current technique of applying a coating by hand is hard to control. Although it creates a repeatable bearing from a static point of view, it does not from a dynamic point of view. A method yielding a more consistent coating, resulting in the same performance for the static and dynamic characteristics, would be very interesting.

**Alternative ways to create a surface restrictive coating to carbon** For ductile materials there are more options to get a surface restrictive layer than there are for brittle materials. For other materials such as porous alumina there is the possibility of choosing a different grain size before sintering[10]. For porous metals it's possible to create a surface loading effect with the burs that occur during machining [19]. Maybe it is possible to do a similar thing with porous graphite to create a layer at the surface of the bearing.

**Changing the working principle of the test-setup** As it is now unclear what causes the error between the experiment and the model, rendering it impossible to say anything about the performance of the model. It is important to simplify the test set-up and to extract more data from it. As the original measurement setup relied on the eigenfrequency moving in and out of the negative damping frequencies of the bearing. It is only possible to measure around the crossover frequency of the bearing.

To improve on these points a set-up using a shaker as depicted in Figure 6.1 would be more suited. This set-up has far less moving parts that have to be considered in the dynamics and it takes away the dependency of the test on the eigenfrequency of the system. In this set-up the counter-surface is mounted to a shaker acting as an input to the system. The bearing is standing on top only weighted down by a mass and is kept from moving side to side by a flexure, assuming that the amplitude of the shaker is kept small there will be little to no parasitic motion. When mounting the weight to the bearing

special care needs to be taken in making sure that the connection is very rigid and simple, to avoid creating a dynamically more complex system.

By measuring both the vertical movement of the counter-surface and that of the bearing, the transmission between the two can be calculated and the bearing dynamics extracted. There are some downsides to this set-up as it is limited, due to practical reasons, to small bearings only as the load is supplied by gravity. To verify the model and the set-up, it is recommended to start with a small uncoated bearing to have an idea of the error before moving to coated bearings.

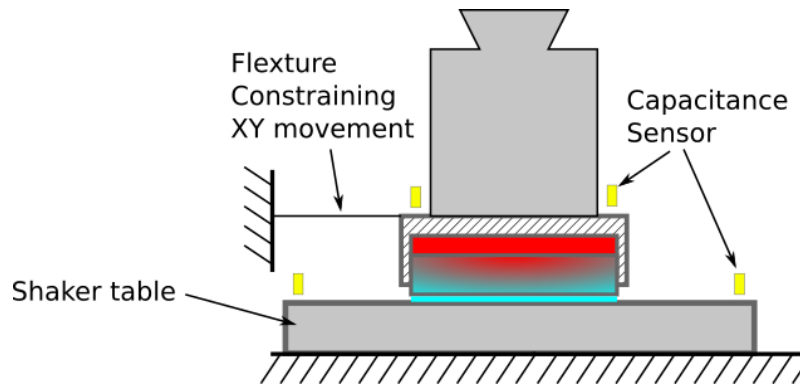


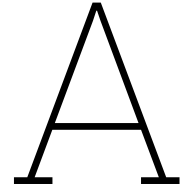
**Figure 6.1:** Proposal for improved testing set-up

# References

- [1] New Way Air Bearings. *Media Packet*. Web Page. 2023. URL: <https://www.newwayairbearings.com/about-us/company/media-packet/>.
- [2] G. Belforte et al. "Permeability and inertial coefficients of porous media for air bearing feeding systems". In: *Journal of Tribology* 129.4 (2007). Cited By :30 Export Date: 19 April 2022, pp. 705–711. DOI: 10.1115/1.2768068. URL: <https://www.scopus.com/inward/record.uri?eid=2-s2.0-35348969365&doi=10.1115%2f1.2768068&partnerID=40&md5=4ae459b6fcb757fe2532a9dcf049eec2>.
- [3] Farid Al-Bender. *Air bearings : theory, design and applications*. Hoboken, NJ: John Wiley and Sons, Inc., 2021. ISBN: 9781118511497. URL: <http://dx.doi.org/10.1002/9781118926444%20http://search.ebscohost.com/login.aspx?direct=true&scope=site&db=nlebk&db=nlabk&AN=2726154>.
- [4] H. S. Chang, Z. S. Wang, and D. C. Sun. "An Experimental Investigation of the Stability of Externally Pressurized Gas-Lubricated Porous Thrust Bearings". In: *Journal of Lubrication Technology* 105.4 (1983), pp. 630–637. ISSN: 0022-2305. DOI: 10.1115/1.3254695. URL: <https://doi.org/10.1115/1.3254695>.
- [5] A. K. Chattopadhyay and B. C. Majumdar. "Dynamic Characteristics of Finite Porous Journal Bearings Considering Tangential Velocity Slip". In: *Journal of Tribology* 106.4 (1984), pp. 534–536. ISSN: 0742-4787. DOI: 10.1115/1.3260977. URL: <https://doi.org/10.1115/1.3260977>.
- [6] Specialty Components. *Product page LCAP150*. Web Page. 2023. URL: <https://www.specialtycomponents.com/Products/lcap150/>.
- [7] Specialty Components. *Product page SRA100-R45*. Web Page. 2023. URL: <https://www.specialtycomponents.com/Products/sra100-r45/>.
- [8] Henry Darcy. *Les fontaines publiques de la ville de Dijon: exposition et application des principes à suivre et des formules à employer dans les questions de distribution d'eau*. Vol. 1. Victor dalmont, 1856.
- [9] Bernard J. Hamrock, Steven R. Schmid, and Bo O. Jacobson. *Fundamentals of fluid film lubrication*. Electronic Book. 2004.
- [10] Y. B. P. Kwan. "Processing and fluid flow characteristics of hot isostatically pressed porous alumina for aerostatic bearing applications". 1 online resource. Thesis. 1996.
- [11] Y. B. P. Kwan and J. Corbett. "A simplified method for the correction of velocity slip and inertia effects in porous aerostatic thrust bearings". In: *Tribology International* 31.12 (1998), pp. 779–786. ISSN: 0301-679X. DOI: [https://doi.org/10.1016/S0301-679X\(98\)00101-7](https://doi.org/10.1016/S0301-679X(98)00101-7). URL: <https://www.sciencedirect.com/science/article/pii/S0301679X98001017>.
- [12] Y. B. P. Kwan and J. Corbett. "Porous aerostatic bearings-an updated review". In: *Wear* 222.2 (1998), pp. 69–73. ISSN: 0043-1648. DOI: 10.1016/S0043-1648(98)00285-3.
- [13] Hao Liu and Ying Xu. "Gas permeability measurement in porous graphite under steady-state flow". In: *Materials Research Express* 9.2 (2022), p. 025603. ISSN: 2053-1591. DOI: 10.1088/2053-1591/ac50d7. URL: <http://dx.doi.org/10.1088/2053-1591/ac50d7>.
- [14] T. S. Luong et al. "Numerical and experimental analysis of aerostatic thrust bearings with porous restrictors". In: *Tribology International* 37.10 (2004), pp. 825–832. ISSN: 0301-679X. DOI: 10.1016/j.triboint.2004.05.004.
- [15] B. C. Majumdar. "Dynamic Characteristics of Externally Pressurized Rectangular Porous Gas Thrust Bearings". In: *Journal of Lubrication Technology* 98.1 (1976), pp. 181–186. ISSN: 0022-2305. DOI: 10.1115/1.3452762. URL: <https://doi.org/10.1115/1.3452762>.

- [16] M. C. Majumder and B. C. Majumdar. "Theoretical Analysis of Pneumatic Instability of Externally Pressurized Porous Gas Journal Bearings Considering Velocity Slip". In: *Journal of Tribology* 110.4 (1988), pp. 730–733. ISSN: 0742-4787. DOI: 10.1115/1.3261721. URL: <https://doi.org/10.1115/1.3261721>.
- [17] M. C. Majumder and B. C. Majumder. "Study of the pneumatic instability of externally pressurized porous gas thrust bearings with slip velocity". In: *Wear* 124.3 (1988), pp. 261–277. ISSN: 0043-1648. DOI: [https://doi.org/10.1016/0043-1648\(88\)90217-7](https://doi.org/10.1016/0043-1648(88)90217-7). URL: <https://www.sciencedirect.com/science/article/pii/0043164888902177>.
- [18] M Miyatake, S Yoshimoto, and J Sato. "Whirling instability of a rotor supported by aerostatic porous journal bearings with a surface-restricted layer". In: *Proceedings of the Institution of Mechanical Engineers, Part J: Journal of Engineering Tribology* 220.2 (2006), pp. 95–103. DOI: 10.1243/13506501jet89. URL: <https://journals.sagepub.com/doi/abs/10.1243/13506501JET89>.
- [19] H. Mori and H. Yabe. "Theoretical Investigation of Externally Pressurized Gas-Lubricated Porous Journal Bearing With Surface-Loading Effect". In: *Journal of Lubrication Technology* 95.2 (Apr. 1973), pp. 195–202. ISSN: 0022-2305. DOI: 10.1115/1.3451768. eprint: [https://asmedigitalcollection.asme.org/tribology/article-pdf/95/2/195/5663856/195\\_1.pdf](https://asmedigitalcollection.asme.org/tribology/article-pdf/95/2/195/5663856/195_1.pdf). URL: <https://doi.org/10.1115/1.3451768>.
- [20] Yuta Otsu, Masaaki Miyatake, and Shigeka Yoshimoto. "Dynamic Characteristics of Aerostatic Porous Journal Bearings With a Surface-Restricted Layer". In: *Journal of Tribology* 133.1 (2010). ISSN: 0742-4787. DOI: 10.1115/1.4002730. URL: <https://doi.org/10.1115/1.4002730>.
- [21] D. W. Parkins and W. T. Stanley. "Characteristics of an Oil Squeeze Film". In: *Journal of Lubrication Technology* 104.4 (Oct. 1982), pp. 497–502. ISSN: 0022-2305. DOI: 10.1115/1.3253268. eprint: [https://asmedigitalcollection.asme.org/tribology/article-pdf/104/4/497/5918806/497\\_1.pdf](https://asmedigitalcollection.asme.org/tribology/article-pdf/104/4/497/5918806/497_1.pdf). URL: <https://doi.org/10.1115/1.3253268>.
- [22] P. Plessers and R. Snoeys. "Dynamic stability of mechanical structures containing externally pressurized gas-lubricated thrust bearings". In: *Journal of Tribology* 110.2 (1988). Cited By :9 Export Date: 23 March 2023, pp. 271–278. DOI: 10.1115/1.3261598. URL: <https://www.scopus.com/inward/record.uri?eid=2-s2.0-0023994913&doi=10.1115%2f1.3261598&partnerID=40&md5=4f830897d784f7ba9120f83837374548>.
- [23] N. S. Rao. "Analysis of Dynamic Tilt Stiffness and Damping Coefficients of Externally Pressurized Porous Gas Journal Bearings". In: *Journal of Lubrication Technology* 100.3 (1978), pp. 359–363. ISSN: 0022-2305. DOI: 10.1115/1.3453185. URL: <https://doi.org/10.1115/1.3453185>.
- [24] N. S. Rao and B. C. Majumdar. "Analysis of Pneumatic Instability of Externally Pressurized Porous Gas Journal Bearings". In: *Journal of Lubrication Technology* 101.1 (1979), pp. 48–53. ISSN: 0022-2305. DOI: 10.1115/1.3453276. URL: <https://doi.org/10.1115/1.3453276>.
- [25] NS Rao. "Analysis of the stiffness and damping characteristics of an externally pressurized porous gas journal bearing". In: *Journal of Lubrication Technology* 99.2 (1977), pp. 295–301.
- [26] W H Rasnick. *AIR-BEARING REWORK AND IMPREGNATION*. Report. 1972. URL: <https://www.osti.gov/biblio/4623649>.
- [27] W H Rasnick et al. *Porous graphite air-bearing components as applied to machine tools*. Conference Paper. 1974. URL: <https://www.osti.gov/biblio/5110726><https://www.osti.gov/servlets/purl/5110726>.
- [28] W. H. Rasnick and Philip J. Steger. *GAS BEARING AND METHOD OF MAKING SAME*. Patent. 1973. URL: <https://www.freepatentsonline.com/3721479.html>.
- [29] Dah-Chen Sun. "Stability Analysis of an Externally Pressurized Gas-Lubricated Porous Thrust Bearing". In: *Journal of Lubrication Technology* 95.4 (1973), pp. 457–468. ISSN: 0022-2305. DOI: 10.1115/1.3451857. URL: <https://doi.org/10.1115/1.3451857>.
- [30] Dah-chen Sun. "Stability of Gas-Lubricated, Externally Pressurized Porous Journal Bearings". In: *Journal of Lubrication Technology* 97.3 (1975), pp. 494–505. ISSN: 0022-2305. DOI: 10.1115/1.3452645. URL: <https://doi.org/10.1115/1.3452645>.

- [31] Wikipedia contributors. *Porosity* — *Wikipedia, The Free Encyclopedia*. [Online; accessed 16-August-2023]. 2023. URL: <https://en.wikipedia.org/w/index.php?title=Porosity&oldid=1141983405>.
- [32] S. Yoshimoto and K. Kohno. "Static and Dynamic Characteristics of Aerostatic Circular Porous Thrust Bearings (Effect of the Shape of the Air Supply Area)". In: *Journal of Tribology* 123.3 (2000), pp. 501–508. ISSN: 0742-4787. DOI: 10.1115/1.1308027. URL: <https://doi.org/10.1115/1.1308027>.
- [33] Chaoqun Zeng et al. "Three-dimensional flow state analysis of microstructures of porous graphite restrictor in aerostatic bearings". In: *Tribology International* 159 (2021), p. 106955. ISSN: 0301-679X. DOI: <https://doi.org/10.1016/j.triboint.2021.106955>. URL: <https://www.sciencedirect.com/science/article/pii/S0301679X21001031>.



## Baseline bearing

To plot some of the figures in chapter 3 a baseline situation is needed. The specifications of this bearing can be seen below:

- diameter:  $D = 100 \text{ mm}$
- height:  $H = 4 \text{ mm}$
- supply pressure:  $P_s = 6 \cdot 10^5 \text{ Pa}$
- ambient pressure  $P_a = 1 \cdot 10^5 \text{ Pa}$
- porosity: 15%
- permeability:  $\kappa_v = 4 \cdot 10^{-15} \text{ m}^2$   $\kappa_i = 4 \cdot 10^{-11} \text{ m}$
- normalized permeability:  $K_v = 1 \cdot 10^{-12} \text{ m}$   $K_i = 1 \cdot 10^{-8}$

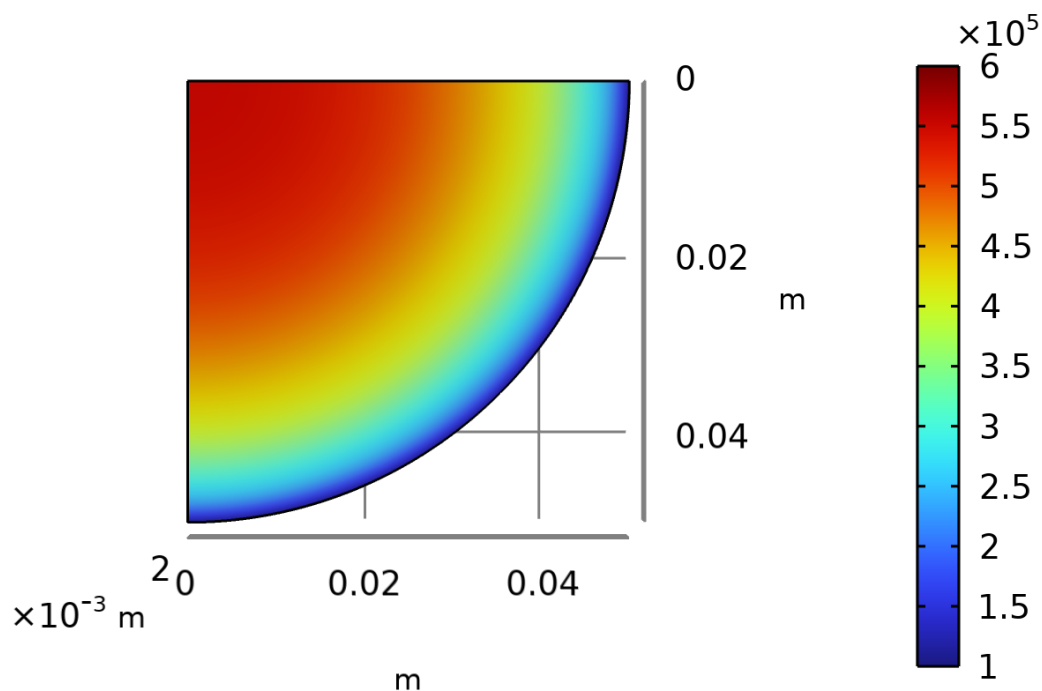


**Figure A.1:** Calculated Pressure distribution (Pa) at 13  $\mu\text{m}$  flying height



A.1. baseline static Performance

With the parameters above the pressure distribution underneath the bearing is calculated (figure A.1). By integrating the pressure distribution minus the ambient pressure over the surface of the bearing, the load capacity can be calculated. From this it's possible to plot the load capacity vs flying height (figure A.2) and stiffness vs flying height (figure A.3).

From the load capacity and flying height plots we can see that a operating point at 13  $\mu\text{m}$  is optimal for this bearing. At this point the stiffness of the bearing is at its highest point at a value of 145 N/ $\mu\text{m}$  and the load capacity is around 2.5 kN.

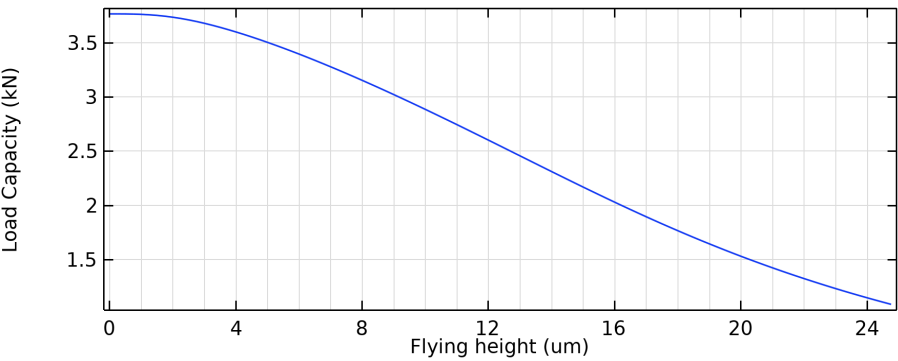


Figure A.2: Load capacity of baseline bearing.

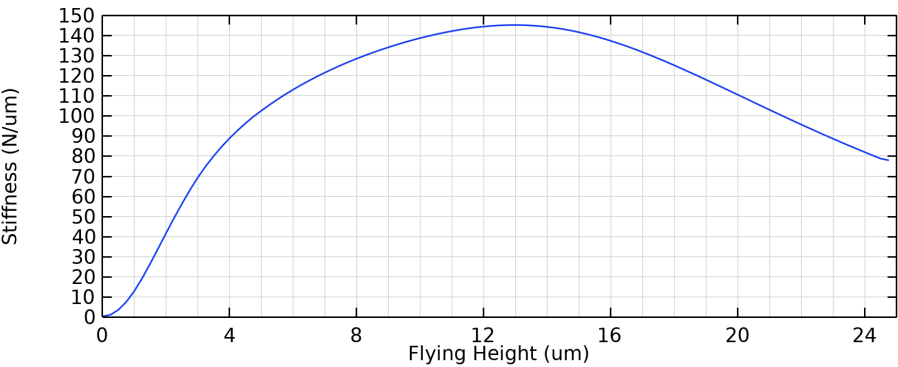


Figure A.3: Static stiffness of baseline bearing.

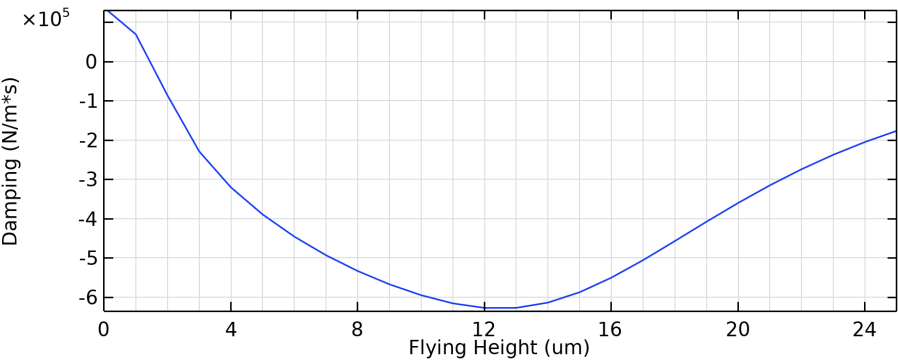
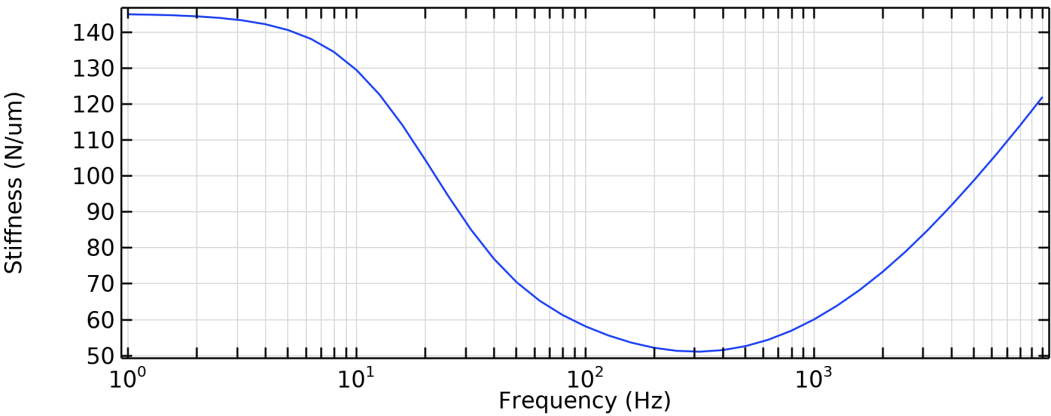


Figure A.4: Low frequency damping of baseline bearing.

**A.2. baseline dynamic performance at operating point**

Now that the optimal operating point from a static point of view is found at 13  $\mu\text{m}$ , it is important to check the dynamic performance of the bearing at this operating point. If we analyse the bearing by using a perturbation around the operating point, the following stiffness (figure A.5) and damping (figure A.6) characteristics are found as a function of frequency.



**Figure A.5:** dynamic stiffness of baseline bearing around flying height of 13  $\mu\text{m}$ .

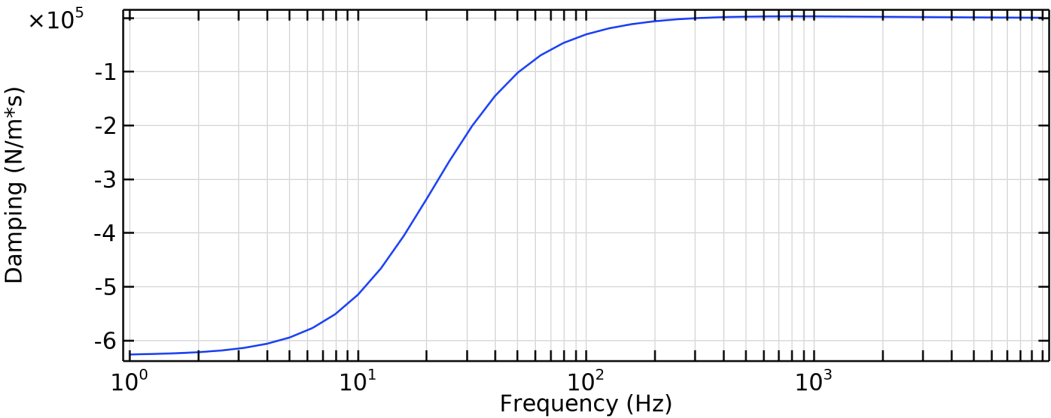


**Figure A.6:** dynamic damping of baseline bearing around flying height of 13  $\mu\text{m}$ .

# B

## COMSOL implementation

In this appendix the implementation of all formula's introduced in Chapter 2 is shown.

### B.1. Parameters

Before we can start the model some definitions need to be made in the Parameters section. The geometric variables have been excluded. Note that some definitions such as the film height need to be changed for bearings that don't have a constant film height over their entire surface.

Name	value	Description
H0	constant[um]	film height
H0_pert	constant[um]	perturbation of film height
P_supply	constant[Pa]	absolute supply pressure
P_ambient	constant[Pa]	the ambient pressure
pert_freq	constant[Hz]	perturbation frequency
omega	$(2 \cdot \pi) \cdot \text{pert\_freq}$	perturbation frequency [rad/s]
allow_xy_flow	0 or 1	switching variable for allowing flow in the x and y direction
allow_nonlin	0 or 1	switching variable for switching on and of the forchheimer term
Horous	constant[mm]	height of porous block
Hcoat	constant[um]	height of the coating
mu	constant[Pa s]	dynamic viscosity
Rs	constant [m <sup>2</sup> /s <sup>2</sup> K]	specific gas constant
T0	constant[K]	absolute temperature of the supply
M_moving	constant[kg]	moving mass in system used for plotting nyquist and bode plots(optional)
epsilon_porous	constant between 0 and 1	porosity of porous material
epsilon_coating	constant between 0 and 1	porosity of porous material
Kv_total_before_coating	constant[m]	Total viscous normalized permeability before coating
Ki_total_before_coating	constant[]	Total inertial normalized permeability before coating
Kv_total_after_coating	constant[m]	Total viscous normalized permeability after coating
Ki_total_after_coating	constant[]	Total inertial normalized permeability after coating

Name	value	Description
kv_porous	$Kv\_total\_before\_coating * H_{porous}$	permeability of porous material viscous component
ki_porous	$Ki\_total\_before\_coating * H_{porous}$	permeability of porous material inertial component
kv_coating	$1 / (1 / Kv\_total\_after\_coating ((H_{porous} - H_{coat}) / H_{porous}) / Kv\_total\_befor\_coating) * H_{coat}$	permeability of coating viscous component
ki_coating	$1 / (1 / Ki\_total\_after\_coating ((H_{porous} - H_{coat}) / H_{porous}) / Ki\_total\_befor\_coating) * H_{coat}$	permeability of coating viscous component

## B.2. Model setup

The model was implemented in COMSOL 6.0. To start off a 3D geometry is needed for this model to be created. Since this geometry is bearing specific it will not be discussed in detail in this appendix, but note that for this model to work a geometry is needed representing the porous material and a geometry is needed representing the bearing surface. For fully porous bearings the bearing surface is simply one of the sides of the porous material.

To start of 5 items need to be created under definitions:

- Variables: Bearing variables
- Variables: Stiffness variables
- Variables: Porous material properties
- Variables: Coating material properties (optional)
- Integration: Integration over bearing surface

After this a set of 10 physics modules are needed to model al the different formula's listed in Chapter 2:

- General Form Boundary PDE: Reynolds Static
- General Form PDE: Darcy Static
- Domain ODEs and DAEs: qx static
- Domain ODEs and DAEs: qy static
- Domain ODEs and DAEs: qx static
- General Form Boundary PDE: Reynolds Perturbation
- General Form PDE: Darcy Perturbation
- Domain ODEs and DAEs: qx perturbation
- Domain ODEs and DAEs: qy perturbation
- Domain ODEs and DAEs: qx perturbation

The total component tree for the bearing should look something like in figure B.1

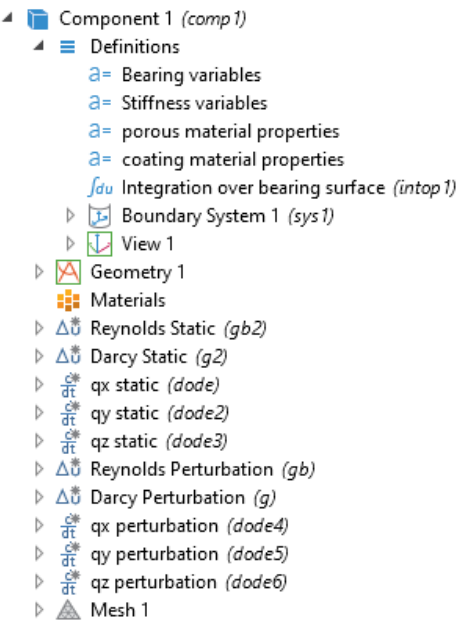


Figure B.1: Component modules

B.3. Definitions

B.3.1. Bearing variables

This set of variables contains the definition of the load capacity needed for the normal calculation and the absolute load capacity needed to calculate the secant stiffness of the bearing.

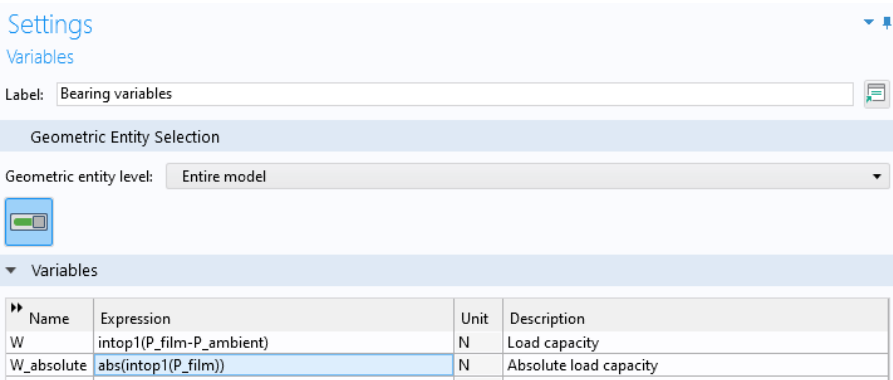


Figure B.2: Definitions: Bearing variables

B.3.2. Stiffness variables

This set of variables contains the formula's for the calculation of the dynamic stiffness (eq. 2.32) and the dynamic damping (eq. 2.33).

Settings

Variables

Label: 

Stiffness variables

Geometric Entity Selection

Geometric entity level: 

Entire model

Variables

Name	Expression	Unit	Description
K_dynamic	$-\text{real}(\text{intop1}((P_{\text{film\_pert}})/H0\_pert))$	N/m	Frequency dependant Stiffness
D_damping	$-\text{imag}(\text{intop1}((P_{\text{film\_pert}})/H0\_pert)/(\omega))$	kg/s	Frequency dependant Damping

Figure B.3: Definitions: Stiffness variables

### B.3.3. Porous material properties

This set of variables contains the material properties for the porous material and is not defined in the entire model, only in the porous material that hasn't had a coating applied to it (optional).

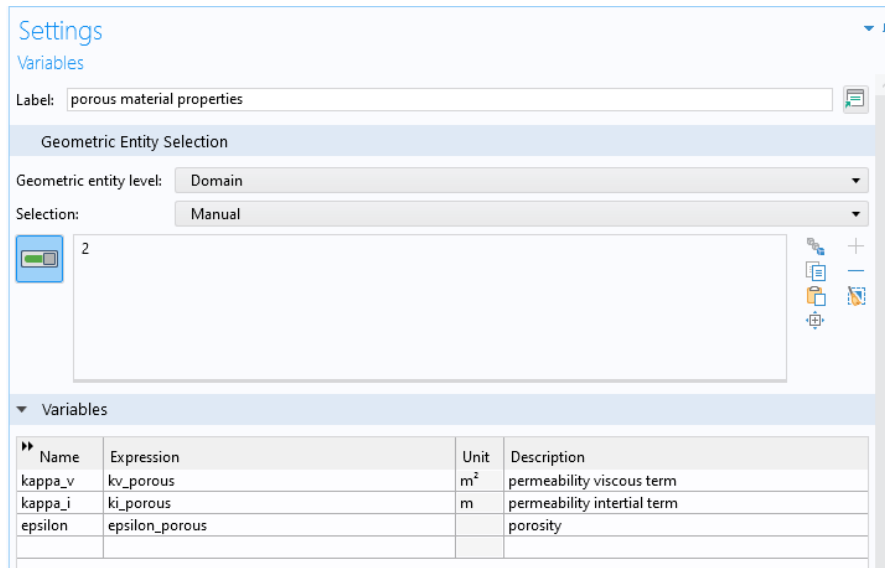


Figure B.4: Definitions: porous material properties

### B.3.4. Coating material properties

This set of variables contains the material properties for the surface restrictive layer or coating that is applied to the surface of the bearing and is an optional feature to add to the model.

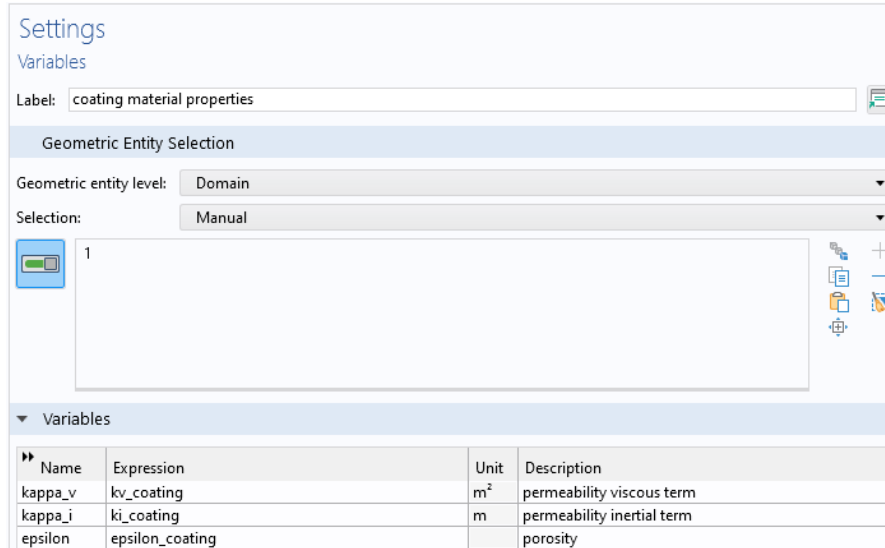
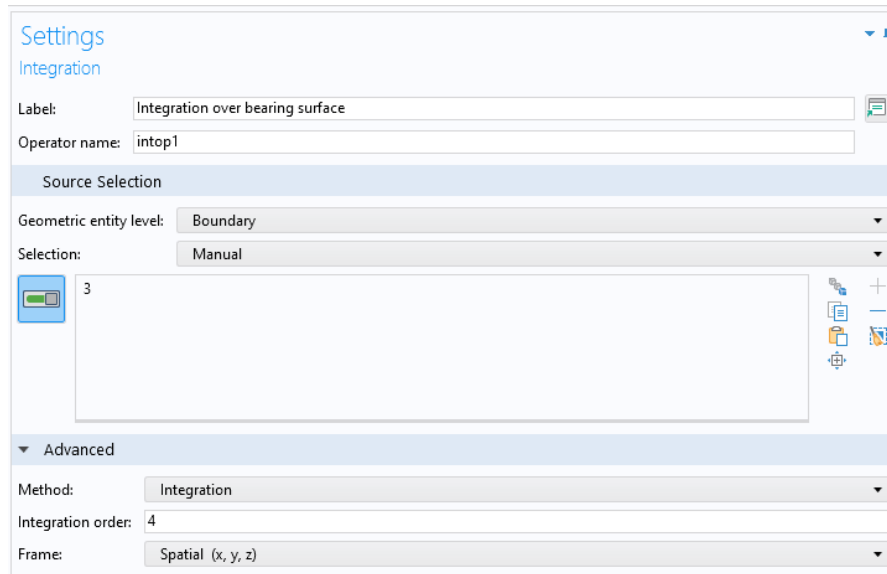


Figure B.5: Definitions: coating material properties

### B.3.5. Integration over bearing surface

This integration is defined as the integral over the bearing surface and is used as a function in other parts of the model.



The screenshot shows a 'Settings Integration' dialog box. At the top, the title is 'Settings' with a sub-tab 'Integration'. Below this, there are two input fields: 'Label:' with the value 'Integration over bearing surface' and 'Operator name:' with the value 'intop1'. A section titled 'Source Selection' contains two dropdown menus: 'Geometric entity level:' set to 'Boundary' and 'Selection:' set to 'Manual'. Below these is a large empty rectangular area with a small icon on the left and a toolbar on the right. The 'Advanced' section is expanded, showing three settings: 'Method:' set to 'Integration', 'Integration order:' set to '4', and 'Frame:' set to 'Spatial (x, y, z)'.

**Figure B.6:** Definitions: Integration over bearing surface



## B.4. Physics

### B.4.1. General form boundary PDE: Reynolds static

This physics module contains all the physics and boundary conditions linked to the porous film. The variable solved for in this module is the variable  $P_{\text{film}}$ .

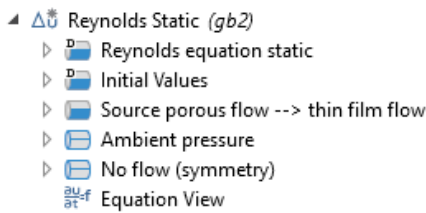


Figure B.7: Physics: Reynolds Static: Modules

### General settings

The settings for the module can be seen below. Note that a choice can be made here for the element order. In this model a high element order was chosen over increasing the amount of elements but it might be a good idea to play around with these settings to see what gives the best accuracy and solving time for the particular geometry.

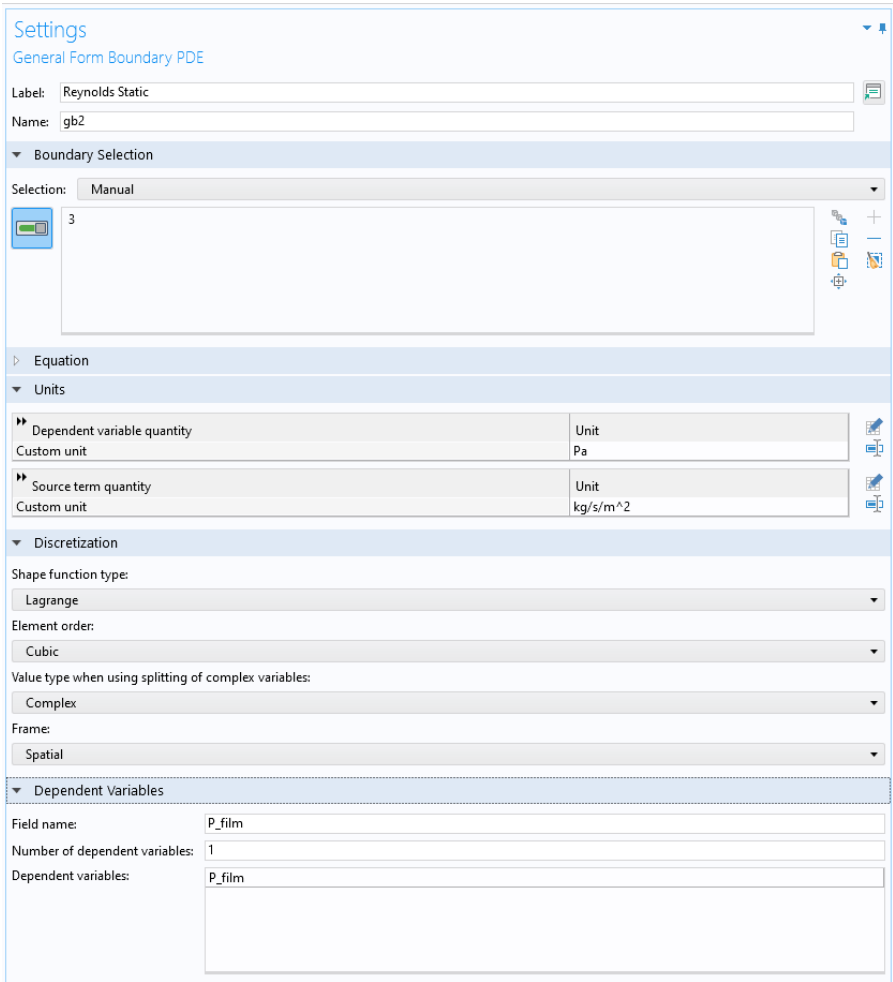


Figure B.8: Physics: Reynolds Static: General Settings

### Reynolds equation static

These are the equations describing the Reynolds equation as can be seen in Equation 2.6. Not that compared the z term is also defined while the equation in chapter 2 doesn't contain a z term. This is because the COMSOL module will only calculate the components parallel to the surface. This means for example that a surface parallel to the xy-surface automatically sets the flux in the z direction to zero.

The formula's for the flux in the x, y and z directions are in COMSOL code:

```
flux_x = -(P_film*H0^3)/(12*mu*Rs*T0)*dtang(P_film,x)
flux_y = -(P_film*H0^3)/(12*mu*Rs*T0)*dtang(P_film,y)
flux_z = -(P_film*H0^3)/(12*mu*Rs*T0)*dtang(P_film,z)
```

The screenshot shows the 'Settings' window for the 'Reynolds equation static' physics interface. The 'General Form PDE' tab is selected. The 'Label' is 'Reynolds equation static'. The 'Boundary Selection' section shows 'All boundaries' selected. The 'Equation' section shows the 'Conservative Flux' with the following equations for x, y, and z components:

Component	Equation	Units
x	$-(P_{\text{film}} \cdot H_0^3) / (12 \cdot \mu \cdot R_s \cdot T_0) \cdot \text{dtang}(P_{\text{film}}, x)$	kg/(m·s)
y	$-(P_{\text{film}} \cdot H_0^3) / (12 \cdot \mu \cdot R_s \cdot T_0) \cdot \text{dtang}(P_{\text{film}}, y)$	kg/(m·s)
z	$-(P_{\text{film}} \cdot H_0^3) / (12 \cdot \mu \cdot R_s \cdot T_0) \cdot \text{dtang}(P_{\text{film}}, z)$	kg/(m·s)

The 'Source Term' section shows the source term  $f$  set to 0, with units kg/(m²·s). The 'Damping or Mass Coefficient' section shows the damping coefficient  $d_a$  set to 0, with units s²/m. The 'Mass Coefficient' section shows the mass coefficient  $e_a$  set to 0, with units s¹/m.

**Figure B.9:** Physics: Reynolds static: equations

### Initial values

For the system to solve correctly an initial value higher than zero is required due to a singularity at  $P_{\text{film}} = 0$ . The average value between the supply pressure and the ambient pressure seems to converge quickly.



Figure B.10: Physics: Reynolds static: initial conditions

### Source porous flow --> thin film flow

This is the coupling between the flow in the porous material and the flow in the thin film. This boundary condition can be found in equation 2.22.

The equation in COMSOL code for the source is:

$$\text{source} = -\text{domflux.P\_porousx} \cdot n_x - \text{domflux.P\_porousy} \cdot n_y - \text{domflux.P\_porousz} \cdot n_z$$



Figure B.11: Physics: Reynolds static: Source porous flow → thin film flow

**Ambient pressure**

This boundary condition can be found at Equation 2.23, prescribes that the pressure at the edges of the bearing-surface should be equal to the ambient pressure.

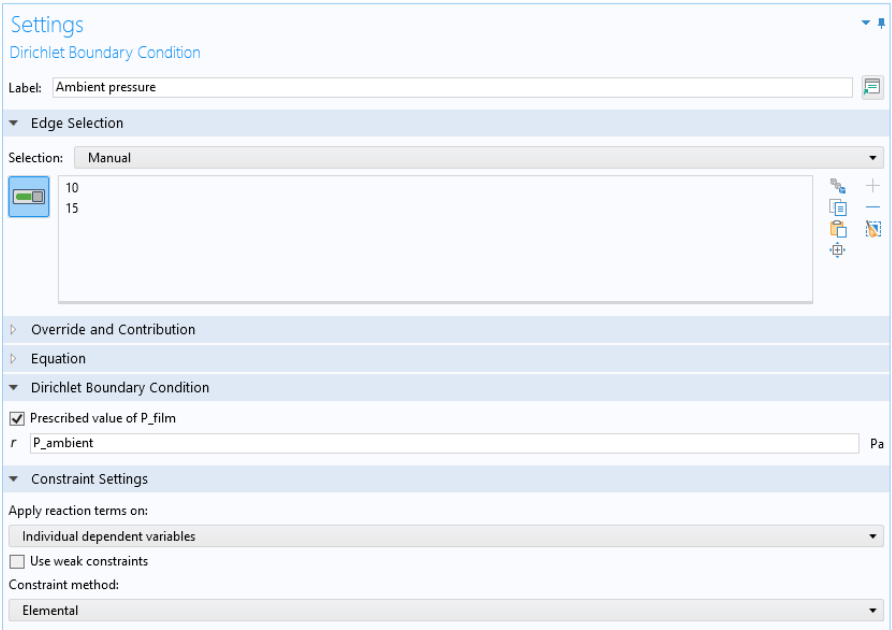


Figure B.12: Physics: Reynolds static: Ambient pressure

**No flow (symmetry)**

This boundary condition wasn't described in Chapter 2 as it isn't part of the fundamental physics of the problem. If the problem is symmetrical, for example when studying a rectangular bearing the bearing is symmetrical in 2 planes which allows for a huge reduction in the elements required to solve the problem. This boundary condition needs to be added at the symmetry planes.

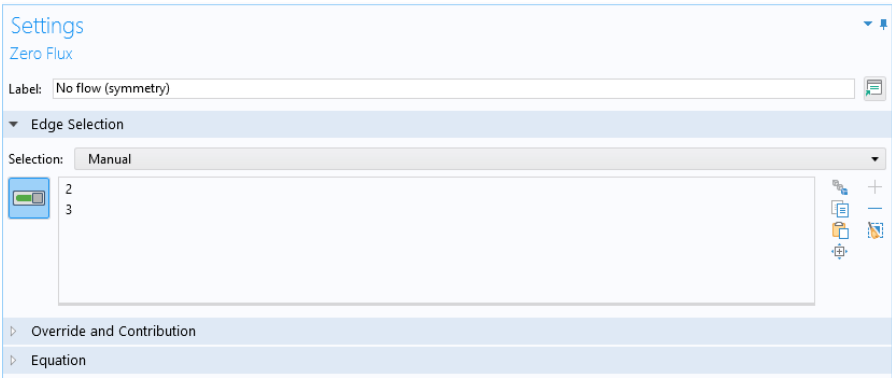


Figure B.13: Physics: Reynolds static: No flow(symmetry)

### B.4.2. General form PDE: Darcy static

This module contains all the physics for the static Darcy - Forchheimer equation. The variable solved in this module is  $P_{\text{porous}}$ . This module is not independent and needs  $q_x$ ,  $q_y$  and  $q_z$  to function.

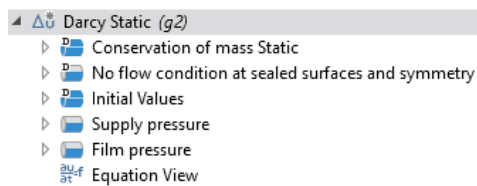


Figure B.14: Physics: Darcy static: modules

### General settings

The settings for the module can be seen below. Note that a choice can be made here for the element order. In this model a high element order was chosen over increasing the amount of elements but it might be a good idea to play around with these settings to see what gives the best accuracy and solving time for the particular geometry.

Figure B.15: Physics: Darcy static: General Settings

### Conservation of mass static

This module contains Equation 2.9, a difference between the equation and the application in comsol is that a switching variable has been added to only allow for flow in the Z-direction. This switching functionality is only for debug purposes as serves to compare the model with a 2D model in the XY-plane.

The formula's for the flux in the x, y and z directions are in COMSOL code:

```
flux_x = -(P_porous/Rs/T0)*qx*allow_xy_flow
flux_y = -(P_porous/Rs/T0)*qy*allow_xy_flow
flux_z = -(P_porous/Rs/T0)*qz
```

The screenshot shows the 'Settings' window for the 'Conservation of mass Static' module. The 'Domain Selection' section shows 'All domains' selected. The 'Conservative Flux' section shows the following flux components:

Component	Formula	Unit
$\Gamma_x$	$-(P_{porous}/Rs/T0)*qx*allow\_xy\_flow$	$kg/(m^2 \cdot s)$
$\Gamma_y$	$-(P_{porous}/Rs/T0)*qy*allow\_xy\_flow$	$kg/(m^2 \cdot s)$
$\Gamma_z$	$-(P_{porous}/Rs/T0)*qz$	$kg/(m^2 \cdot s)$

The 'Source Term' section shows the source term  $f$  set to 0, with units  $kg/(m^3 \cdot s)$ . The 'Damping or Mass Coefficient' section shows the damping coefficient  $d_a$  set to 0, with units  $s^2/m^2$ . The 'Mass Coefficient' section shows the mass coefficient  $e_a$  set to 0, with units  $s^3/m^2$ .

Figure B.16: Physics: Darcy static: Conservation of mass Static

### No flow condition at sealed surfaces and symmetry

This boundary condition can be found in Chapter 2 at Equation 2.26. And prevents flow through any surfaces that are sealed as mentioned in Chapter 2. This no flow condition is also used in blocking flow when the amount of elements is reduced by utilizing symmetry planes in the problem.

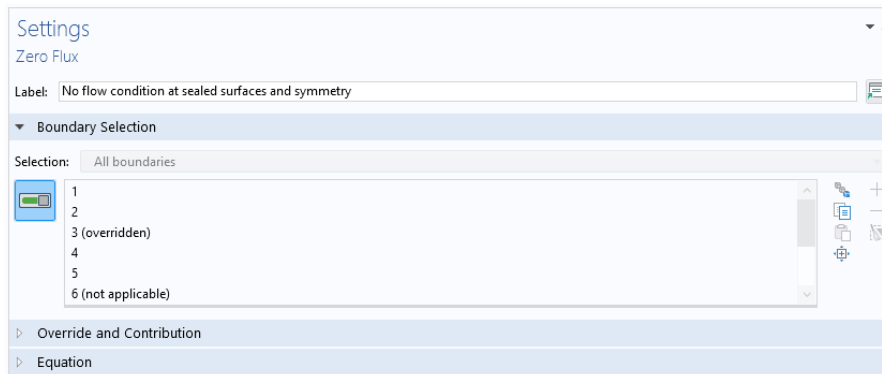


**Figure B.17:** Physics: Darcy static: No flow condition at sealed surfaces and symmetry

### Initial values

For the system to solve correctly an initial value higher than zero is required due to a singularity at  $P_{\text{porous}} = 0$ . The average value between the supply pressure and the ambient pressure seems to converge quickly.



**Figure B.18:** Physics: Darcy static: Initial Values

**Supply pressure**

This boundary condition can be found in Chapter 2 at Equation 2.27. The pressure at the feeding side of the porous material is prescribed to be at the supply pressure.



Figure B.19: Physics: Darcy static: Supply pressure

**Film pressure**

This boundary condition can be found in Chapter 2 at Equatioin 2.28 and prescribes that the pressure at the bearing surface is equal to the pressure in the thin film of air in the bearing gap.

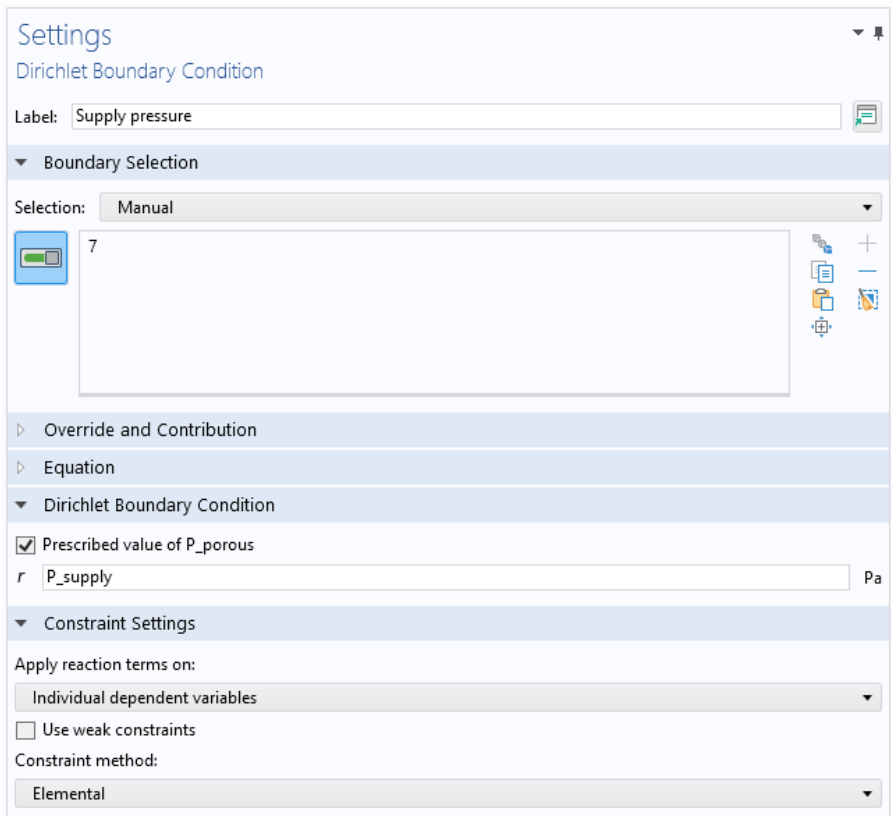


Figure B.20: Physics: Darcy static: Film pressure



### B.4.3. Domain ODEs and DAEs: qx static (same as qy and qz)

This module calculates the value of  $q_x$  as a function of the pressure gradient which is needed in the mass balance of the Darcy module. Because the relationship between the pressure gradient and the flow is implicit an extra module is needed to solve this equation. If only linear Darcy is considered without the inertial Forchheimer term, this module can be eliminated. The module is very similar to the  $q_y$  and  $q_z$  modules, the only thing that needs to be done is replace  $x$  in all equations by either  $y$  or  $z$  to get the other two. The initial conditions in this module can be left at their default 0 values because there are no singularities.

#### General settings

To ensure that the module converges quickly it is recommend to match the element type order with the Darcy Static module.

The screenshot shows the 'Settings' window for 'Domain ODEs and DAEs'. The 'Label' is 'qx static' and the 'Name' is 'dode'. Under 'Domain Selection', 'All domains' is selected, and a list shows domains 1 and 2. The 'Equation' section is collapsed. Under 'Units', the 'Dependent variable quantity' has a 'Custom unit' of 'm/s', and the 'Source term quantity' has a 'Custom unit' of 'N\*m^-3'. Under 'Discretization', 'Shape function type' is 'Discontinuous Lagrange', 'Element order' is 'Cubic', 'Value type when using splitting of complex variables' is 'Complex', and 'Frame' is 'Spatial'. Under 'Dependent Variables', the 'Field name' is 'qx', the 'Number of dependent variables' is '1', and the 'Dependent variables' list contains 'qx'.

Units	
Dependent variable quantity	Unit
Custom unit	m/s
Source term quantity	Unit
Custom unit	N*m <sup>-3</sup>

Dependent Variables	
Field name:	qx
Number of dependent variables:	1
Dependent variables:	qx

Figure B.21: Physics: qx static: General Settings

**qx static**

The equation described here can be found in Chapter 2 as Equation 2.8. There is a difference between the equation in Chapter 2 and the implementation that the version in COMSOL contains. A switching variable is used to switch off the non-linear term to get from Darcy-Forchheimer to the normal Darcy description.

The relation for finding qx in COMSOL code:

```
source term = -P_porousx-mu/kappa_v*qx-(P_porous/Rs/T0)/kappa_i*abs(qx)*qx*allow_nonlin
```

The screenshot shows the 'Settings' window for a 'Distributed ODE' in COMSOL. The 'Label' is 'qx static'. Under 'Domain Selection', 'All domains' is selected, and domains 1 and 2 are listed. The 'Source Term' section shows the equation  $f = -P_{\text{porous}}x - \mu/k_{\text{v}}qx - (P_{\text{porous}}/R_s/T_0)/k_{\text{i}}\text{abs}(qx)*qx*\text{allow\_nonlin}$  with units  $\text{N/m}^3$ . The 'Damping or Mass Coefficient' section shows  $d_a = 0$  with units  $\text{kg/m}^3$ . The 'Mass Coefficient' section shows  $e_a = 0$  with units  $\text{kg}\cdot\text{s}/\text{m}^3$ .

**Figure B.22:** Physics: qx static: equation

### B.4.4. General form boundary PDE: Reynolds perturbation

The Reynolds perturbation module contains all equations related to the perturbation of the Reynolds equation. The variable solved in this module is  $p_{\text{pert}}$ .

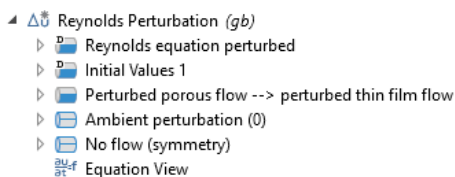


Figure B.23: Physics: Reynolds perturbation: modules

#### General settings

The general settings for the module can be seen below. Note that for the best results the element order should be the same as the static Reynolds module.

Settings  
General Form Boundary PDE

Label: Reynolds Perturbation

Name: gb

Boundary Selection

Selection: Manual

3

Equation

Units

Dependent variable quantity	Unit
Custom unit	Pa

Source term quantity	Unit
Custom unit	kg/s/m <sup>2</sup>

Discretization

Shape function type:  
Lagrange

Element order:  
Cubic

Value type when using splitting of complex variables:  
Complex

Frame:  
Spatial

Dependent Variables

Field name: P\_film\_pert

Number of dependent variables: 1

Dependent variables: P\_film\_pert

Figure B.24: Physics: Reynolds perturbation: General Settings

### Reynolds equation perturbed

The equation described here can be found in Chapter 2 as Equation 2.17. The equation was expanded and then simplified using MATLAB.

The relation for the perturbed Reynolds equation in COMSOL code:

```
flux_x = -(H0^3*P_film*dtang(P_film_pert,x) +
H0^3*dtang(P_film,x)*P_film_pert +
H0^3*P_film_pert*dtang(P_film_pert,x) +
H0_pert^3*P_film*dtang(P_film,x) +
H0_pert^3*P_film*dtang(P_film_pert,x) +
H0_pert^3*dtang(P_film,x)*P_film_pert +
H0_pert^3*P_film_pert*dtang(P_film_pert,x) +
3*H0*H0_pert^2*P_film*dtang(P_film,x) +
3*H0^2*H0_pert*P_film*dtang(P_film,x) +
3*H0*H0_pert^2*P_film*dtang(P_film_pert,x) +
3*H0*H0_pert^2*dtang(P_film,x)*P_film_pert +
3*H0^2*H0_pert*P_film*dtang(P_film_pert,x) +
3*H0^2*H0_pert*dtang(P_film,x)*P_film_pert +
3*H0*H0_pert^2*P_film_pert*dtang(P_film_pert,x) +
3*H0^2*H0_pert*P_film_pert*dtang(P_film_pert,x))/(12*Rs*T0*mu)
flux_y = -(H0^3*P_film*dtang(P_film_pert,y) +
H0^3*dtang(P_film,y)*P_film_pert +
H0^3*P_film_pert*dtang(P_film_pert,y) +
H0_pert^3*P_film*dtang(P_film,y) +
H0_pert^3*P_film*dtang(P_film_pert,y) +
H0_pert^3*dtang(P_film,y)*P_film_pert +
H0_pert^3*P_film_pert*dtang(P_film_pert,y) +
3*H0*H0_pert^2*P_film*dtang(P_film,y) +
3*H0^2*H0_pert*P_film*dtang(P_film,y) +
3*H0*H0_pert^2*P_film*dtang(P_film_pert,y) +
3*H0*H0_pert^2*dtang(P_film,y)*P_film_pert +
3*H0^2*H0_pert*P_film*dtang(P_film_pert,y) +
3*H0^2*H0_pert*dtang(P_film,y)*P_film_pert +
3*H0*H0_pert^2*P_film_pert*dtang(P_film_pert,y) +
3*H0^2*H0_pert*P_film_pert*dtang(P_film_pert,y))/(12*Rs*T0*mu)
flux_z = -(H0^3*P_film*dtang(P_film_pert,z) +
H0^3*dtang(P_film,z)*P_film_pert +
H0^3*P_film_pert*dtang(P_film_pert,z) +
H0_pert^3*P_film*dtang(P_film,z) +
H0_pert^3*P_film*dtang(P_film_pert,z) +
H0_pert^3*dtang(P_film,z)*P_film_pert +
H0_pert^3*P_film_pert*dtang(P_film_pert,z) +
3*H0*H0_pert^2*P_film*dtang(P_film,z) +
3*H0^2*H0_pert*P_film*dtang(P_film,z) +
3*H0*H0_pert^2*P_film*dtang(P_film_pert,z) +
3*H0*H0_pert^2*dtang(P_film,z)*P_film_pert +
3*H0^2*H0_pert*P_film*dtang(P_film_pert,z) +
3*H0^2*H0_pert*dtang(P_film,z)*P_film_pert +
3*H0*H0_pert^2*P_film_pert*dtang(P_film_pert,z) +
3*H0^2*H0_pert*P_film_pert*dtang(P_film_pert,z))/(12*Rs*T0*mu)
source = -(H0*P_film_pert*omega*i + H0_pert*P_film*omega*i +
H0_pert*P_film_pert*omega*2i)/(Rs*T0)
```

Settings  
General Form PDE

Label: Reynolds equation perturbed

Boundary Selection

Selection: All boundaries

1 (not applicable)  
2 (not applicable)  
3  
4 (not applicable)  
5 (not applicable)  
6 (not applicable)

Override and Contribution

Equation

Conservative Flux

$-(H_0^3 P_{film\_pert} \frac{\partial}{\partial x} (P_{film\_pert, x}) + H_0^3 \frac{\partial}{\partial x} (P_{film\_pert} P_{film\_pert, x}) + H_0^3 P_{film\_pert} \frac{\partial}{\partial x} (P_{film\_pert, x}) + H_0^3 P_{film\_pert} \frac{\partial}{\partial x} (P_{film\_pert, x}))$	x	
$-(H_0^3 P_{film\_pert} \frac{\partial}{\partial y} (P_{film\_pert, y}) + H_0^3 \frac{\partial}{\partial y} (P_{film\_pert} P_{film\_pert, y}) + H_0^3 P_{film\_pert} \frac{\partial}{\partial y} (P_{film\_pert, y}) + H_0^3 P_{film\_pert} \frac{\partial}{\partial y} (P_{film\_pert, y}))$	y	kg/(m·s)
$-(H_0^3 P_{film\_pert} \frac{\partial}{\partial z} (P_{film\_pert, z}) + H_0^3 \frac{\partial}{\partial z} (P_{film\_pert} P_{film\_pert, z}) + H_0^3 P_{film\_pert} \frac{\partial}{\partial z} (P_{film\_pert, z}) + H_0^3 P_{film\_pert} \frac{\partial}{\partial z} (P_{film\_pert, z}))$	z	

Source Term

$f$   $-(H_0^3 P_{film\_pert} \omega^2 i + H_0^3 P_{film\_pert} \omega^2 i + H_0^3 P_{film\_pert} \omega^2 i) / (R_s T_0)$  kg/(m<sup>2</sup>·s)

Damping or Mass Coefficient

$d_a$  0 s<sup>2</sup>/m

Mass Coefficient

$e_a$  0 s<sup>2</sup>/m

Figure B.25: Physics: Reynolds perturbation: Reynolds equation perturbed

### Initial values

For the perturbed Reynolds equations there are no requirements for the initial conditions because there are no singularities.

Settings  
Initial Values

Label: Initial Values

Boundary Selection

Selection: All boundaries

1 (not applicable)  
2 (not applicable)  
3  
4 (not applicable)  
5 (not applicable)  
6 (not applicable)

Override and Contribution

Initial Values

Initial value for  $P_{film\_pert}$ :  
 $P_{film\_pert}$  0 Pa

Initial time derivative of  $P_{film\_pert}$ :  
 $\frac{\partial P_{film\_pert}}{\partial t}$  0 Pa/s

Figure B.26: Physics: Reynolds perturbation: Initial Values

**Perturbed porous flow --> perturbed thin film flow**

This module contains the link between the perturbed flow in the porous material and the perturbed flow in the thin film in the bearing gap. The equation can be found in Chapter 2 as Equation 2.24.

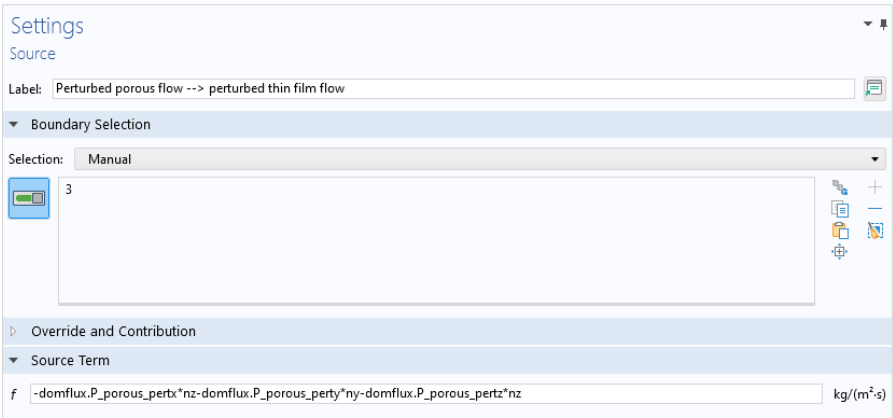


**Figure B.27:** Physics: Reynolds perturbation: Perturbed porous flow --> perturbed thin film flow

**Ambient perturbation**

This module contains the constraint that the perturbed pressure at the edge, where the ambient pressure is present, is equal to 0. This equation can be found in Chapter 2 as Equation 2.25.



**Figure B.28:** Physics: Reynolds perturbation: Ambient perturbation

**No flow (symmetry)**

This optional boundary condition is not described in Chapter 2 as it is not part of the fundamental physics. It is used to reduce the amount of elements by utilizing that the problem is symmetrical.

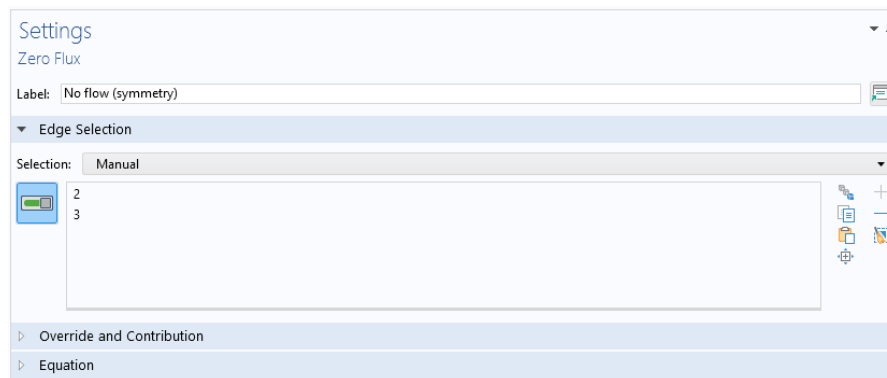


**Figure B.29:** Physics: Reynolds perturbation: No flow (symmetry)

B.4.5. General form PDE: Darcy perturbation

The Reynolds perturbation module contains the equations needed to evaluate the perturbation of the porous flow. The variable solved in this equation is `p_porous_pert`.

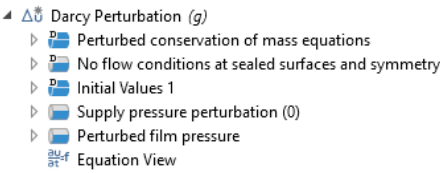


Figure B.30: Physics: Darcy perturbation: modules

General settings

The general settings for the module can be seen below. Note that for the best results the element order needs to be the same as for the Static Darcy module.

Settings

General Form PDE

Label: Darcy Perturbation

Name: g

Domain Selection

Selection: All domains

1

2

Equation

Units

Dependent variable quantity

Unit

Custom unit

Pa

Source term quantity

Unit

Custom unit

kg/s/m^3

Discretization

Shape function type:

Lagrange

Element order:

Cubic

☐ Compute boundary fluxes

☐ Apply smoothing to boundary fluxes

Value type when using splitting of complex variables:

Complex

Frame:

Spatial

Dependent Variables

Field name:

P\_porous\_pert

Number of dependent variables:

1

Dependent variables:

P\_porous\_pert

Figure B.31: Physics: Darcy perturbation: General Settings



### Perturbed conservation of mass equations

In this module the equations for the conservation of mass in the Darcy equations is perturbed. The equation can be found in Chapter 2 under Equation 2.21.

The relation for the perturbed Darcy conservation of mass equation in COMSOL code:

```
flux_x = -(P_porous*qx_pert+P_porous_pert*qx)/Rs/T0*allow_xy_flow
flux_y = -(P_porous*qy_pert+P_porous_pert*qy)/Rs/T0*allow_xy_flow
flux_z = -(P_porous*qz_pert+P_porous_pert*qz)/Rs/T0
source = P_porous_pert*i*omega/Rs/T0*epsilon
```

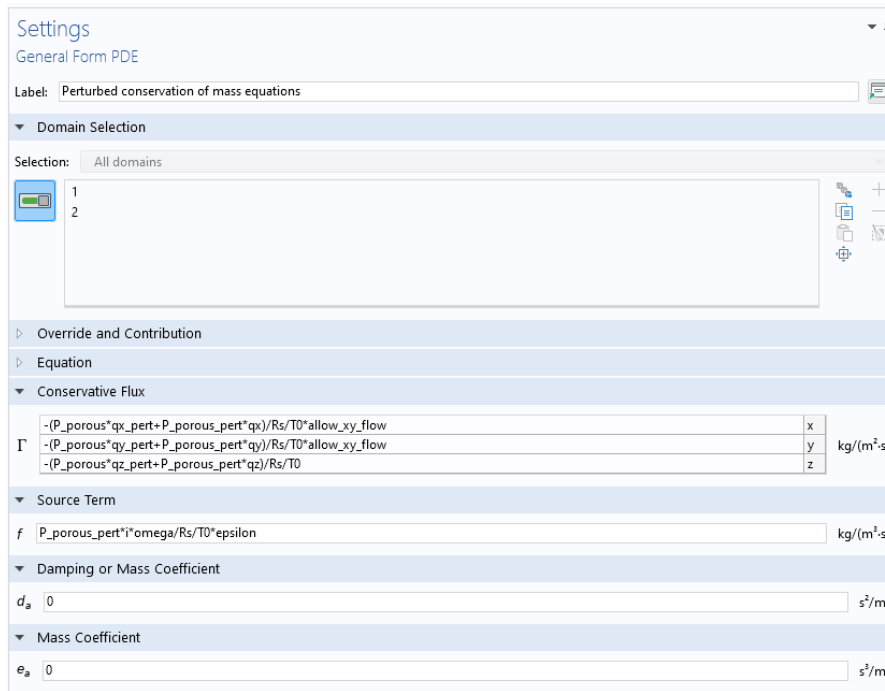


Figure B.32: Physics: Darcy perturbation: Perturbed conservation of mass equations

### No flow conditions at sealed surfaces and symmetry

In this module the no flow conditions is set which is described in Chapter 2 under Equation 2.29. It is applied at the surfaces where there is no flow due to the sides are sealed or due to symmetry.

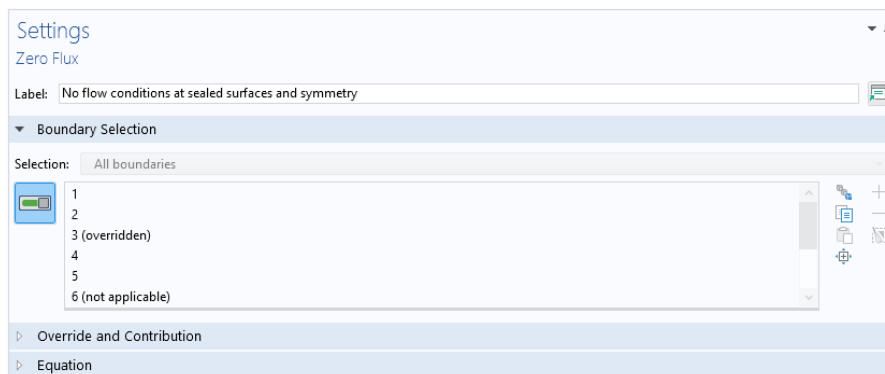



Figure B.33: Physics: Darcy perturbation: No flow conditions at sealed surfaces and symmetry

### Initial values

For the Perturbed Darcy equations there are no requirements for the initial conditions because there are no singularities.



Settings  
Initial Values

Label: Initial Values 1

Domain Selection

Selection: All domains

1  
2

Override and Contribution

Initial Values

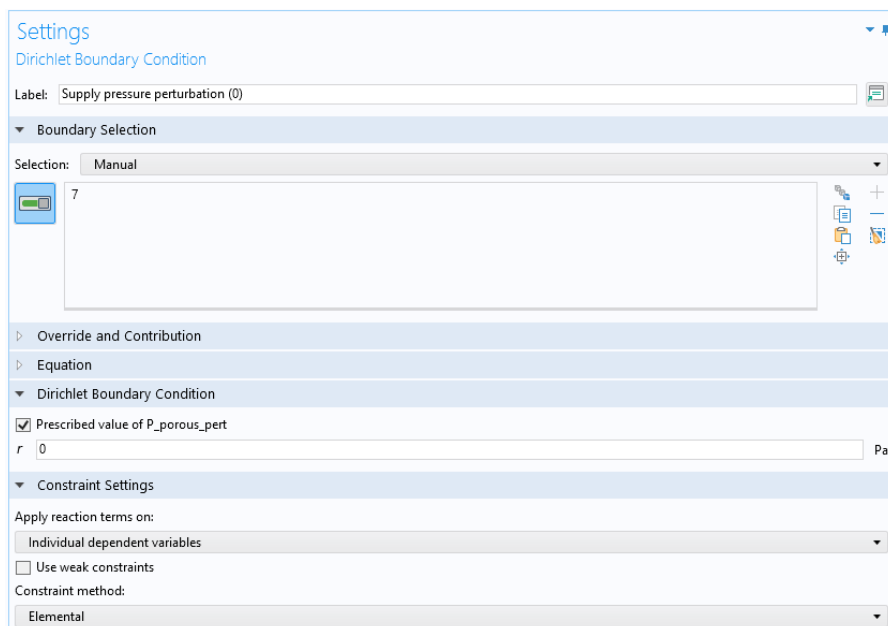
Initial value for  $P_{\text{porous\_pert}}$ :  
 $P_{\text{porous\_pert}}$  0 Pa

Initial time derivative of  $P_{\text{porous\_pert}}$ :  
 $\frac{\partial P_{\text{porous\_pert}}}{\partial t}$  0 Pa/s

**Figure B.34:** Physics: Darcy perturbation: Initial Values

### Supply pressure perturbation

This module contains the constraint that the perturbed pressure, at the sides where the supply pressure is present, is equal to 0. This equation can be found in Chapter 2 to as Equation 2.30.



Settings  
Dirichlet Boundary Condition

Label: Supply pressure perturbation (0)

Boundary Selection

Selection: Manual

7

Override and Contribution

Equation

Dirichlet Boundary Condition

☒ Prescribed value of  $P_{\text{porous\_pert}}$   
 $r$  0 Pa

Constraint Settings

Apply reaction terms on:  
 Individual dependent variables

☐ Use weak constraints

Constraint method:  
 Elemental

**Figure B.35:** Physics: Darcy perturbation: Supply pressure perturbation

**Perturbed film pressure**

This module links the perturbed film pressure  $p_{\text{film\_pert}}$  with the perturbed porous pressure  $p_{\text{porous\_pert}}$  at the bearing surface. This equation can be found in Chapter 2 as Equation 2.31.

The screenshot shows the 'Settings' window for a 'Dirichlet Boundary Condition' in COMSOL Multiphysics. The window is titled 'Settings' and has a sub-header 'Dirichlet Boundary Condition'. The 'Label' field is set to 'Perturbed film pressure'. Under the 'Boundary Selection' section, the 'Selection' is set to 'Manual' and a list of boundaries is shown with '3' selected. The 'Override and Contribution' section is collapsed. The 'Equation' section is expanded, showing the 'Dirichlet Boundary Condition' with the 'Prescribed value of  $P_{\text{porous\_pert}}$ ' checked. The variable  $r$  is set to  $P_{\text{film\_pert}}$  and the unit is 'Pa'. The 'Constraint Settings' section is expanded, showing 'Apply reaction terms on:' set to 'Individual dependent variables', 'Use weak constraints' unchecked, and 'Constraint method:' set to 'Elemental'.

**Figure B.36:** Physics: Darcy perturbation: Perturbed film pressure

### B.4.6. Domain ODEs and DAEs: qx perturbation (same as qy and qz)

This module calculates the value of  $q_x$  as a function of the perturbed pressure gradient which is needed in the mass balance of the perturbed Darcy module. Because the relationship between the pressure gradient and the flow is implicit an extra module is needed to solve this equation. If only linear Darcy is considered without the inertial Forchheimer term, this module can be eliminated. The module is very similar to the  $q_y$  and  $q_z$  modules, the only thing that needs to be done is replace  $x$  in all equations by either  $y$  or  $z$  to get the other two. The initial conditions in this module can be left at their default 0 values because there are no singularities.

#### General settings

To ensure that the module converges quickly it is recommend to match the element type order with the Darcy Static module.

The screenshot shows the 'Settings' window for 'Domain ODEs and DAEs'. The 'Label' is 'qx perturbation' and the 'Name' is 'dode4'. Under 'Domain Selection', the 'Selection' is 'All domains'. The 'Equation' section is expanded. Under 'Units', there are two rows: 'Dependent variable quantity' with 'Unit' 'm/s' and 'Source term quantity' with 'Unit' 'Pa/m'. Under 'Discretization', 'Shape function type' is 'Discontinuous Lagrange', 'Element order' is 'Cubic', 'Value type when using splitting of complex variables' is 'Complex', and 'Frame' is 'Spatial'. Under 'Dependent Variables', 'Field name' is 'qx\_pert', 'Number of dependent variables' is '1', and 'Dependent variables' is 'qx\_pert'.

Units	
Dependent variable quantity	Unit
Custom unit	m/s
Source term quantity	Unit
Custom unit	Pa/m

Dependent Variables	
Field name:	qx_pert
Number of dependent variables:	1
Dependent variables:	qx_pert

Figure B.37: Physics: qx perturbation: General Settings

**qx perturbed**

This module contains the actual description to calculate the perturbed flow from the perturbed pressure gradient in the x direction. The equation can be found in Chapter 2 as equation 2.19. The variable switching variable `allow_nonlin` is used to switch the model into a mode that only looks at the viscous component of the permeability and is only used for testing purposes.

The relation for the perturbed flows equation in COMSOL code:

```
source = -P_porous_pertx-mu/kappa_v*(qx_pert)-
          ((P_porous+P_porous_pert)*abs(qx+qx_pert)*(qx+qx_pert)-
           P_porous*abs(qx)*qx)/Rs/T0/kappa_i*allow_nonlin
```

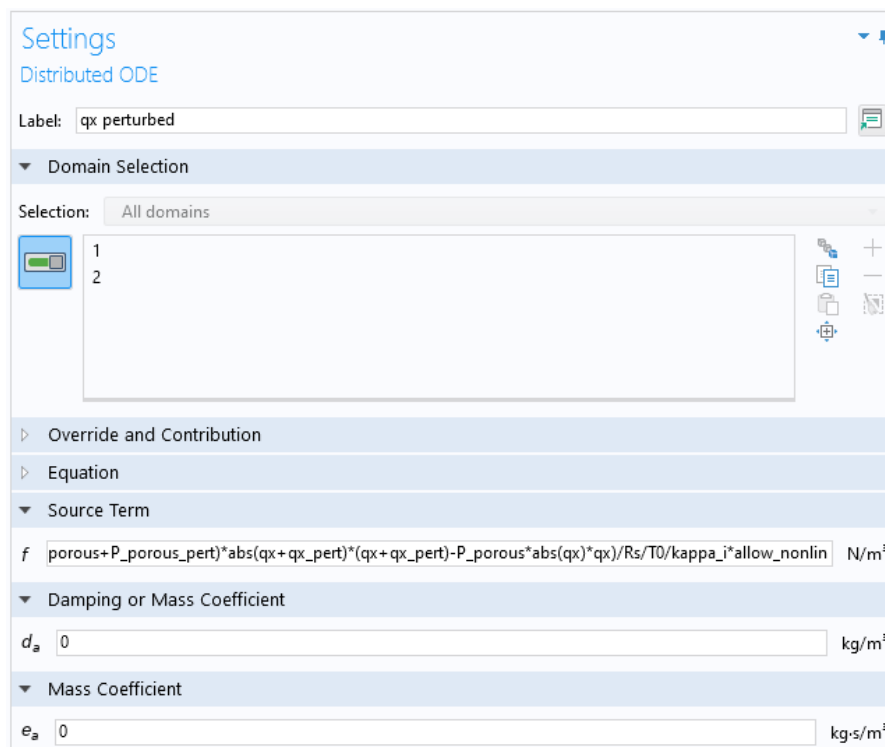
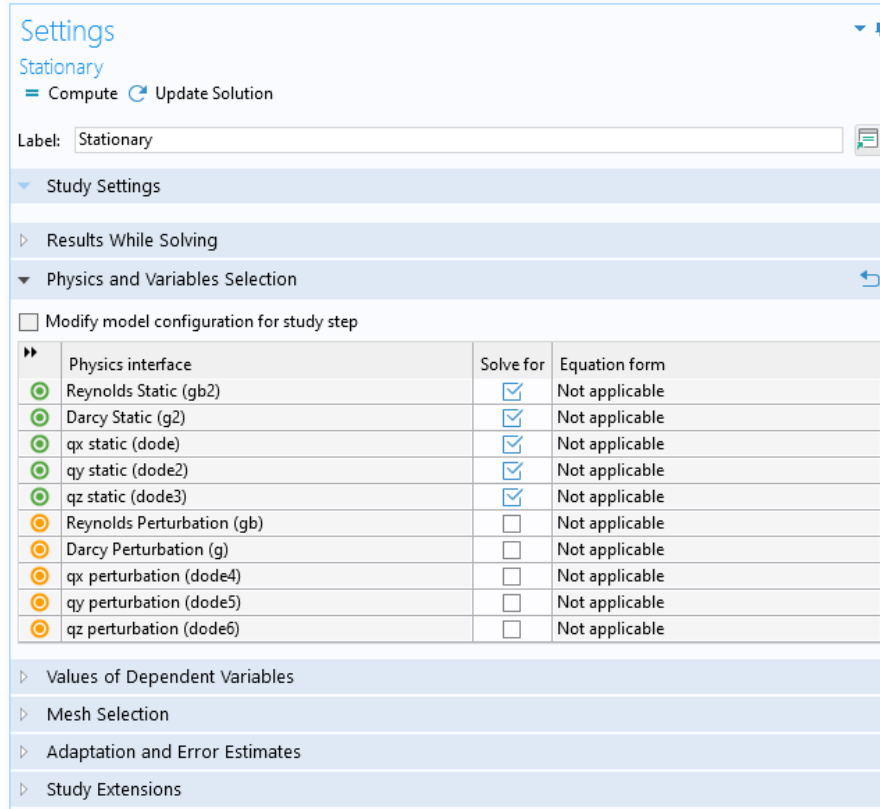


**Figure B.38:** Physics: qx perturbation: General Settings

## B.5. Solver settings

The model is set up in 2 steps. It is possible to do it all in one step but this is inefficient and will result in very long calculation times. To set the solver up we need to set up two stationary study steps. The first study step is used to solve all the stationary equations. The second is used to loop through the dynamic equations for different frequency's. In the screen-shots below all settings that were changed from their default are visible.



**Settings**  
Stationary  
Compute Update Solution

Label: Stationary

Study Settings

Results While Solving

Physics and Variables Selection

☐ Modify model configuration for study step

Physics interface	Solve for	Equation form
Reynolds Static (gb2)	<input checked="" type="checkbox"/>	Not applicable
Darcy Static (g2)	<input checked="" type="checkbox"/>	Not applicable
qx static (dode)	<input checked="" type="checkbox"/>	Not applicable
qy static (dode2)	<input checked="" type="checkbox"/>	Not applicable
qz static (dode3)	<input checked="" type="checkbox"/>	Not applicable
Reynolds Perturbation (gb)	<input type="checkbox"/>	Not applicable
Darcy Perturbation (g)	<input type="checkbox"/>	Not applicable
qx perturbation (dode4)	<input type="checkbox"/>	Not applicable
qy perturbation (dode5)	<input type="checkbox"/>	Not applicable
qz perturbation (dode6)	<input type="checkbox"/>	Not applicable

Values of Dependent Variables

Mesh Selection

Adaptation and Error Estimates

Study Extensions

**Figure B.39:** Solver settings: Stationary Step 1

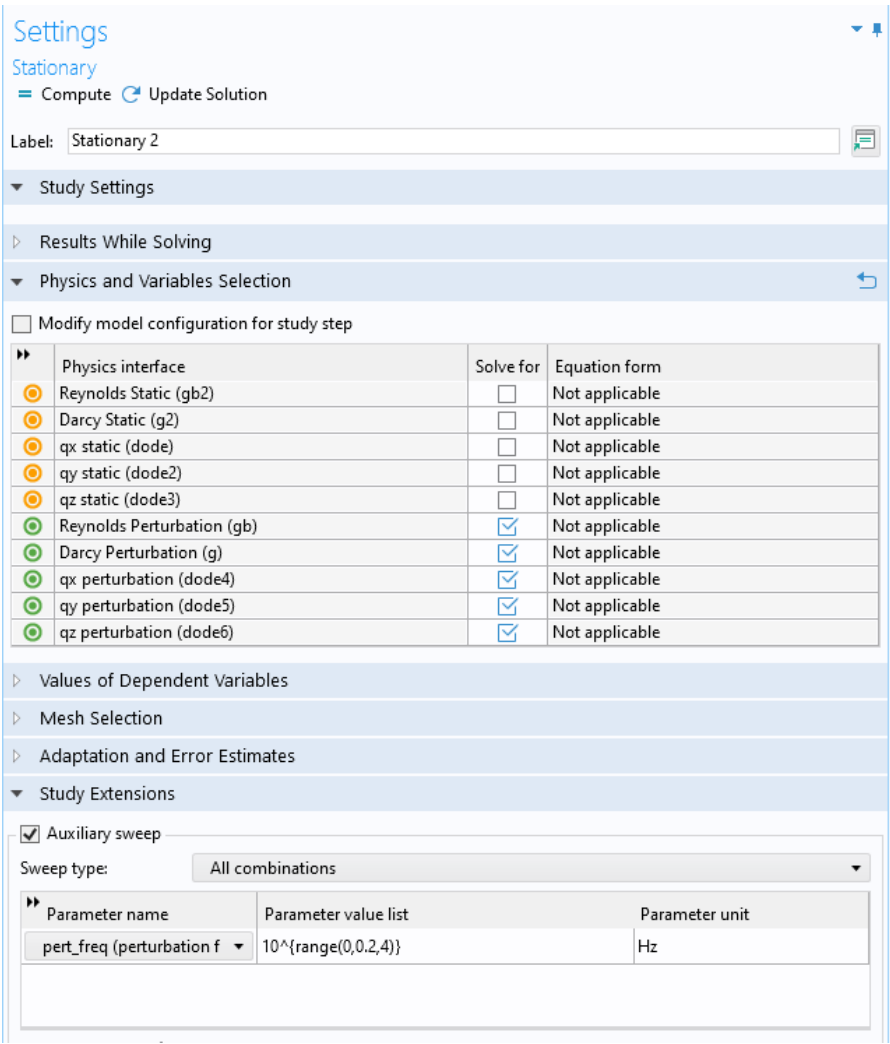


Figure B.40: Solver settings: Stationary Step 2

By default COMSOL will try to solve these steps using a segregated solver. This solver was found to be unable to converge within a realistic time frame. To solve this problem the solver can be modified to solve the selected modules as a fully coupled system of equations. To do this, go into the solver configurations that are generated by COMSOL and set both solves to fully coupled.

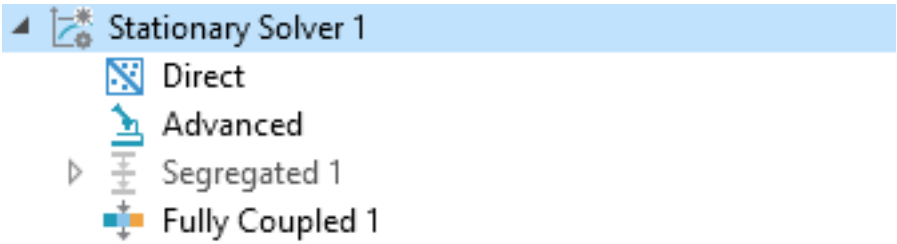


Figure B.41: Solver settings: Setting solvers to fully coupled

## B.6. Suggestions for figures

From the output data it is possible to create many different kinds of plots some suggestions are:

### Pressure profile static

Create a plot for the Static Pressure profile by first creating a 3D plot. Inside the plot create a surface in which the expression is set to  $P_{\text{porous}}$ . This creates a plot of the pressure profile of the static solution. This is useful for checking if all the boundary conditions are correct and to check if the solution is smooth. If for example the solution is not as expected, first check all boundary conditions that could influence the anomaly. If the solution shows artefacts that coincide with the boundaries of the elements, for example lines of high pressure along the edges of the elements, check if there are enough elements in this area or if the order of the elements is high enough.

### Perturbation pressure profile

Create a plot for the perturbed pressure profile by first creating a 3D plot. Inside the plot create a Surface in which the expression is set to  $P_{\text{porous\_pert}}$ . This creates a plot of the pressure profile of the perturbed solution. This is useful for checking if all the boundary conditions are correct and to check if the solution is smooth. If for example the solution is not as expected, first check all boundary conditions that could influence the anomaly. If the solution shows artefacts that coincide with the boundaries of the elements, for example lines of high pressure along the edges of elements, check if there are enough elements in this area or if the order of the elements is high enough. For the perturbation it is necessary to have more elements near the bearing surface because the derivatives of the perturbed pressure near the surface can get quite high.

### B.6.1. Dynamic stiffness

Create a plot for the dynamic stiffness by creating a 1D plot. Inside this 1D plot create a Global with the expression  $K_{\text{dynamic}}$ . It is a good check for the model to evaluate the low and high frequency stiffness, which can be calculated by evaluating the tangent and secant stiffness in a static model.

### Dynamic damping

Create a plot for the Dynamic damping by creating a 1D plot. Inside this 1D plot create a Global with the expression  $D_{\text{dynamic}}$ .

### Nyquist

If a loop function is known for the system describing both the bearing and the system, it is simple to create a Nyquist plot inside of COMSOL. Create a 1D plot and insert under more plots the Nyquist plot. For the expression insert the loop gain formula. For a simple 1D system consisting only of the air bearing and a simple mass the loop function is:

$$\text{loop\_fuction} = -(K_{\text{dynamic}}/M_{\text{moving}})/(\omega)^2 - (D_{\text{damping}}/M_{\text{moving}})/(\omega)*i$$

To make a Nyquist plot for the stability of a more complex system, this might not be the most suitable solution. For more complex systems it might be easier to use this model to create the stiffness and damping characteristics and use that as an input to a more elaborate model of the system dynamics.